The Dissolution of Mineral Phosphate in Soil

D. Phil Thesis
G.J.D. Kirk
St. Cross College
Hilary Term 1985

Abstract

The use of cheap, sparingly soluble calcium phosphate fertilizers is increasingly widespread, particularly in the extensive agriculture systems of the tropics where very high yields are not sought, and phosphate deficiency is a major limitation to crop production. At present there is little quantitative understanding of the factors determining the rates of dissolution of calcium phosphates in soils. Existing quantitative treatments are inadequate, being either empirical or based on over-simplified theory. By developing a precise model of the dissolution process, it should be possible to short-cut the usual practice of running extensive field trials to establish the responses over a wide range of soil conditions and management practices.

In this thesis a model which makes no arbitrary assumptions is developed for predicting the rates of dissolution of dicalcium phosphate dihydrate (DCPD) in soils. DCPD is the initial reaction product of the dissolution of many phosphatic fertilizers, and is an important fertilizer in its own right; the mechanisms governing its dissolution in soils are basically the same for other, more complex calcium phosphates. The simple case of a planar layer of DCPD in contact with soil is considered first to introduce the principles of the model. This is the simplest system for measuring experimentally the solute concentration profiles close to the dissolving surface, in order to test the model. The model is then extended to describe the dissolution of granules of DCPD in soil.

The model comprises numerical solutions of mathematical equations describing the diffusion and reaction of calcium, phosphate and base in soil. The concentrations of calcium, phosphate and hydrogen ions in the soil solution at the mineral/soil boundary are found (a) from the ion activity product of DCPD and (b) by equating the fluxes of calcium, phosphate and base across the boundary (1 mol of DCPD gives 1 mol each of calcium, phosphate and base). In the granular system, the diminution of the granules as they dissolve, and the effect of neighbouring particles on each other are allowed for.

The solute concentration profiles predicted for the planar system agreed with experimentally measured profiles; and the predicted net rates of dissolution of granules of DCPD agreed with the rates determined by a radioactive-tracer technique, in which ^{45}Ca dissolved from labelled DCPD is recovered from the soil with an extractant, saturated with respect to DCPD. Thus all important processes have been accounted for in the model. Since the theory is non-specific, the model should apply equally well to most other soils.

The model has nine input parameters : the concentrations of calcium and phosphate in the native soil solution, the native soil pH, the phosphate and lime potential buffer capacities of the soil, the moisture status, the diffusion impedance factor, and the rate of application and particle size of the DCPD. A sensitivity analysis of the model showed that the rate is particularly dependent on particle size, rate of application, and the pH and concentration of calcium in the soil solution. If the granules are so far apart that they do not influence each other, after the very early

stages the rate of dissolution is independent of the soil buffer terms. But for typical rates and methods of application, neighbouring granules will influence each other, and the consequent interactions between the rate determining variables are complex.

The extension of the model to describe the dissolution of carbonate-apatites, and hence rock phosphates, is discussed.

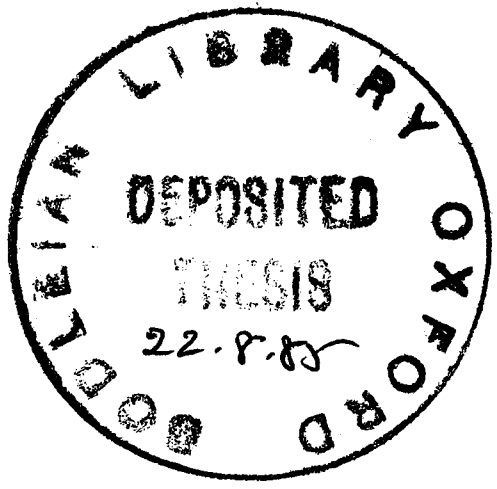
THE DISSOLUTION OF MINERAL PHOSPHATE IN SOIL

Thesis submitted for the degree of

Doctor of Philosophy

at the

University of Oxford



by

G.J.D. KIRK

St. Cross College

Hilary Term 1985

To my father, Joseph Dunn Kirk.

CONTENTS

	Acknowledgements	iv
	List of Main Symbols	v
1	Introduction	1
2	A Model of the Dissolution of a Planar Layer of DCPD in Soil.	4
3	Experimental Assessment of the Planar Model.	47
4	A Model of the Dissolution of Granules of DCPD in Soil.	76
5	Experimental Assessment of the Granular Model.	98
6	Applications of the Model	107
	Appendices	136
	References	154

Acknowledgements

I am greatly indebted to my supervisor, Peter Nye, who has shown me unreasonable patience and discretion throughout this research; and to my colleagues, Peter Darrah and Rachhpal Singh.

For domestic support I wish to thank John Baker, Hermann Bauer, Gillian Bendle, Fred Honey, Barbara Library, Dick Martin, Gladys Office, Tony Probitts, Frank Roche, Paddy Selwood and Jeni Tree.

The research was funded by the Natural Environment Research Council.

LIST OF MAIN SYMBOLS

Symbol	Definition and Units
a_i	initial radius of granule, dm
a_s	radius of granule at a particular time, dm
Δa	amount by which granule surface has retreated at a particular time, dm
b_{HS}	lime potential buffer capacity, (-d[HS]/d(pH-1/2pCa))
C_L	concentration of $H_2PO_4^-$ in solution, mol dm^{-3} of solution
C_S	concentration of all adsorbed phosphate species, mol dm^{-3} of whole soil
$[Ca^{2+}]_L$	concentration of Ca^{2+} in solution, mol dm^{-3} of solution
$[Ca^{2+}]_S$	concentration of Ca^{2+} on soil solid, mol dm^{-3} of whole soil
D_L	diffusion coefficient of solute in free solution, subscripted P, H and C for $H_2PO_4^-$, H^+ and HCO_3^- respectively, $dm^2\ s^{-1}$
f	diffusion impedance factor
F_P, F_B	fluxes of phosphate and base, mol $dm^{-2}\ s^{-1}$
$[H^+]_L$	concentration of H_3O^+ in solution, mol dm^{-3} of solution
$[HB]_L$	concentration of acid HB, in solution, mol dm^{-3} of solution
[HS]	concentration of titratable soil acid with respect to the native soil, mol dm^{-3}
I	ionic strength
K_{SP}	solubility product of DCPD
K_2	second dissociation constant of H_3PO_4
K_3	equilibrium constant for the formation of $CaH_2PO_4^+$

K_d	apparent dissociation constant of H_2CO_3
K_s	solubility of CO_2 in water, mol dm^{-3}
M	amount of substance dissolved, mol
mw	molecular weight
P_{CO_2}	pressure of CO_2, atm
r	radial distance from centre of particle, dm
Δr	radial distance step, dm
R	radial distance from centre of particle to zone of influence of neighbouring particle, dm
S_L	concentration of solute in solution, mol dm^{-3} of solution
t	time, s
Δx	planar distance step, dm
x	distance, dm
X	length of soil block, dm
z	ionic valence (cations + , anions -)
λ	ion activity coefficient
θ	volumetric moisture content
θ_g	gravimetric moisture content
ρ	moist bulk density, kg dm^{-3} of whole soil

Additional subscripts: L, liquid phase; S, solid phase; j, distance step.

Superscripts: ' value in native soil; t, time step.

1

INTRODUCTION

The use of sparingly soluble, mineral phosphate fertilizers is increasingly widespread (Lehr, 1980), particularly in the extensive agriculture systems of the tropics where very high yields are not sought and phosphate deficiency is a major limitation to crop production. In addition to their relative cheapness and the fact that they are often locally available, the chemistry of sparingly soluble phosphates makes them well suited to many tropical soils. Thus, the acidity of the soils favours a reasonable rate of dissolution, but, unlike water-soluble phosphates, mineral phosphates do not dissolve so rapidly that the dissolved phosphate largely becomes occluded on soil surfaces, before it can be utilised by plants. With the continuing development of acid-tolerant plant species, sparingly soluble phosphates are likely to be increasingly important in tropical agriculture as it becomes possible to farm these soils in their native, acid state (Sanchez and Salinas, 1981).

At present there is little quantitative understanding of the soil factors determining the rates of dissolution of mineral phosphates. Existing quantitative treatments are either empirical or based on over-simplified theory (for a review see Khasawneh and Doll, 1978). This is a serious practical omission because without a quantitative framework, one cannot decide what are the optimal management practices for the use of these minerals; obviously the avoidance of wastage is particularly apposite in tropical farming. In addition to being able to determine the correct rates of application, one needs to know the effects of fineness of division, the benefits to be gained from placement regimes, and what the residual value of the dissolved, as well as the undissolved phosphate, is likely to be. The complexity of the mineral/soil reaction is such that

only a rigorous treatment can satisfactorily answer such questions by enabling prediction of how the rate of dissolution responds to variations in natural conditions and management practices.

The difficulties in developing accurate models of fertilizer dissolution are legion. Most fertilizers are not pure salts and so do not have fixed solubilities. In any case, dissolution of pure salts is not necessarily congruent. The large solute concentrations that occur near fertilizers cause simultaneous precipitation, sorption and displacement reactions. Furthermore, it is necessary to account for the diffusion of several ions from the fertilizer into the soil, and they may influence each other's mobilities.

This thesis is concerned with the development of a mechanistic model, capable of predicting the solute concentration profiles developed around dissolving dicalcium phosphate dihydrate (DCPD). DCPD was chosen because it is the initial reaction product of the dissolution of many phosphatic fertilizers, and is an important fertilizer in its own right. The model should provide a basis from which to advance to more complex fertilizers such as rock phosphate. The thesis is divided into two stages: firstly the simple case of a planar source of DCPD in contact with soil is considered to introduce the main concepts and to establish what the important processes are. This is the simplest system for measuring experimentally the solute concentration profiles close to the dissolving surface. The basic model is then extended to the more practically relevant system of individual granules of DCPD dissolving in soil. Certain aspects of the model are discussed in relation to the soil used for the experimental work, but the theory is non-specific and applies to soils in general. Since the work is intended as a starting point from which to advance to other mineral phosphates, and it is hoped that in the

future that work will be taken up, the development of the model is given in some detail. Thus a full description is given of the solutions of the equations used in the model, and the way in which the solutions were programed is explained. The final chapter is concerned with the sensitivity of the model to its input variables, and serves to identify the important rate controlling factors in the dissolution of granules of DCPD in soil.

SI units are used, except where they are obviously inconvenient: thus, for example, the distance axes of solute concentration profiles are given in mm rather than decimal powers of a metre.

2

A MODEL OF THE DISSOLUTION OF A PLANAR LAYER OF DCPD IN SOIL

In this chapter, the simple case of a planar layer of DCPD in contact with soil (fig. 2.1) is considered to introduce the main concepts. This is the simplest system for measuring experimentally the solute concentration profiles close to the dissolving surface.

2.1 Rate Limiting Processes in Crystal Dissolution

The dissolution of crystals in aqueous solution comprises two distinct processes: transfer of material from the crystalline phase to the solution at the crystal surface (the surface process), and transfer of dissolved material from the crystal/solution interface to the bulk solution (the bulk-diffusion process). If the rate of the surface process greatly exceeds that of bulk-diffusion, the rate of dissolution will be controlled by the rate of diffusion, and vice versa.

Commonly, surface process are discussed in terms of nucleation models (eg. Christoffersen, 1980), which apply to crystal growth as well as dissolution. In these models, the probability of an ion escaping from the crystal surface is related to the growth of microscopic holes centered on surface defects. At such points, the lattice energy is decreased so that interionic bonds are weaker and ions can escape more easily. The change in Gibbs free energy for hole formation, ΔG_{diss}, is a function of the change in surface free energy which is related to the initial hole size and the increase in surface area resulting from hole formation. Thus for holes smaller than a critical size, ΔG_{diss} is positive and these holes tend to be infilled. Larger holes, however, will expand since ΔG_{diss} is

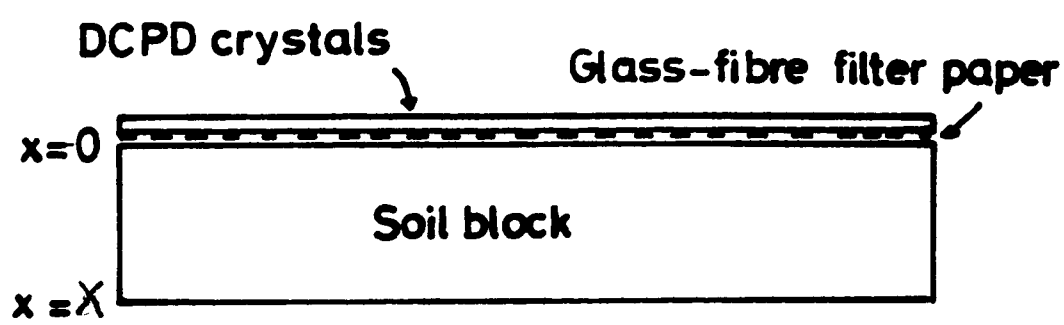


Fig. 2.1. The experimental system.

negative, and will continue to expand (both into the crystal and across the face) until a layer is removed from the entire crystal surface (mononuclear dissolution) or until they link up with adjacent holes (polynuclear dissolution). Mononuclear dissolution tends to remove a layer of thickness proportional to the area of the crystal face, whereas the thickness of a layer removed by polynuclear dissolution is independent of the face area.

A simple means of establishing whether the surface process or bulk-diffusion is rate controlling for a particular crystal in water, is to study its dissolution in stirred suspension. Dissolution limited by diffusion will be accelerated by stirring whereas surface process limited dissolution should be unaffected. The temperature dependence and hence activation energy of dissolution provides further evidence since, if the overall reaction is fast enough to be diffusion controlled, it will have a low activation energy in the range 15-30 kJ mol^{-1} (Glasstone et al, 1941). If surface processes are rate limiting, the activation energy will be higher.

Aqueous dissolution of DCPD appears to be limited by bulk-diffusion processes since it is accelerated by stirring and has a low activation energy (15.9 kJ mol^{-1}) (Nancollas and Marshall (1971); Huffman et al (1957)). In soils, solute diffusion is generally restricted and is sure to limit the rate of dissolution if no other transport process is operating; but in addition to diffusive movement, solutes may be transported through soil by mass flow of solution due to leaching, or as a result of vapour gradients which cause counter-fluxes of water and solute. The present study has been limited to situations in which leaching does not occur, but in other circumstances, leaching of calcium would increase the rate of dissolution. Movement of water vapour can occur where very

high solute concentrations arise. Thus, vapour diffuses rapidly towards the dissolving mineral, leaving a dry zone in the soil bulk. Saturated solution subsequently moves into the soil in response to the blotting action of the dry zone, forming a wetting front which is sharp due to the high surface tension of the concentrated solution. Thus Lindsay and Stephenson (1959) observed distinct wet and dry bands around particles of monocalcium phosphate (MCP) dissolving in a fine sandy loam. If such processes operate in DCPD dissolution, movement of solute away from the mineral/soil interface would be very fast so that surface processes could be rate limiting. However, MCP has a much higher solubility than DCPD and gives rise to solutions that are several molar in phosphate. The vapour pressure gradient about dissolving DCPD would be insufficient to cause significant vapour movement. Similarly osmotic movement can be discounted.

2.2 The Composition of the Solid Phase

If a solid and a solution are in equilibrium, the chemical potential of components occuring in both phases must be the same throughout. The chemical potential, μ_i of a particular component in a given phase is related to its activity, a_i by the conventional expression

$$\mu_i = \mu_i^\circ + RT \ln a_i$$

where superscript $^\circ$ refers to the standard state. Thus any factor changing the activity of the solid phase will change the solid's solubility. A number of factors may alter the activity of a solid phase in a soil system. Isomorphous substitution of foreign ions in the crystal lattice (solid solution formation) may occur. Possible invading ions in DCPD dissolution in soil are Al^{3+} and Fe^{3+}, but their concentrations are typically very small compared with the calcium concentration at the

mineral/soil interface, so the rate of solid solution formation is in practice very low. Dehydration of DCPD to its polymorph, DCP, should be considered, but is unlikely to occur at the water activity at normal temperatures and pressures in a soil pore above wilting point. The formation of less soluble phases such as octacalcium phosphate and hydroxyapatite is more likely. However, a lot of work has been done on the stability of calcium phosphates in the $CaO-P_2O_5-H_2O$ system (eg. Arnold, 1950; Brown and Lehr, 1959) and it is clear that these phases are formed only very slowly under typical soil conditions, and thus DCPD is a metastable phase and its dissolution is congruent.

The activity of solid DCPD is therefore constant throughout dissolution and a simple solubility product relationship can be used to describe the dissolution equilibrium, with the activity of the solid phase set equal to unity.

2.3 The Composition of the Soil Solution at the Mineral/Soil Interface

The precipitation-dissolution reaction of DCPD in aqueous solution is

$$CaHPO_4.2H_2O \rightleftharpoons Ca^{2+} + HPO_4^{2-} + 2H_2O \qquad (2.31)$$

Thus $$K_{SP} = (Ca^{2+})_L(HPO_4^{2-})_L$$

where the terms in parentheses are ionic activities. For the purposes of the present study, it is convenient to work in concentrations. The conversion of activities to concentrations using the Davies equation, is described in section 2.4.

In neutral and acid soils, most of the phosphate will be present as monovalent orthophosphoric acid in accordance with the equilibrium

$$HPO_4^{2-} + H_2O \rightleftharpoons H_2PO_4^- + OH^-$$

which is conventionally written

$$H_2PO_4^- \rightleftharpoons HPO_4^{2-} + H^+ \qquad (2.32)$$

Thus DCPD dissolution causes a rise in pH. The propagation of this rise in pH through the soil bulk can be considered in terms of a spread of "base" outward, effected by the diffusion of conjugate acid-base pairs in the soil. I define the amount of soil base as the amount of strong acid required to bring the soil back to the lime potential of the native soil. Thus increases in the amount of soil base are equivalent to decreases in the amount of soil acid.

The total amounts of calcium and phosphate dissolved are further increased by the formation of complex ions, the most important of which is

$CaH_2PO_4^+$, as given by the equilibrium

$$Ca^{2+} + H_2PO_4^- \rightleftharpoons CaH_2PO_4^+ \qquad (2.33)$$

The concentrations of other calcium-orthophosphate complexes, such as $CaHPO_4$, and complexes with Mg^{2+}, Fe^{2+}, and Fe^{3+} are negligible at the pH's (3.5 to 6.5) and ion concentrations of the present system.

Fig. 2.2 shows the relative contributions of the different phosphate species to the composition of an aqueous solution with $[Ca^{2+}] = 10^{-3}$ mol dm^{-3}. The equilibrium constants for equations (2.31) to (2.33) at 20°C are pK_{SP} 6.699 (self determined for the DCPD used), pK_2 7.213 (Bates and Acree, 1943), and pK_3 -0.914 (Moreno et al, 1968). Values refer to activities on a mol dm^{-3} scale.

Moreno et al (1960b) give evidence of complexing of calcium with dissolved organic matter to explain an apparent super-saturation of an acid soil solution in equilibrium with DCPD. But it seems unlikely that sufficient organic matter could be dissolved by either phosphate or base, to complex an appreciable amount of calcium. The concentration of dissolved organic matter in a typical soil solution is of the order of a few µmol dm^{-3}, and in the acid woodland soil used in the present study, the concentration was found to be less than 10 µmol dm^{-3}, even at quite high phosphate concentrations. This possibility has therefore been dismissed.

The major phosphate species in solution are therefore $H_2PO_4^-$, HPO_4^{2-}, and $CaH_2PO_4^+$. Near the interface, the flux of HPO_4^{2-} will be important in relation to the propagation of the pH rise at the interface (see below and fig. 2.6), and the $CaH_2PO_4^+$ concentration will be important in relation to the the balance of ionic

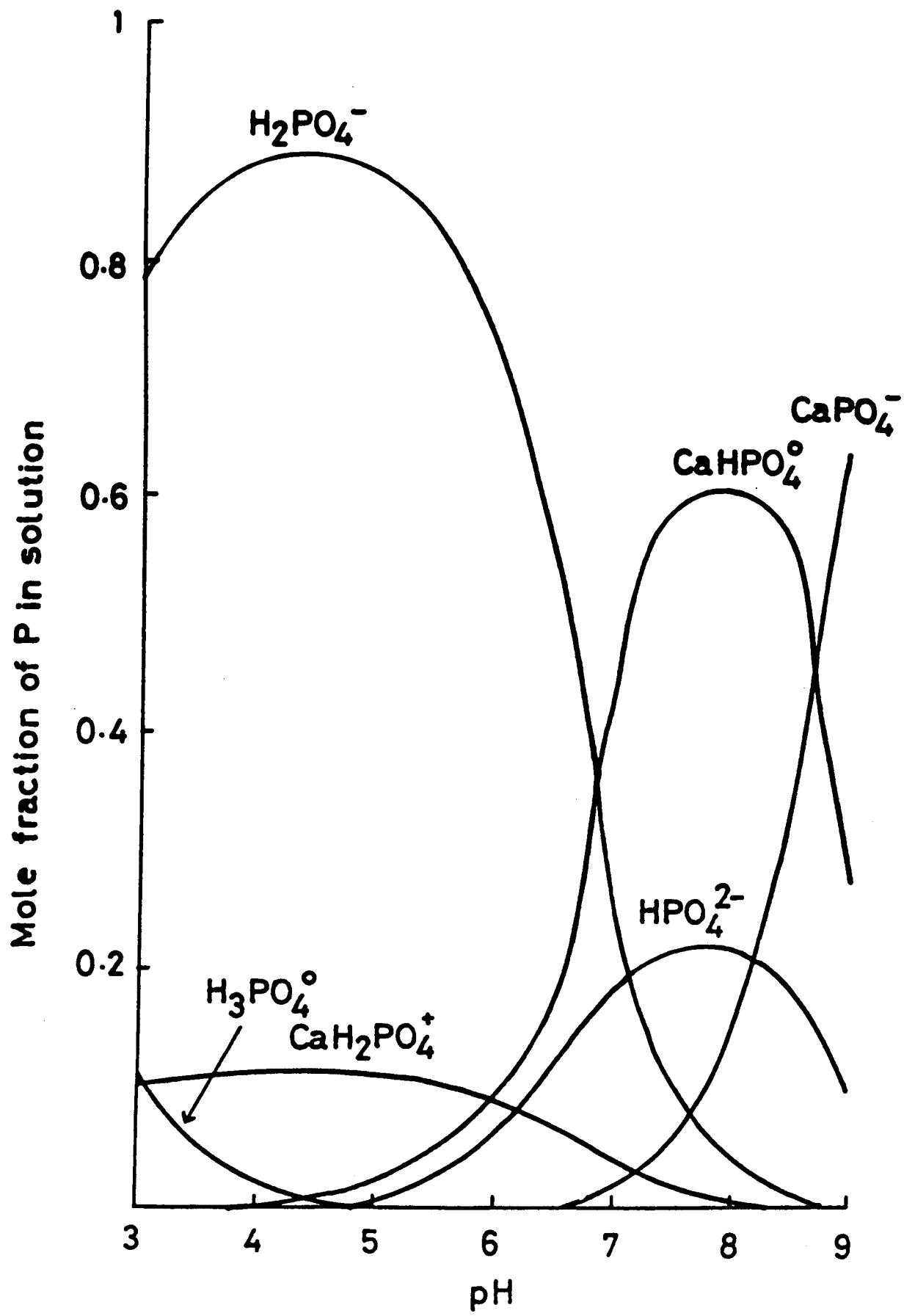


Fig. 2.2. The major phosphate species in solution at different pH's. $[Ca^{2+}] = 5 \times 10^{-3}$ mol dm^{-3}.

charges (see fig. 2.7). However, the net flux of phosphate will be little influenced by these components since their concentrations are small compared to that of $H_2PO_4^-$, and they need not be considered in the phosphate continuity equation.

In a static system of DCPD in water at equilibrium, the concentrations of calcium, phosphate and acid ions in solution could be calculated using the equilibrium constants for equations (2.31) to (2.33). However, in a non-equilibrium system, to find the concentrations of ions at the DCPD/water or DCPD/soil interface, one needs to know, in addition to the solubility product relationship, the rates of removal of solutes from the interface. In the simple case of a salt containing one cation and one anion, dissolving in water, both ions would be expected to move at the same rate, the ion with greater mobility being slowed down by the one with less, and vice versa. The concentration gradients of the two ions in the bulk solution would therefore be the same, as would their concentrations at the interface, which could be determined directly from the salt's solubility product. The present problem, however, involves a number of ions whose fluxes in individual volumes of the soil bulk will be coupled but not equal, resulting in different concentration gradients. Thus, for example, if base moved away from the interface more slowly than calcium and phosphate, the composition of the interface soil solution would tend towards the basic end of the solubility isotherm. Since one mol of Ca^{2+}, $H_2PO_4^-$ and OH^- is produced for each mol of DCPD dissolved, steady state is attained when the fluxes of calcium, phosphate and base at the interface, are all equal; otherwise dissolution would not be continuous. The problem, therefore, is to find the steady state concentration gradients at the interface which satisfy this equal flux requirement, as well as the solubility product relationship.

It is not necessary to obtain solutions to diffusion equations for each of the components, calcium, phosphate and base, to calculate their concentration gradients, because if one knows the gradients of two, the third may be obtained by balancing the ionic charges for electroneutrality. Writing the correct equations for calcium diffusion is difficult because its interaction with surface sites is not a simple function of its solution concentration, depending also on the concentrations of competing cations in the soil solution. Exchange of calcium with other metal cations, such as K^+, will be negligible in most circumstances. Thus changes in the concentration of calcium in solution will be controlled by changes in the concentrations of the anions entering the soil from the mineral. It is therefore expedient to take calcium as the balancing ion, and solve the diffusion equations for phosphate and soil base.

It is thereby possible to obtain three equations describing the propagation of the component species through the soil, which, as will be shown, can be expressed in terms of the three working concentration variables, $[H_2PO_4^-]_L$, $[H^+]_L$ and $[Ca^{2+}]_L$.

Description of the Model

2.4 The Propagation of Phosphate, Base and Calcium into the Soil

a) Phosphate

Movement of phosphate in soils occurs by diffusion through the pore network, accompanied by adsorption onto the solid phase on which it is essentially immobile. The continuity equation for such a diffusion plus reaction process is

$$\theta\frac{\partial C_L}{\partial t} = \frac{\partial}{\partial x}\left[D_{LP}\theta f\frac{\partial C_L}{\partial x}\right] - \frac{\partial C_S}{\partial t} \qquad (2.41)$$

(after Crank, 1975, eqn.14.2). Evaluating the reaction term, $\partial C_S/\partial t$, is difficult, owing to the complex nature of the phosphate-surface interaction, and the difficulty of obtaining experimental data that correctly describes the reaction rate in the micro-environment of a soil aggregate (Brewster et al, 1975). But if the rate of reaction is fast compared to the rate of diffusion, equilibrium between adjacent solid and liquid phases will be effectively instantaneous, and the problem is much simpler. Equilibrium data obtained for the present soil in shaken suspension experiments (see section 3.1) fitted a Freundlich equation over the relevant solution concentration range (5×10^{-5} to 5×10^{-2} mol dm^{-3}):

$$C_S = aC_L^{\,b}$$

This equation satisfactorily describes phosphate sorption data for many soils (Barrow, 1978). Differentiating with respect to C_L

$$dC_S/dC_L = abC_L^{b-1} \qquad (2.42)$$

Thus $$\frac{\partial C_S}{\partial t} = \frac{dC_S}{dC_L}\frac{\partial C_L}{\partial t} = abC_L^{b-1}\frac{\partial C_L}{\partial t}$$

Substituting in equation (2.41) and rearranging

$$\frac{\partial C_L}{\partial t} = \frac{D_{LP}\theta f}{\theta + abC_L^{b-1}}\frac{\partial^2 C_L}{\partial x^2} \qquad (2.43)$$

This treatment of the sorption reaction has two limitations. Firstly, it does not take account of the slow reaction between phosphate and soils. This is probably acceptable for periods up to a few weeks, which is as long as DCPD particles persist in acid soils. For longer times one would have to incorporate a kinetic component to account for the additional phosphate sorbed by slow reaction.

Secondly, the treatment does not include the fact that phosphate sorption is likely to vary at different pHs. Thus, for soils in which hydrogen ions tend to solubilise phosphate, one might expect that the spread of base away from the mineral should reduce the concentration of phosphate in solution and enhance the rate of dissolution (Nye, 1983, gives a mathematical treatment of such systems).

Infact, kinetic and pH effects were found to be unimportant for the present soil, and this is discussed in detail in section 3.1.

b) Soil Base

A theoretical treatment of the propagation of changes of pH in soils has been given by Nye (1972). pH changes are brought about by the transfer of protons carried by conjugate acid-base pairs. Arrival of a base from a region of high pH is followed by reaction with the soil and simultaneous removal of the conjugate acid, resulting in a decrease in the acidity of the exchange complex and a rise in pH.

The continuity equation for this process is obtained by summing the contributions of the individual acid and bases involved. Thus

$$\frac{\partial[HS]}{\partial t} = \frac{\partial}{\partial x}\left[\theta f \; \Sigma \; D_{LHB} \frac{\partial[HB]_L}{\partial x}\right] \qquad (2.44)$$

where HB is the conjugate acid of base B. In very acid soils, H_3O^+-H_2O will be the major acid-base pair in the bulk of the soil, but close to the DCPD the contributions of the pairs H_2CO_3-HCO_3^- and $H_2PO_4^-$-HPO_4^{2-} will also be significant since the interface pH and phosphate concentration are high. Thus

$$\frac{\partial[HS]}{\partial t} = \frac{\partial}{\partial x}\theta f\left(D_{LH}\frac{\partial[H^+]_L}{\partial x} - D_{LP}\frac{\partial[HPO_4^{2-}]_L}{\partial x} - D_{LC}\frac{\partial[HCO_3^-]_L}{\partial x}\right) \qquad (2.45)$$

The components of equation (2.45) must now be expressed in terms of the three working variables, $[H_2PO_4^-]_L$, $[H^+]_L$, and $[Ca^{2+}]_L$:

$[HCO_3^-]_L$ - This may be expressed in terms of $[H^+]_L$ by considering the equilibria in the H_2CO_3-CO_2-H_2O system. Thus, under conditions of constant pressure of carbon dioxide,

$$[HCO_3^-]_L = K_d K_s P_{CO_2} / [H^+]_L \qquad (2.46)$$

pK_d=6.381, pK_s=1.41 (Stumm and Morgan, 1981); P_{CO_2}=0.005 (see section 3.5).

$[HPO_4^{2-}]$ - This may be expressed in terms of $[H_2PO_4^-]_L$ and $[H^+]_L$ using reaction (2.32).

[HS] - Because the calcium gradient is steep (see fig. 2.4) and calcium will exchange with hydrogen ions on soil surfaces, changes in [HS] must be expressed in terms of changes in lime potential, not simply in terms of changes in pH. The lime potential buffer capacity, b_{HS} is defined by the relation

$$\Delta[HS] = -b_{HS}\Delta(pH-1/2pCa) \qquad (2.47)$$

This equation is preferable to other semi-empirical cation exchange equations because its logarithmic format can allow for the fact that the affinity of an exchange surface for a given cation varies with the proportion of sites already occupied by it. Thus b_{HS} is often reasonably constant over a wide range of lime potentials. Now,

$$\frac{\partial[HS]}{\partial t} = -\frac{d[HS]}{d(pH-1/2pCa)}\frac{\partial(1/2pCa-pH)}{\partial t} = b_{HS}\frac{\partial(1/2pCa-pH)}{\partial t} \qquad (2.48)$$

In practice the differences in the activity coefficient terms in (1/2pCa-pH) cancel in the range of ionic strengths in the present system: eg. at the interface (where the ionic strength is greatest), I=0.02, $[H^+]_L=10^{-5}$ and $[Ca^{2+}]_L=5\times10^{-3}$ mol dm^{-3} (see fig. 2.7),

giving pH-1/2pCa=3.79 as compared to $p[H^+]_L - 1/2p[Ca^{2+}]_L = 3.85$. Thus equation (2.48) may be written

$$\frac{\partial[HS]}{\partial t} = \frac{b_{HS}}{2.3}\left(\frac{1}{[H^+]_L}\frac{\partial[H^+]_L}{\partial t} - \frac{1}{2[Ca^{2+}]_L}\frac{\partial[Ca^{2+}]_L}{\partial t}\right) \qquad (2.49)$$

By equating the RHS of (2.45) to the RHS of (2.49), and substituting for $[HCO_3^-]$ and $[HPO_4^{2-}]$, we have an expression for the diffusion of soil base in terms of the working variables, $[H_2PO_4^-]_L$, $[H^+]_L$ and $[Ca^{2+}]_L$,

$$\frac{b_{HS}}{2.3}\left(\frac{1}{[H^+]_L}\frac{\partial[H^+]_L}{\partial t} - \frac{1}{2[Ca^{2+}]_L}\frac{\partial[Ca^{2+}]_L}{\partial t}\right) = \qquad (2.410)$$

$$\theta f \frac{\partial}{\partial x}\left(D_{LH}\frac{\partial[H^+]_L}{\partial x} - D_{LP}K_2\frac{\partial[H_2PO_4^-]_L/[H^+]_L}{\partial x} - D_{LC}K^*\frac{\partial 1/[H^+]_L}{\partial x}\right)$$

where $K^* = K_d K_s P_{CO_2}$.

As with phosphate, there is a kinetic component to the reaction of acids and bases with soils. Experimentally this was found to be insignificant for the present soil over the time of interest (section 3.2), in agreement with Ameloko (1983). It is therefore reasonable to assume that the reaction is complete instantaneously.

c) Calcium

Having obtained the concentration profiles of phosphate and soil base, the calcium profile can be calculated by balancing its concentration in any incremental soil volume against the concentrations of the other ions in accord with the requirement of electroneutrality. The positive charge in any part of the soil must be balanced by the negative charge. Thus for

cations M^{z+} and anions A^{z-},

$$\Sigma(z_i[M_i^{z+}]) + \Sigma(z_i[A_i^{z-}]) = 0$$

In the present system, the major species in the liquid phase are Ca^{2+}, H_3O^+, $CaH_2PO_4^+$, $H_2PO_4^-$, HPO_4^{2-}, HCO_3^- and Cl^- (NO_3^- resulting from the mineralisation of soil organic N may be significant in biologically active systems and could be allowed for; in the present system biological activity has been inhibited - see section 3.5). Hence

$$[Ca^{2+}]_L = 1/2([H_2PO_4^-]_L+2[HPO_4^{2-}]_L+[HCO_3^-]_L + [Cl^-]_L-[H^+]_L-[CaH_2PO_4^+]_L) \quad (2.411)$$

Chloride is very mobile in soils because it is non-adsorbed and its ions might be expected to diffuse in response to the electric potential gradient set up by the diffusion of the other ions. But in practice its movement is negligible in this system because its solution concentration is much smaller than the concentrations of the other ions. Thus in considering changes with time in the concentration of the ions at a given position in the soil, $\Delta[Cl^-] = 0$, and

$$\Delta[Ca^{2+}]_L = 1/2(\Delta[H_2PO_4^-]_L+2\Delta[HPO_4^{2-}]_L+\Delta[HCO_3^-]_L - \Delta[H^+]_L-\Delta[CaH_2PO_4^+]_L) \quad (2.412)$$

Over a time interval, $\Delta[H_2PO_4^-]_L$ and $\Delta[H^+]_L$ are given by the solutions of equations (2.43) and (2.410), and $[CaH_2PO_4^+]_L$, $[HPO_4^{2-}]_L$ and $[HCO_3^-]_L$ can be expressed in terms of $[H_2PO_4^-]_L$, $[H^+]_L$ and $[Ca^{2+}]_L$ using equations (2.33), (2.32) and (2.46).

In the solid phase, changes in $[Ca^{2+}]$ must balance the changes in the concentrations of the other sorbed ions. Implicit in the treatment of the propagation of soil base is the assumption that sorption of $H_2PO_4^-$ occurs without exchange of titratable acid or base. This is in accord with experimental work in which no pH change was found with phosphate sorption (section 3.1). Since there is no exchange of acid or base, $H_2PO_4^-$ sorption must be accompanied by sorption of an equivalent amount of Ca^{2+} to maintain the charge balance. Changes in the concentration of acid ions on the solid, expressed by $\Delta[HS]-\theta\Delta[H^+]_L$, are also balanced by sorption of an equivalent amount of Ca^{2+}. Thus, summing over all the significant changes affecting the solid,

$$\Delta[Ca^{2+}]_S = 1/2[\Delta[H_2PO_4^-]_S-(\Delta[HS]-\theta\Delta[H^+]_L)] \qquad (2.413)$$

Diffusion coefficients in free solution

Values for the diffusion coefficients in free solution at 20°C were calculated using the Nernst-Einstein relation (Robinson and Stokes, 1968):

$$D_{Li} = RT\ \mu_i/(z_iF)^2 \qquad (2.414)$$

where μ_i is the molar ionic conductivity (Ω^{-1} dm^2 mol^{-1}) and F is the Faraday.

Table 2.1

Calculated diffusion coefficients in free solution at 20°C.

ion	D_L, dm^2 s^{-1}
H^+	8.40×10^{-7}
$H_2PO_4^-$	8.90×10^{-8}
HCO_3^-	1.08×10^{-7}
Cl^-	2.00×10^{-7}
Ca^{2+}	1.55×10^{-7}

[The values for Ca^{2+} and Cl^- are required in the section following]

The effect of diffusion potentials

Diffusing ions are electrically coupled so that an electric potential exists between them. The effect of these "diffusion potentials" is to slow down the more mobile ions and to accelerate the slower ones, thus D_L values should be adjusted accordingly, as the program runs. Nye (1966) has considered such mixed ion systms: from his equation (10)

$$D_{LA}^{*} = D_{LA} + \frac{z_A D_{LA} C_{LA}}{dC_{LA}/dx} \frac{\Sigma z_i D_{Li} dC_{Li}/dx}{\Sigma z_i^2 D_{Li} C_{Li}} \qquad (2.415)$$

where D_{LA}^{*} is the modified diffusion coefficient for ion A and subscript i refers to all co- and counter-ions. Notice that z_i and dC_i/dx may be positive or negative.

The effect of the diffusion potential on the diffusion coefficients is not great and does not justify the increased CPU time that results from its incorporation, thus it was omitted from the final program. The reason for the lack of an effect is that the most concentrated ions (calcium and phosphate) have similar mobilities, and the most mobile ion (hydrogen) has a relatively low concentration.

The effect of ionic strength

The ionic strength of the soil solution near the dissolving mineral will be appreciable, so to calculate solute concentrations, the thermodynamic equilibrium constants (which refer to ionic activities) must be adjusted for the differences in individual ionic activity coefficients. The Davies (1962) equation gives the activity coefficients of individual ions, λ_i in terms of the ionic strength, I and a coefficient, A, for electrostatic and

geometric factors,

$$\log \lambda_i = -Az_i^2\left(\frac{I^{1/2}}{1+I^{1/2}}-.3I\right) \qquad (2.416)$$

A=0.524 for water at 293K.

The effect of the ionic strength on the equilibrium constants is significant. The ionic strength of the interface solution is about 0.02 mol dm^{-3} giving activity coefficients of 0.87 for the monovalent ions and 0.57 for the divalent ones.

2.5 The Boundary Conditions for the Solutions of the Continuity Equations

The Interface Boundary

The problem is to find the steady state concentrations of the ions at the interface, subject to the boundary conditions (a) the fluxes of calcium, phosphate and base out of the boundary are equal, and (b) the concentrations of the component ions are in accord with the solubility product relationship (equations (2.31) and (2.32)).

Because the concentrations cannot be calculated until the fluxes are known, and vice versa, an iterative procedure is required whereby the values are successively adjusted until concordance is achieved. As explained above, the concentration of calcium is calculated from the concentrations of the other components, so that, if the fluxes of phosphate and base are equal, the fluxes of all three components must be equal. In the routine outlined below, changes in the fluxes of phosphate and base over a time interval, found from the solutions of equations (2.46) and (2.410), are expressed in terms of the corresponding changes in

$[H^+]_L$ (and hence C_L from the solubility product relationship) by considering the mass balances of phosphate and base in a thin slice of soil at the interface. Starting with an arbitrary concentration of, say, H^+_L, if this concentration is too high, the corresponding flux of H^+ will also be too high and so the concentration calculated for the end of the time interval will be too low. Thus in the next time interval, a lower value will be calculated for the flux and a corresponding higher value for the concentration. The calculation will converge as it is iterated if the slice thickness is not too small (see below), until the fluxes are equal.

Consider a thin slice of soil, Δx, in steady state with the mineral surface (fig. 2.3):

The change in the total amount of phosphate in the slice over a time interval is equal to the difference between the amount entering the slice from the mineral and the amount leaving it into the soil. Thus, over a time interval, Δt

$$(b_p+\theta)(C_L^t-C_L)\Delta x = M-F_p\Delta t \qquad (2.51)$$

where b_p is the phosphate buffer power, dC_S/dC_L (equation (2.42)), M the amount of DCPD dissolved per unit area, and superscript t refers to the end of the time interval.

The change in the concentration of soil base in the slice over the time interval is given by the lime potential buffer capacity (equation (2.10)). Thus

$$-\Delta[HS] = \frac{b_{HS}}{2.3}\left(\frac{\Delta[Ca^{2+}]_L}{2[Ca^{2+}]_L} - \frac{\Delta[H^+]_L}{[H^+]_L}\right)$$

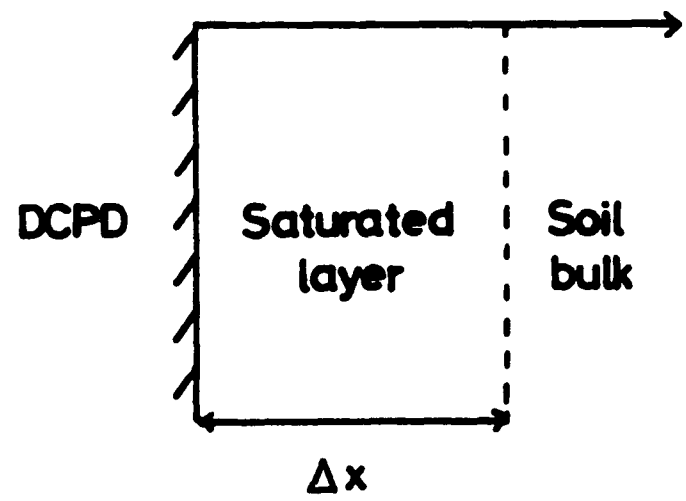


Fig. 2.3. The soil/mineral interface.

by analogy with equation (2.51),

$$\left\{\frac{b_{HS}}{4.6[\bar{Ca}^{2+}]_L}([Ca^{2+}]_L^t-[Ca^{2+}]_L)-\frac{b_{HS}}{2.3[\bar{H}^+]_L}([H^+]_L^t-[H^+]_L)\right\}\Delta x \qquad (2.52)$$

$$= M-F_B\Delta t$$

where $[\bar{H}^+]_L$ and $[\bar{Ca}^{2+}]_L$ are the average values over the time interval.

The C_L variables in (2.51) can be expressed in terms of the $[H^+]_L$ variables using the solubility product relationship

$$C_L^t-C_L = K_{SP}/(K_2[\bar{Ca}^{2+}]_L)([H^+]_L^t-[H^+]_L)$$

Thus the C_L variables can be eliminated from (2.51), and by subtracting (2.52) from the resultant expression, we obtain

$$\left\{(b_P+\theta)\frac{K_{SP}}{K_2[\bar{Ca}^{2+}]_L}+\frac{b_{HS}}{2.3[\bar{H}^+]_L}\right\}([H^+]_L-[H^+]_L)\Delta x \qquad (2.53)$$

$$-\frac{b_{HS}}{4.6[\bar{Ca}^{2+}]_L}([Ca^{2+}]_L^t-[Ca^{2+}]_L)\Delta x = (F_B-F_P)\Delta t$$

Hence

$$[H^+]_L^t = [H^+]_L+\left\{(F_B-F_P)\Delta t+\frac{b_{HS}}{4.6[\bar{Ca}^{2+}]_L}([Ca^{2+}]_L-[Ca^{2+}]_L^t)\Delta x\right\}/\Psi\Delta x \qquad (2.54)$$

where Ψ is the term in curly brackets in (2.53).

We thus have an expression for the change in $[H^+]_L$ over a time step, in terms of the fluxes of phosphate and base out of the slice, and the change in $[Ca^{2+}]_L$.

The flux of phosphate is given by

$$F_P = -D_{LP}\theta f \, \partial[H_2PO_4^-]_L/\partial x$$

and the flux of soil base by

$$F_B = \theta f\left(D_{LH}\frac{\partial[H^+]_L}{\partial x} - D_{LP}\frac{\partial[HPO_4^{2-}]_L}{\partial x} - D_{LC}\frac{\partial[HCO_3^-]_L}{\partial x}\right)$$

Thus for an arbitrary starting value of $[H^+]_L$, a corresponding set of concentration profiles can be calculated to find F_B and F_P (see section 2.6), $[Ca^{2+}]_L^t$ can be calculated iteratively using equation (2.412), and hence $[H^+]_L^t$ can be found. The value of $[H^+]_L^t$ should quickly adjust as the calculation is iterated until $F_B=F_P$. Since the starting value of $[H^+]_L$ is arbitrary, so is Δx which can therefore be chosen so as to damp oscillations in the calculation. A small value will produce violent changes in $[H^+]_L$ because the amount of H^+ in the slice will be of the same order of magnitude as the change in the amount over the time interval. Thus the program may crash. On the other hand, a large value will result in slow adjustment and, in any case, be physically unrealistic. In practice a value of $\Delta x=10^{-4}$ dm was found convenient. During a run, the value of $[H^+]_L$ settled after about 20 time steps (ie less than 1 hour). Thereafter it changed very slowly in sympathy with the changing fluxes of phosphate and base.

The Initial Conditions and the Condition at x=X

Formally, the conditions imposed by experimental design may be written

for eqn. (2.43)	$C_L=C_L'$	$0<x\leqslant X$	$t=0$
	$dC_L/dx=0$	$x=X$	$t>0$
for eqn. (2.410)	$[H^+]_L=[H^+]_L'$	$0<x\leqslant X$	$t=0$
	$d[H^+]_L/dx=0$	$x=X$	$t>0$

where superscript ' refers to concentrations in the native soil.

2.6 The Numerical Solutions of the Continuity Equations

Equations (2.43) and (2.410) were expressed in finite-difference form using the Crank-Nicolson implicit method (Smith, 1965), and solved using the algorithm described by Richtmyer (1957, chapter 6, section 5). This procedure involves converting the set of finite-difference equations for each continuity equation, to the form

$$-W_j S^t_{j+1} + X_j S^t_j - Y_j S^t_{j-1} = Z_j \qquad (2.61)$$

where j denotes a distance step (j=1 is the DCPD surface) and t a time step. Z_j is known being a function of the current S values, and coefficients W_j, X_j and Y_j are either constants or are functions of the solute concentration, S.

The set of equations (2.61) are then solved inductively using the relation

$$S^t_j = E_j S^t_{j+1} + F_j \qquad (2.62)$$

where
$$E_j = W_j/(X_j - Y_j E_{j-1}) \qquad (2.63)$$

and
$$F_j = (Z_j + Y_j F_{j-1})/(X_j - Y_j E_{j-1}) \qquad (2.64)$$

starting from $S_{j=1}$ which is known from the interface boundary conditions. The procedure is presented below in detail for phosphate, to demonstrate the principles, and in outline for soil base. Subscript L has been omitted for clarity, and $[H^+]_L$, $[Ca^{2+}]_L$, $[HPO_4^{2-}]_L$ and $[HCO_3^-]_L$ are written H, Ca, P2, and HC respectively.

a) Phosphate

The Crank-Nicolson form of equation (2.43) is

$$C_j^t - C_j = \frac{D_L \theta f \Delta t}{\theta + abC_j^{b-1} 2\Delta x^2}(C_{j+1}^t + C_{j+1} - 2C_j^t - 2C_j + C_{j-1}^t + C_{j-1}) \qquad (2.65)$$

Let $\alpha = D_L \theta f \Delta t / (\theta + abC_L^{b-1} 2\Delta x^2)$

Now (2.65) may be written

$$-\alpha C_{j+1}^t + (1+2\alpha)C_j^t - \alpha C_{j-1}^t = \alpha C_{j+1} + (1-2\alpha)C_j + \alpha C_{j-1}$$

If $W_{Pj} = \alpha$, $X_{Pj} = (1-2\alpha)$ and $Y_{Pj} = \alpha$, then

$$-W_{Pj} C_{j+1}^t + X_{Pj} C_j^t - Y_{Pj} C_{j-1}^t = W_{Pj} C_{j+1} + (2-X_{Pj})C_j + Y_{Pj} C_{j-1} = Z_{Pj} \qquad (2.66)$$

(cf. equation (2.61))

The boundary conditions

(i) The x=X boundary condition is that there be no transfer of material across the boundary (ie. out of the soil block). Thus

$$\partial C / \partial x = 0 = C_{N+1} - C_{N-1}$$

ie.
$$C_{N+1} = C_{N-1}$$

Substituting in (2.66) and rearranging

$$C_N^t = \frac{(W_{PN} + Y_{PN})C_{N+1}^t}{X_{PN}} + \frac{Z_{PN}}{X_{PN}} \qquad (2.67)$$

By reference to (2.62) it is apparent that

$$E_{PN} = (W_{PN}+Y_{PN})/X_{PN} \tag{2.68}$$

and

$$F_{PN} = Z_{PN}/X_{PN} \tag{2.69}$$

(ii) The surface (x=0) concentration is calculated from the balanced fluxes of phosphate and base and the solubility product relationship, as described in section 2.5.

From (2.63) and (2.64),

$$E_{Pj} = (X_{Pj+1}-W_{Pj+1}/E_{Pj+1})/Y_{Pj+1} \tag{2.610}$$

and

$$F_{Pj} = \{F_{Pj+1}(X_{Pj+1}-Y_{Pj+1}E_{Pj+1})-Z_{Pj+1}\}/Y_{Pj+1} \tag{2.611}$$

and from (2.62)

$$C^t_{j+1} = (C_j-F_{Pj})/E_{Pj} \tag{2.612}$$

Thus by evaluating E_{PN} and F_{PN} from (2.68) and (2.69), E_{Pj} and F_{Pj} can be found for j=(N-1 to 1), and hence C^t_j can be found for j=(2 to N).

b) Soil base

Differencing the RHS of equation (2.45) gives

$$\frac{\partial[HS]}{\partial t} = \frac{\theta f}{2\Delta x^2}\,[D_{LH}(H^t_{j+1}+H_{j+1}-2H^t_j-2H_j+H^t_{j-1}+H_{j-1}) \qquad (2.613)$$

$$-D_{LP}(P2^t_{j+1}+P2_{j+1}-2P2^t_j-2P2_j+P2^t_{j-1}+P2_{j-1})$$

$$-D_{LC}(HC^t_{j+1}+HC_{j+1}-2HC^t_j-2HC_j+HC^t_{j-1}+HC_{j-1})]$$

$[HPO_4^{2-}]_L$ and $[HCO_3^-]_L$ are functions of $[H^+]_L$, but they are best evaluated separately to avoid generating terms in $1/[H^+]_L$.

If $[Ca^{2+}]_L = 1/2([H_2PO_4^-]_L+[Cl^-]_L-[H^+]_L)$, then

$$\frac{\partial[Ca^{2+}]_L}{\partial t} = \frac{(C^t_j-C_j)-(H^t_j-H_j)}{2\Delta t}$$

Thus in (2.49),

$$\frac{\partial[HS]}{\partial t} = \frac{b_{HS}}{2.3\Delta t}\left[\frac{H^t_j-H_j}{\bar{H}_j} - \frac{(C^t_j-C_j)-(H^t_j-H_j)}{4\bar{Ca}_j}\right]$$

where $\bar{H}_j$ and $\bar{Ca}_j$ are the average values over Δt. Thus,

$$\frac{\partial[HS]}{\partial t} = \frac{b_{HS}}{2.3\Delta t}\left[(H^t_j-H_j)(1/\bar{H}_j+1/4\bar{Ca}_j)-\frac{C^t_j-C_j}{4\bar{Ca}_j}\right] \qquad (2.614)$$

Equating the RHS of (2.613) to the RHS of (2.614) and rearranging gives

$$-\beta H^t_{j+1}+(2\beta+1/H_j+1/4Ca_j)H^t_j-\beta H^t_{j-1} = \tag{2.615}$$

$$\beta H_{j+1}+(1/H_j+1/4Ca_j-2\beta)H_j+\beta H_{j-1} + (C^t_j-C_j)/4Ca_j$$

$$- \beta/D_{LH}[D_{LP}(P2^t_{j+1}+P2_{j+1}-2P2^t_j-2P2_j+P2^t_{j-1}+P2_{j-1})$$

$$+ D_{LC}(HC^t_{j+1}+HC_{j+1}-2HC^t_j-2HC_j+HC^t_{j-1}+HC_{j-1})]$$

where $\beta=2.3D_{LH}\theta f\Delta t/(2b_{HS}\Delta x^2)$.

Now by writing $W_{Bj}=\beta$, $X_{Bj}=(2\beta+1/H_j+1/4Ca_j)$ and $Y_{Bj}=\beta$, equation (2.615) may be solved in the same way as (2.66).

2.7 The Method of Programing

The program was written in FORTRAN. It is reproduced in appendix A.

In the course of a time step, the phosphate profile is worked out first and from it the calcium profile using equation (2.412) and assuming, as a first approximation, $[H^+]_L{}^t=[H^+]_L$. The soil base profile is then found from the set of values obtained for C_L and $[Ca^{2+}]_L$. If necessary, the calculation of the $[Ca^{2+}]_L{}^t$ and $[H^+]_L{}^t$ profiles can be repeated until concordance is achieved. The left hand boundary concentrations are adjusted at the begining of each time step, to ensure the fluxes of calcium, phosphate and base are equal.

The effect of ionic strength is incorporated by evaluating at each distance step the term, $.524(I^{1/2}/(1+I^{1/2})-.3I)$ in (2.414), which is common to the activity coefficients of all ions. The term is then used to modify the thermodynamic equilibrium constants, as appropriate. Since the activity coefficients and concentrations are interdependent, the calculation must be performed iteratively until the calculated values agree. Thus the activity coefficients are estimated for assumed values of the appropriate concentrations, the corresponding concentrations are then calculated and the process repeated using these concentrations until concordance is achieved. In practice, iteration is only necessary during the initial stages of profile development when the high concentrations near the interface are changing most rapidly. The values accord after one or two iterations.

The total quantity of DCPD dissolved after a particular time, M_t, is calculated by keeping a tally of the flux of phosphate across the interface boundary. Thus

$$M_t = \sum_0^t (A\ F_p\ \Delta t)$$

where A is the cross sectional area of the soil block and Δt the duration of a time step.

Distance steps of $5x10^{-4}$ dm and time steps of 100 s were found to be convenient. Halving these values made no difference to the results, showing that the finite-differencing is satisfactory. Once the initial profiles were developed, it was possible to gradually increase the time steps during a run, thereby saving CPU time, without affecting the results.

Absolute tests of the accuracy of the numerical solutions of partial differential equations are generally not possible. However, by setting the Freundlich b parameter equal to one, and making the interface phosphate concentration constant, the output could be compared with an analytical solution of equation (2.43):

$$C_{Lj} = C_L' + (C_{LS}-C_L')\mathrm{erf}[x_j/2(D_{eff}t)^{1/2}]$$

where $D_{eff}=D_{LP}\theta f/(\theta+a)$ (after Crank, 1975, equation 3.13).
The results of the numerical and analytical solutions agreed to within 0.1%. It was not possible to make an equivalent check on the solution of equation (2.410) but the total amounts of calcium, phosphate and base dissolved, calculated from the output using Simpson's rule, were equal showing that the solution of equation (2.410) is also correct.

The experimental parameters required by the model are ρ, θ, f, the Freundlich parameters, and b_{HS}.

The Predicted Concentration Profiles

Fig. 2.4 shows the predicted pH and total calcium and phosphate profiles after 96 hours of dissolution, and fig. 2.5 shows the phosphate profiles for other times. The area under the concentration curves indicates the amount of material dissolved; thus the total amounts of calcium and phosphate dissolved are equal. By multiplying the change in lime potential Δ(pH-1/2pCa) by b_{HS}, a similar mass balance could be obtained for base. The amount of DCPD dissolved varies approximately as the square root of time.

The shape of the phosphate profile is due to the logarithmic sorption relationship, which results in a high mobility near the DCPD surface, where the proportion of phosphate in the soil solution is high, and a corresponding low mobility near to the advancing solute front. Thus the profile has a stunted appearance. By contrast, the pH profile is steep near the DCPD surface because the concentrations of H_3O^+ and the other proton carrying species, are low and hence the rate of propagation of the pH rise away from the DCPD is low. The pH profile is correspondingly shallow far from the interface, where the concentration of H_3O^+ is relatively high.

Fig. 2.6 shows the profiles of the proton carrying ions near the interface. The gradient at a given position in the profile, together with its mobility, indicates the flux and hence importance of the ion at that point. Very close to the interface, the HPO_4^{2-}-$H_2PO_4^-$ pair is dominant, although the contributions of the other pairs is significant. Further away, H_2O-H_3O^+ is the only important pair. Thus, very close to the interface, the base HPO_4^{2-} moves into the soil, but only a few tenths of a millimeter away it is neutralised by H^+ moving up to the surface from the bulk soil.

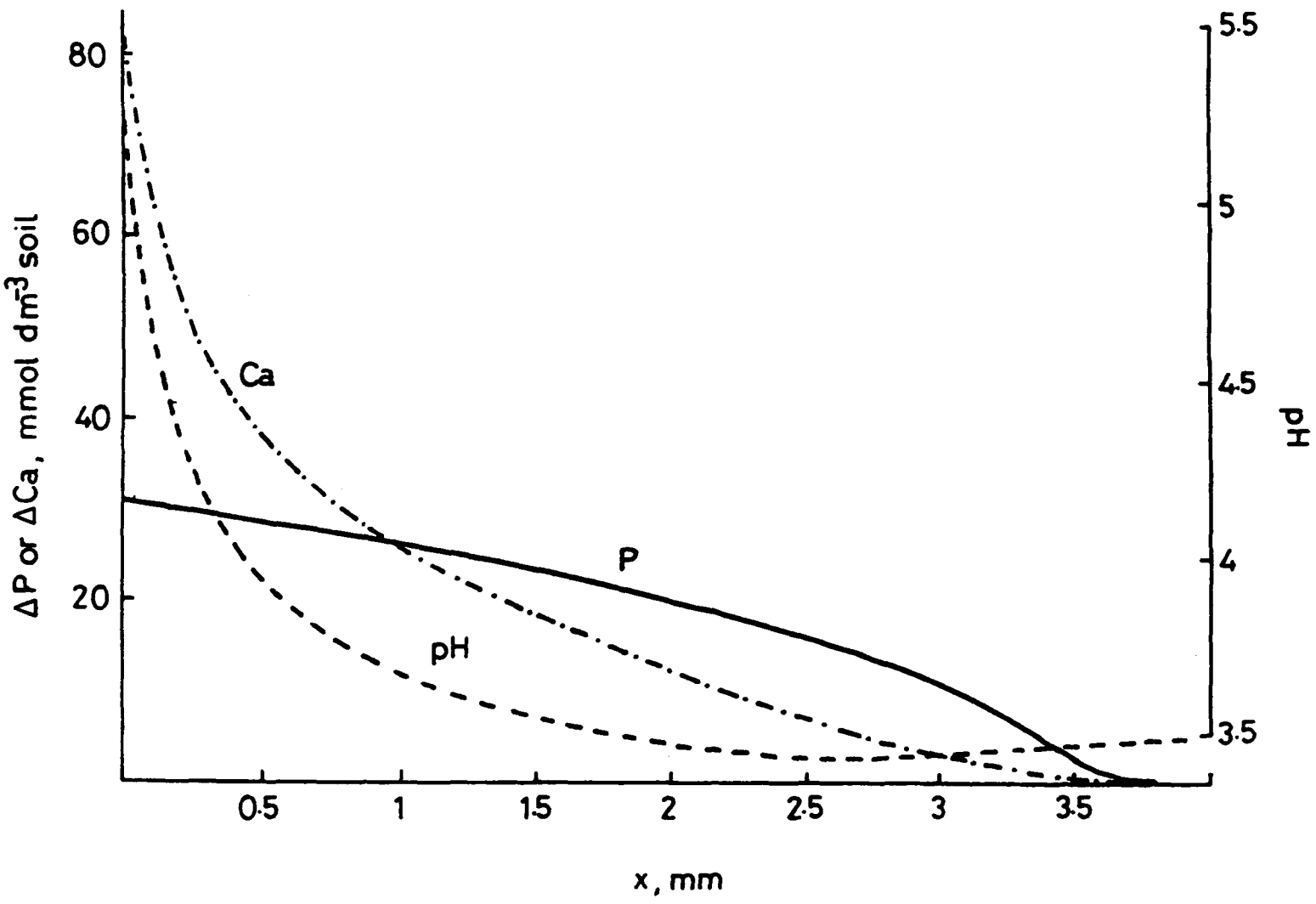


Fig. 2.4. Profiles of pH and changes in total concentrations of phosphate and calcium after 96h. θf=.05, a=.2, b=.3, b_{HS}=.1, native soil pH=3.5.

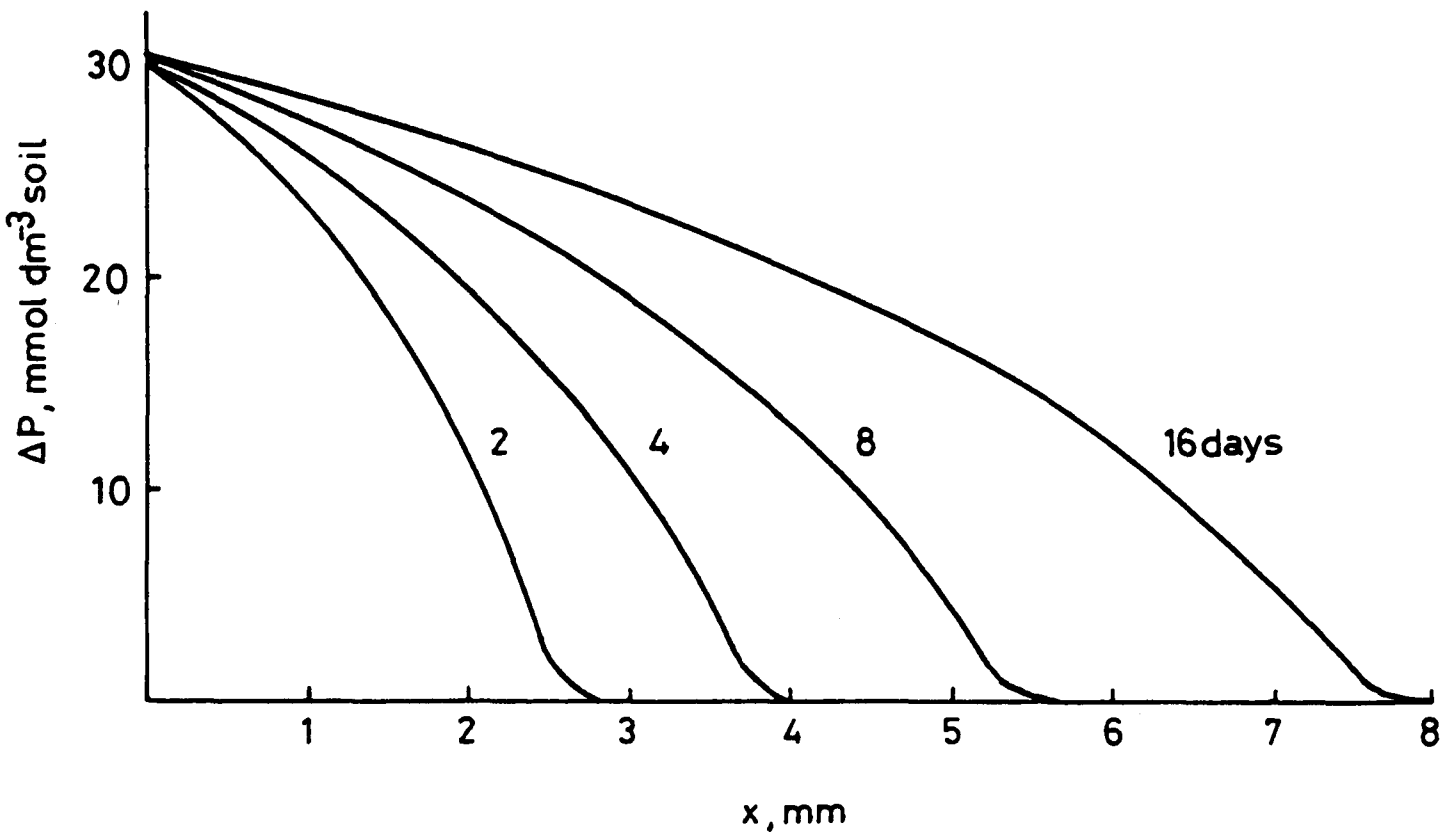


Fig. 2.5. Profiles of changes in total phosphate concentration at different times. Values of soil variables as in Fig. 2.4.

The profiles of the major ions in solution after 96 hours are shown in fig. 2.7. The chloride concentration (which has been assumed to be constant) is included to demonstrate the balance of cationic and anionic charges.

2.8 Discussion

The accuracy of the model depends critically on the precise calculation of the pH and calcium and phosphate concentrations at the interface. Any error in the calculation of one of these will be amplified by its effect on the others. The importance of taking into account the release of base and consequent pH rise at the interface in calculating the interface phosphate concentration, can be seen by considering the concentration that would be obtained using the pH of the native soil:

For every mol of DCPD dissolved, 1 mol of calcium and 1 mol of phosphate are released. Thus, if $[Ca^{2+}]_L'$ is the initial value,

$$[Ca^{2+}]_L = [Ca^{2+}]_L' + [H_2PO_4^-]_L + [HPO_4^{2-}]_L \quad (2.81)$$

From the solubility product relationship,

$$K_{SP} = [Ca^{2+}]_L[HPO_4^{2-}]_L = [Ca^{2+}]_L K_2[H_2PO_4^-]_L/[H^+]_L$$

where K_{SP} and K_2 are corrected values incorporating the appropriate activity coefficients.

Substituting for $[Ca^{2+}]_L$ from equation (2.81) gives a quadratic in $[H_2PO_4^-]_L$. The value thus calculated for $[H_2PO_4^-]_L$ was 9.0×10^{-2} mol dm^{-3} which is almost ten times the value obtained by taking account of the pH rise. Using this value in the solution of

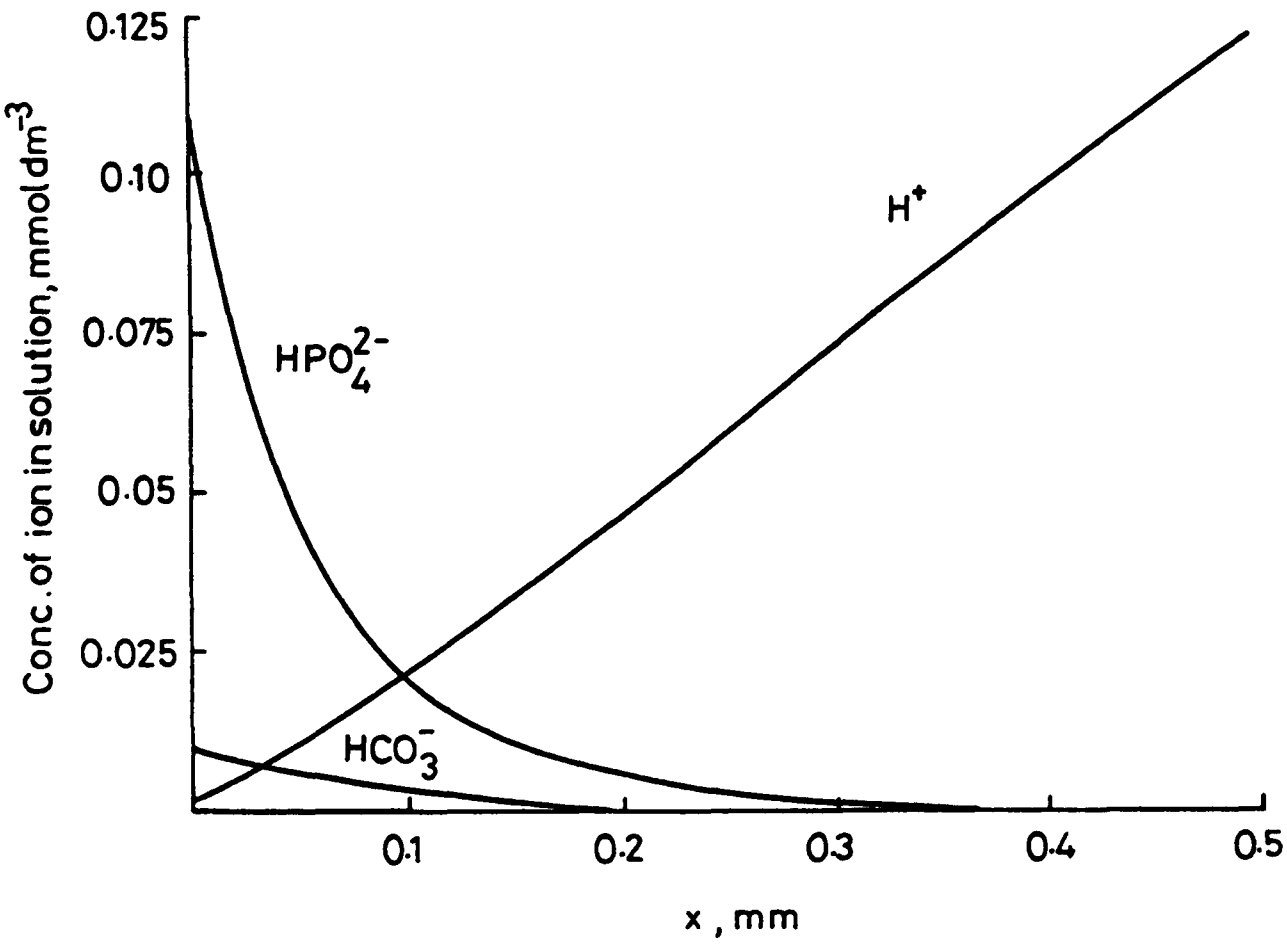


Fig. 2.6. Concentration profiles of important acids and bases in solution after 96h. Values of soil variables as in Fig. 2.4.

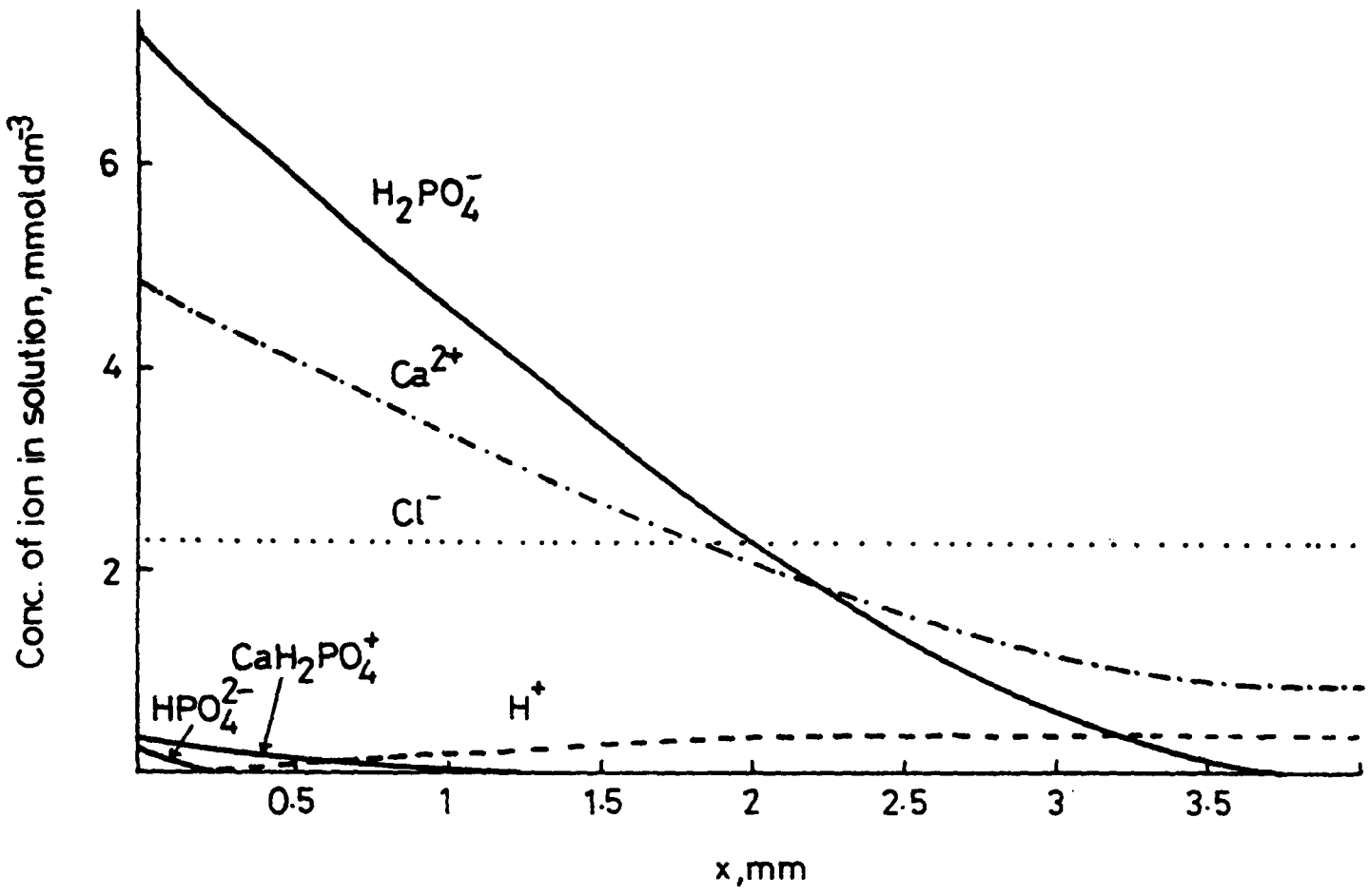


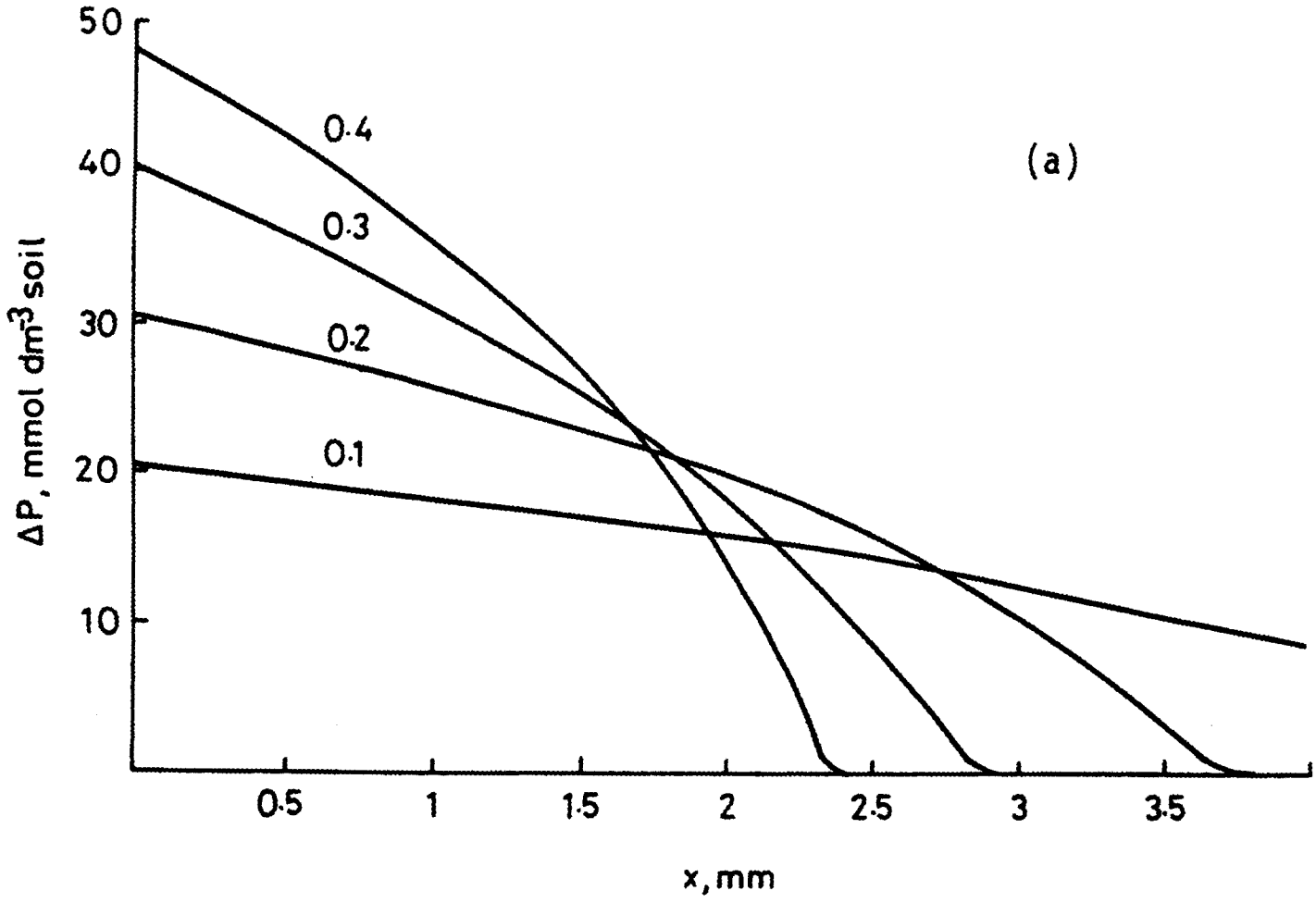
Fig. 2.7. Concentration profiles of major ions in solution after 96h. Values of soil variables as in Fig. 2.4.

equation (2.43), the amount of DCPD dissolved in 96 hours was calculated to be 2.42 mmol, which, compared with 0.37 mmol obtained with the model proper, is an unreasonably large overestimate.

The main parameters on which the calculation of the interface concentrations rely are the phosphate sorption coefficients and b_{HS}. The effect of changes in these parameters on the phosphate profile is shown in figs. 2.8 and 2.9. Since the Freundlich and lime potential buffer equations are logarithmic and we are interested in high phosphate concentrations and low pHs (high H ion concentration in the soil), the model is relatively sensitive to these parameters. The Freundlich parameters determine the effective phosphate diffusion coefficient and hence the spread of phosphate. b_{HS} influences the concentration of phosphate in solution at the interface: a high value results in a small pH rise at the interface and consequently a high concentration of phosphate. A six-fold increase in b_{HS} leads to twice as much phosphate dissolving.

The buffering by the soil of the base released at the interface was accounted for in the model using Nye's (1972) theory of the propagation of pH changes. Previously this theory has not been applied to situations in which the pH and calcium concentration are changing simultaneously. In the present case, however, there is a five-fold change in the calcium concentration between the mineral and the soil bulk, so the calcium gradient cannot be ignored. Calcium ions will exchange with acid ions on the soil solid, so the effect of the calcium gradient is that the pH near the interface is lower than it would be at constant $[Ca^{2+}]$, and hence the rate of dissolution is higher.

Fig. 2.10 shows the effect of different soil pH's on the rate of dissolution. At pH's above neutral, other phases such as octacalcium



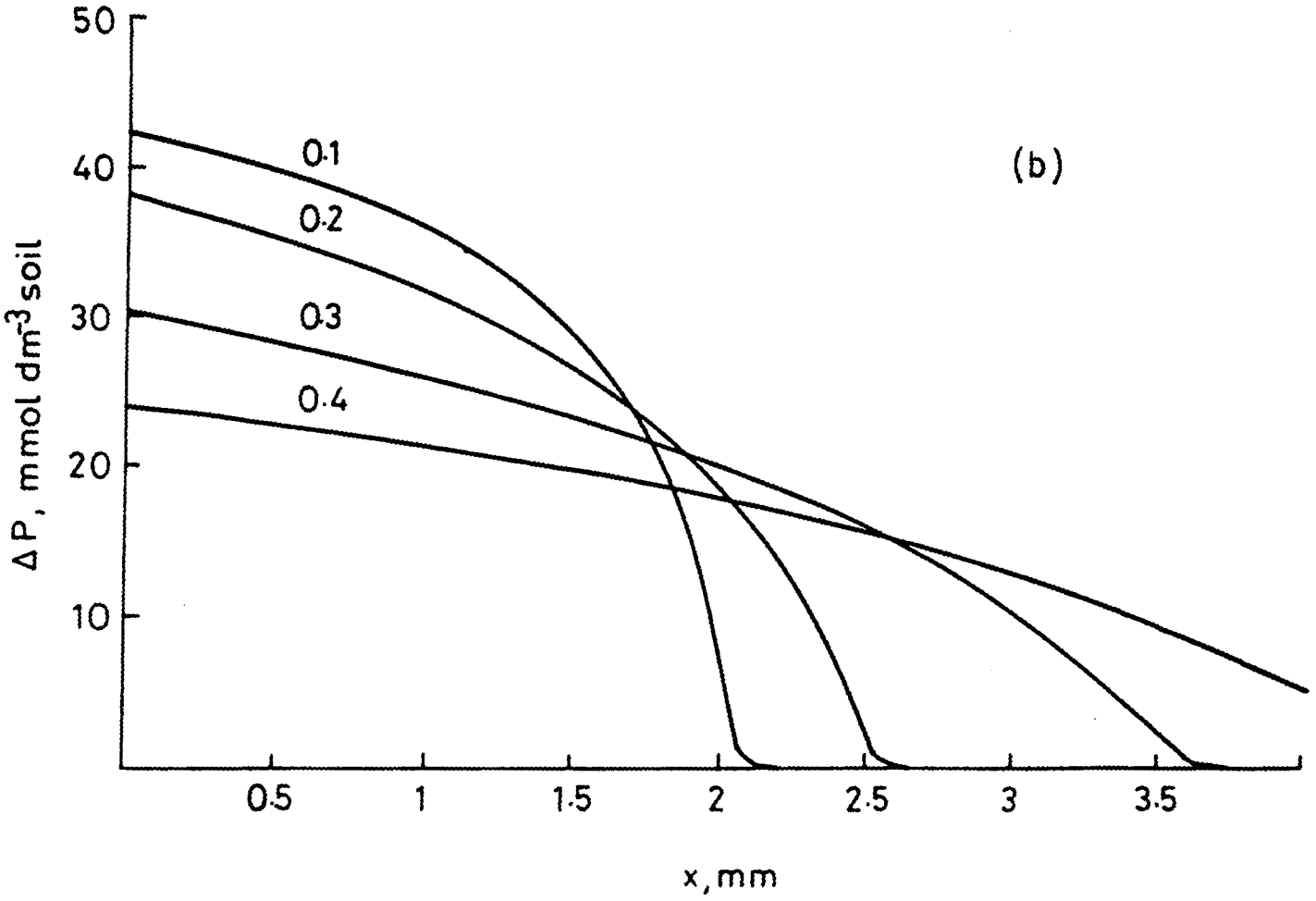


Fig. 2.8. (a) Effect of varying Freundlich a parameter. (b) Effect of varying Freundlich b parameter. Other soil variables and time as in Fig. 2.4.

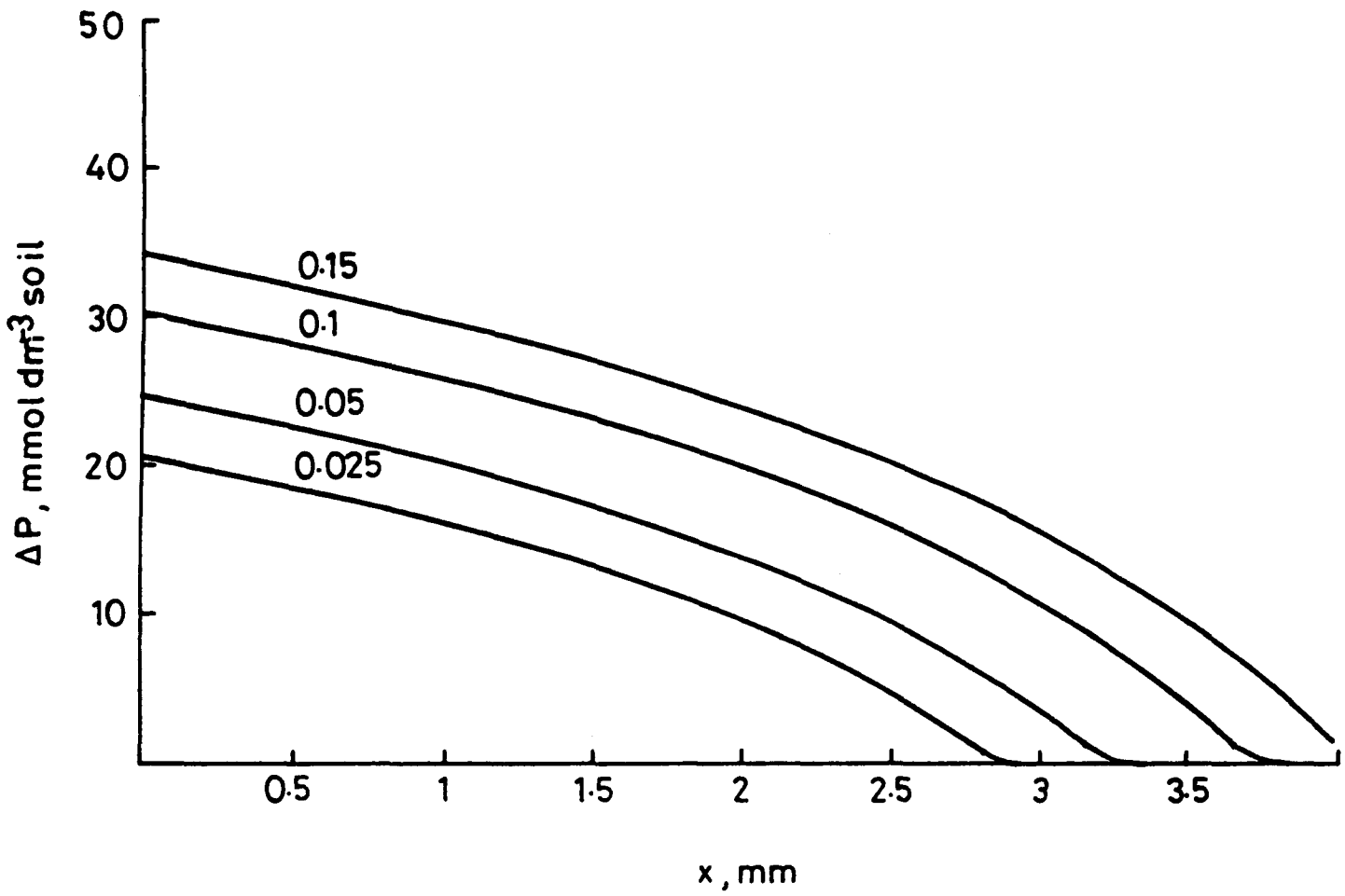


Fig. 2.9. Effect of varying b_{HS}. Other soil variables and time as in Fig. 2.4.

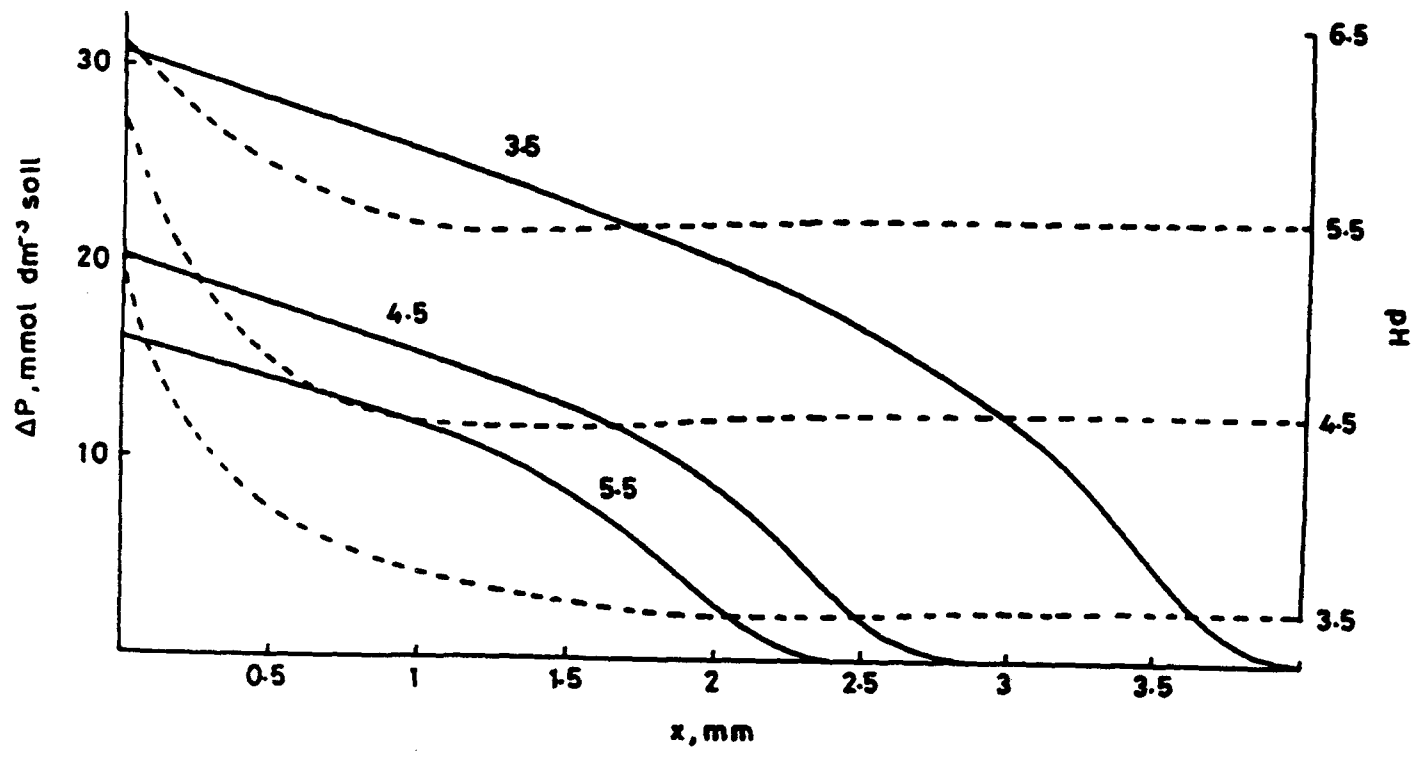


Fig. 2.10. Effect of varying the native soil pH: (——) ΔP, (---) pH. Numbers on ΔP curves are native soil pH's. Other variables and time as in Fig. 2.4.

phosphate may be precipitated, but in acid and slightly-acid soils, the dissolution reaction will be the same.

Any error in the value ascribed to K_{SP} will directly affect the calculation of the interface concentrations. Such errors may arise because of changes in the activity of the dissolving solid phase due to solid solution formation or the precipitation of less soluble phases on the mineral surface. To confirm the conclusion reached in section 2.2 that these processes are unimportant in the present system, the solubility of a sample of weathered DCPD (ie. the residue of undissolved material) was measured and found to be the same as that of the original material. The dissolution of less soluble phosphates, however, is likely to be complicated by these sorts of processes, and they would have to be allowed for in modelling the dissolution of such minerals.

I have aimed to introduce all likely complications to see what was important. The resultant model is somewhat complex although the problem superficially seemed simple. However, a simpler approach would have been inadequate, as has been seen.

3

EXPERIMENTAL ASSESSMENT OF THE PLANAR MODEL

This chapter is concerned with the experimental verification of the planar model. Because the predicted spread of dissolved material is only 2mm in 48 hours, an experimental method is required that is capable of measuring solute concentrations in very thin sections of soil. Experimental evaluation of the major assumptions of the model is also needed: in particular, the effect of phosphate sorption on soil pH, and the effect of changes in pH on sorption must be assessed. In the model, it has been assumed that these effects were negligible.

The Model Parameters

3.1 The Phosphate Sorption Reaction

The Effect of Sorption on Soil pH and Surface Charge

Phosphate "sorption" involves adsorption by fixed- and variable-charge soil constituents and precipitation with other ions in the soil solution. The effect of the net reaction on pH (as distinct from the effect of pH on sorption which is considered below) depends on what the dominant reaction mechanism is for a particular set of experimental conditions. Sorption may involve substitution of phosphate for hydroxyl ions on the soil, in which case the pH of the soil solution should tend to increase. Alternatively phosphate may displace water molecules from the soil so that there is no change in pH and the charge on the adsorbed phosphate ions is balanced by a change in the proportion of cations and anions at exchange sites (Mekaru and Uehara, 1972; Sawhney, 1974), or by specific adsorption of cations (eg. Ca^{2+} - Breeuwsma and Lyklema, 1973; Kinniburgh et al,

1975). If sorption results in a net change in surface charge, b_{HS} may be altered. Precipitation reactions, eg. with Al^{3+}, would not change the surface charge but could change the pH in either direction.

The Effect of pH on Sorption

There is a wealth of literature on this subject (eg. Murmann and Peech, 1969; Lopez-Hernandez and Burnham, 1974; White and Taylor, 1977; Sanchez and Uehara, 1980; Haynes, 1982; Barrow, 1984). A number of factors besides the nature of the soil determine how sorption is effected by pH; in particular, the pH range, the amount of phosphate already on the soil and the nature of the supporting electrolyte are important. In the present system, the pH and phosphate concentration are changing simultaneously and at different rates so we are concerned with the effect of an increase in pH on phosphate that is already sorbed, as well as the effect on phosphate that is arriving by diffusion and being sorbed at new sites. In so far as acid ions solubilise phosphate already on the solid, a reduction in the concentration of acid ions (ie. an increase in pH) should be expected to reduce the amount of phosphate that is re-equilibrating with the solution, and hence increase the amount retained by the solid. On the other hand, an increase in pH will tend to reduce the positivity of variable charge soil components, and hence reduce the amount of new phosphate sorbed by these components. Furthermore, in acid soils, sorption at the high concentrations of the present system is likely to involve precipitation of amorphous alumino-phosphates: thus the effect of pH on the hydrolysis and polymerisation of exchangeable aluminium would also be important.

Sorption Kinetics

There are two distinct rate processes in the sorption reaction: a rapid phase with a half life of less than two hours, and a slow phase which may

continue for several months resulting in a fractional increase in the amount of phosphate sorbed (Barrow and Shaw, 1975). Since the rapid phase is fast compared to the rate of diffusion, it is effectively instantaneous and its kinetics need not be considered. In measuring the rapid phase, a reaction time of 20h is sufficient to ensure equilibrium. If slow reaction occurs to a significant extent as the DCPD dissolves, then an additional term will be needed in equation (2.43). Evaluating this term would be difficult because the reaction rate at a particular point in the soil, at a particular time, depends on the varying phosphate concentration in the soil solution at that time, and hence on the history of the soil at that point; thus it is impossible to give a relation between the reaction rate and the solution concentration (Helfferich, 1962, Chapter 6).

Experimental Methods

The soil used for all the experimental work was an argillic brown sand from Bagley Wood near Oxford, air dried and sieved to <212 μm. Chemical analyses of the sieved fraction are given in Table 3.1. The analytical methods used were those of Nelson and Sommers (1982) (organic matter), Rhoades (1982) (CEC), and Thomas (1982) (exchangeable cations).

Table 3.1

Chemical analyses of Bagley Wood soil (<212 μm)

Total organic matter	9%
CEC (meq/100g)	12.05
Exchangeable cations (meq/100g)	
$Ca^{2+}+Mg^{2+}$	4.62
K^{+}	1.0
$Al^{3+}+H^{+}$	5.28
Soil solution cations (θ_g=0.3)(mmol dm^{-3})*	
Ca^{2+}	0.40
K^{+}	0.25
Al^{3+}	0.081
pH in 10^{-3} mol dm^{-3} $CaCl_2$	3.5

* Data of M.J. Hedley.

a) The 20h Sorption Isotherm

5g samples of air dry soil were weighed into 50 cm^3 polycarbonate centrifuge tubes and to each was added 25 cm^3 of 10^{-3} mol dm^{-3} $CaCl_2$ containing 50 mg dm^{-3} $HgCl_2$ to inhibit microbial activity, and graded amounts of NaH_2PO_4 to give initial concentrations 0.5, 1.0, 2.0, 3.0, 5.0, 10.0, 25.0, 50.0 and 100.0 mmol P dm^{-3}. A high soil:solution (1:5) ratio gives a greater change in solution concentration for a given amount of phosphate sorbed, and hence greater accuracy.

The tubes were shaken end over end at 20°C for 20h. The pHs of the suspensions were measured and found not to deviate by more than 0.05 units from the native soil pH in 10^{-3} mol dm^{-3} $CaCl_2$, and were therefore not adjusted.

The suspensions were then centrifuged at 3000 rpm for 5 minutes and filtered through Whatman No. 42 papers. 5 cm^3 aliquots were diluted and analysed for phosphate by the method of John (1970) (concentration range $1x10^{-5}$ to $5x10^{-8}$ mol P dm^{-3}). Some yellow colouration of the solutions was noticed, presumably due to dissolved organic matter. But when the coloured solutions were run as blanks, diluted appropriately, they gave no absorbance at the wavelength of the phosphate determination (712 nm).

b) The Effect of Sorption on Surface Charge

Three levels of phosphate were established by moistening 20 g samples of air dry soil to θ_g = 0.3 with 1, 10 and 100 mmol dm^{-3} solutions of NaH_2PO_4 in 10^{-3} mol dm^{-3} $CaCl_2$, and incubating for 4 days.

The CECs of the samples were then measured by a method based on that of Rhoades (1982) for acid soils. In this method, the exchange complex is first saturated with Ba^{2+} at the pH and ionic strength of the soil pore solution. The Ba^{2+} is then displaced with Mg^{2+} and the amount displaced estimated from the loss of Mg^{2+} from the displacing solution. For the purposes of the present study it is necessary to minimise desorption of phosphate from the soil, so the number of washings was kept to a minimum. The amount of phosphate on the soil was measured by shaking the residues of the CEC measurements in 1 mol dm^{-3} HCl, and analysing for phosphate.

c) The Effect of pH on Sorption

$15cm^3$ of 10^{-3} mol dm^{-3} $CaCl_2$ + 50mg dm^{-3} $HgCl_2$ were added to 5g samples of air dry soil in 50 cm^3 polycarbonate centrifuge tubes and shaken end-over-end for 1h. The suspension pHs were adjusted by dropwise addition of 0.1 mol dm^{-3} HCl and NaOH, allowing 10 minutes equilibration between each addition.

Four sets of suspensions were prepared in this way, with pH's 3.5, 4.0, 4.5, and 5.0. The soil:solution ratios of the suspensions were then adjusted to 1:4 by addition of 10^{-3}mol dm^{-3} $CaCl_2$, and the tubes shaken for a further 4h after which time no drift in pH was observed. NaH_2PO_4 solutions were then added in 5 cm^3 portions to give solution concentrations 5.0, 10.0, 20.0, 50.0, and 100 mmol P dm^{-3}. The tubes were shaken for 15h, the suspension pH's measured and the filtered solutions analysed for phosphate.

d) The Extent of Slow Reaction

2g samples of air dry soil were shaken end-over-end at 20°C with 10 cm^3 of 10^{-3} mol dm^{-3} $CaCl_2$ + 50 mg dm^{-3} $HgCl_2$ containing graded amounts of NaH_2PO_4 to give initial concentrations in the range 0 to 20 mmol P dm^{-3}. The concentrations of phosphate in solution were measured after shaking for 5, 10, 30, 100, and 200h.

Results and Discussion

A Freundlich isotherm fitted the 20h phosphate sorption data over the solution concentration range $5x10^{-5}$ to $5x10^{-2}$ mol dm^{-3} (fig. 3.1). The fitted equation was

$$P = 0.235C_L^{0.317}$$

where P is the amount of phosphate sorbed, mol kg^{-1} dry soil (r^2=0.997 for the log-log regression).

The difficulty in using a Freundlich isotherm to describe phosphate sorption by soils, is in accounting for the native soil phosphate that is taking part in the equilibration. This explains the poor fit in the low concentration range (<$5x10^{-5}$ mol dm^{-3} in solution) where this quantity is a significant part of the whole. But this is outside the range of interest to us (see fig. 2.7).

The fact that no pH change was observed with phosphate sorption is important: it indicates that there was no displacement of hydroxyl ions from the soil and thus the charge on the adsorbed phosphate ions must be balanced by sorption of an equivalent amount of cations. That is

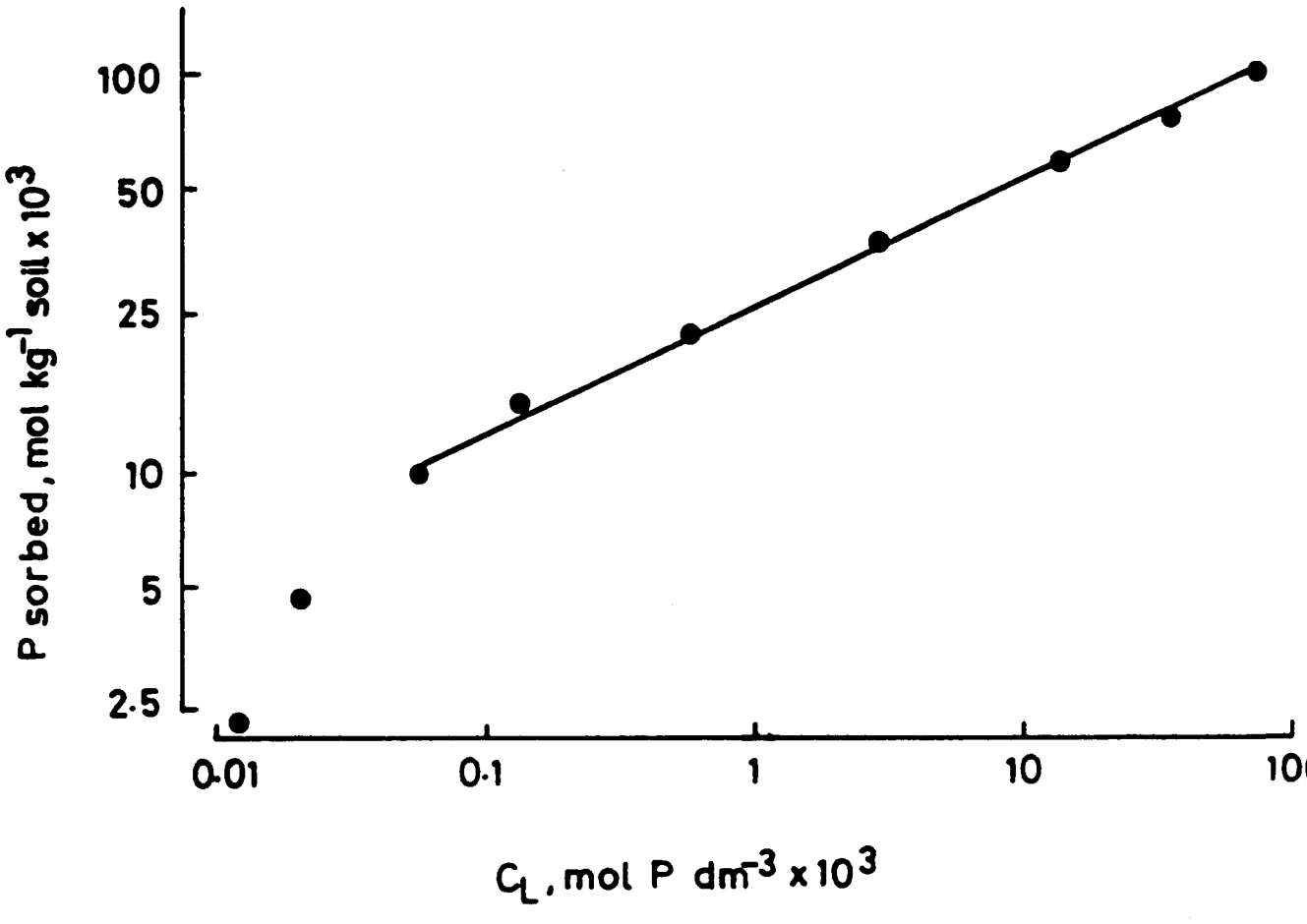


Fig. 3.1. The 20h phosphate sorption isotherm.

$$Soil + M^{+} + H_2PO_4^{-} \rightleftharpoons Soil\text{-}MH_2PO_4$$

This has two implications for the model. One is that the spread of base is not affected by the reaction of $H_2PO_4^-$ with the soil since sorption occurs without exchange of titratable acid or base. The other is that the amount of calcium (equivalent to $2M^+$ in the above equation) on the soil solid at a given position in the soil block, is given by the sum of the amount of phosphate sorbed and the amount of soil acid neutralised by the diffusion of base, the other process conveying charge to the soil surface. This statement requires no assumptions about the disposition of the calcium ions on the soil solid, but there appears to be no change in the cation exchange capacity of the surface (fig. 3.2). Thus b_{HS} is unaltered.

The results of the investigation of the effect of pH on sorption are shown in fig. 3.3. There is no definite trend but there is a tendency towards reduced sorption at higher pH's. This is in accordance with the precipitation of amorphous aluminium phosphates controlling the solution concentration. However, the effect is small at the high concentrations appropriate to the present system: soil base diffusion being slow at the pHs of the present system, the elevated pH near dissolving DCPD falls off more rapidly than the phosphate concentration (see fig. 2.4), so that, in practice, it is only the pH effects at high phosphate concentrations that are relevant anyway. For soils in which there is a marked effect of pH on phosphate sorption, it would be a simple matter to express a and b as functions of pH.

Fig. 3.4 shows the effect of the time of reaction on phosphate sorption. Between 10 and 30 h there is little change in the amount sorbed at a given concentration in solution, showing that the fast reaction reaches

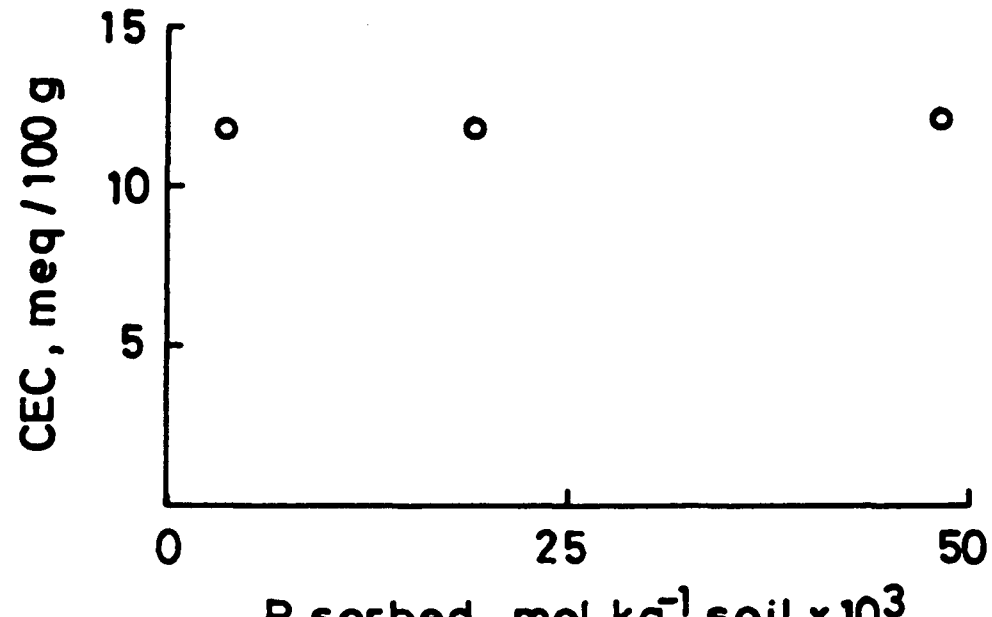


Fig. 3.2. The effect of phosphate sorption on CEC.

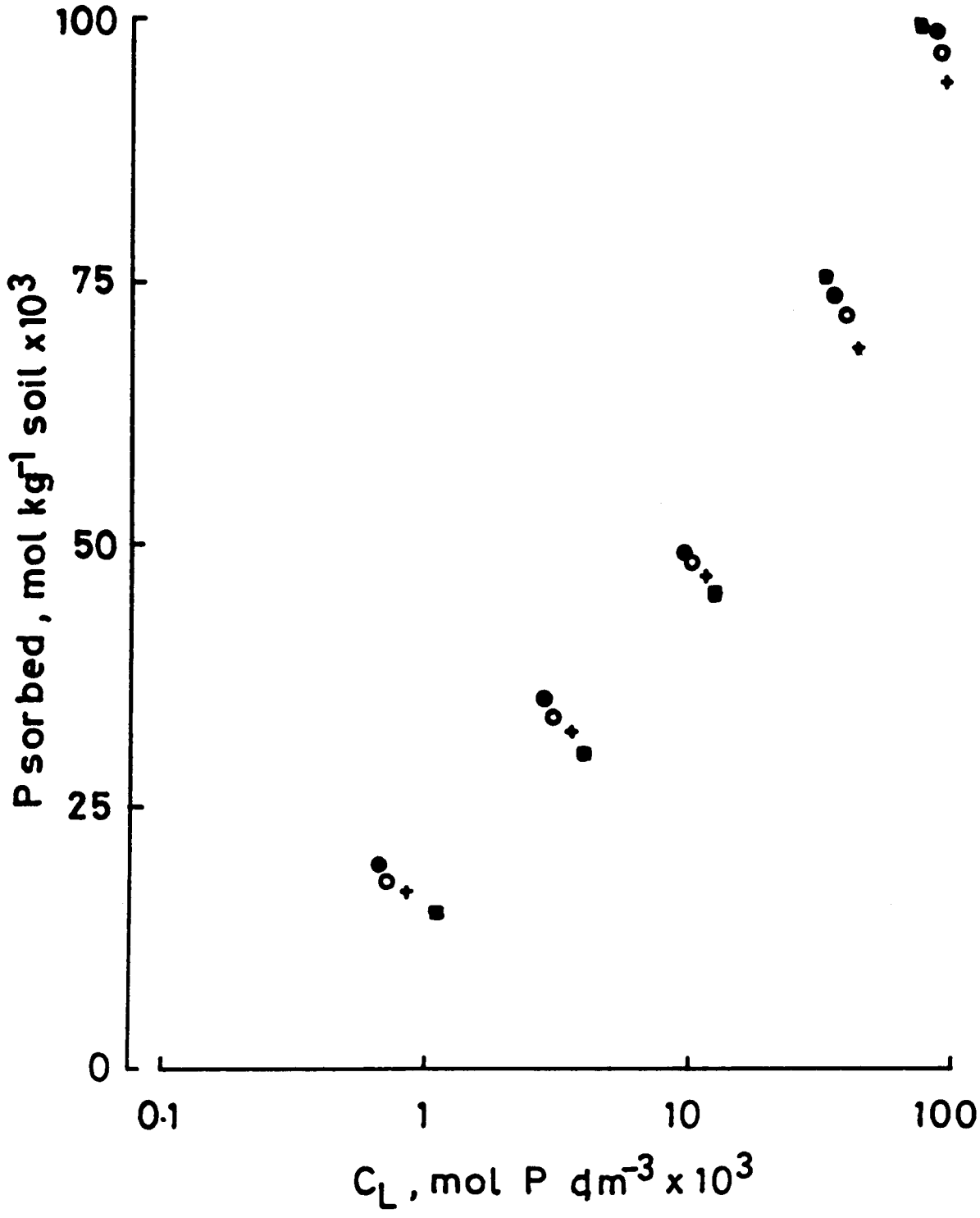


Fig. 3.3. The effect of pH on phosphate sorption: (●) pH 3.5, (o) pH 4.0, (+) pH 4.5, (■) pH 5.0.

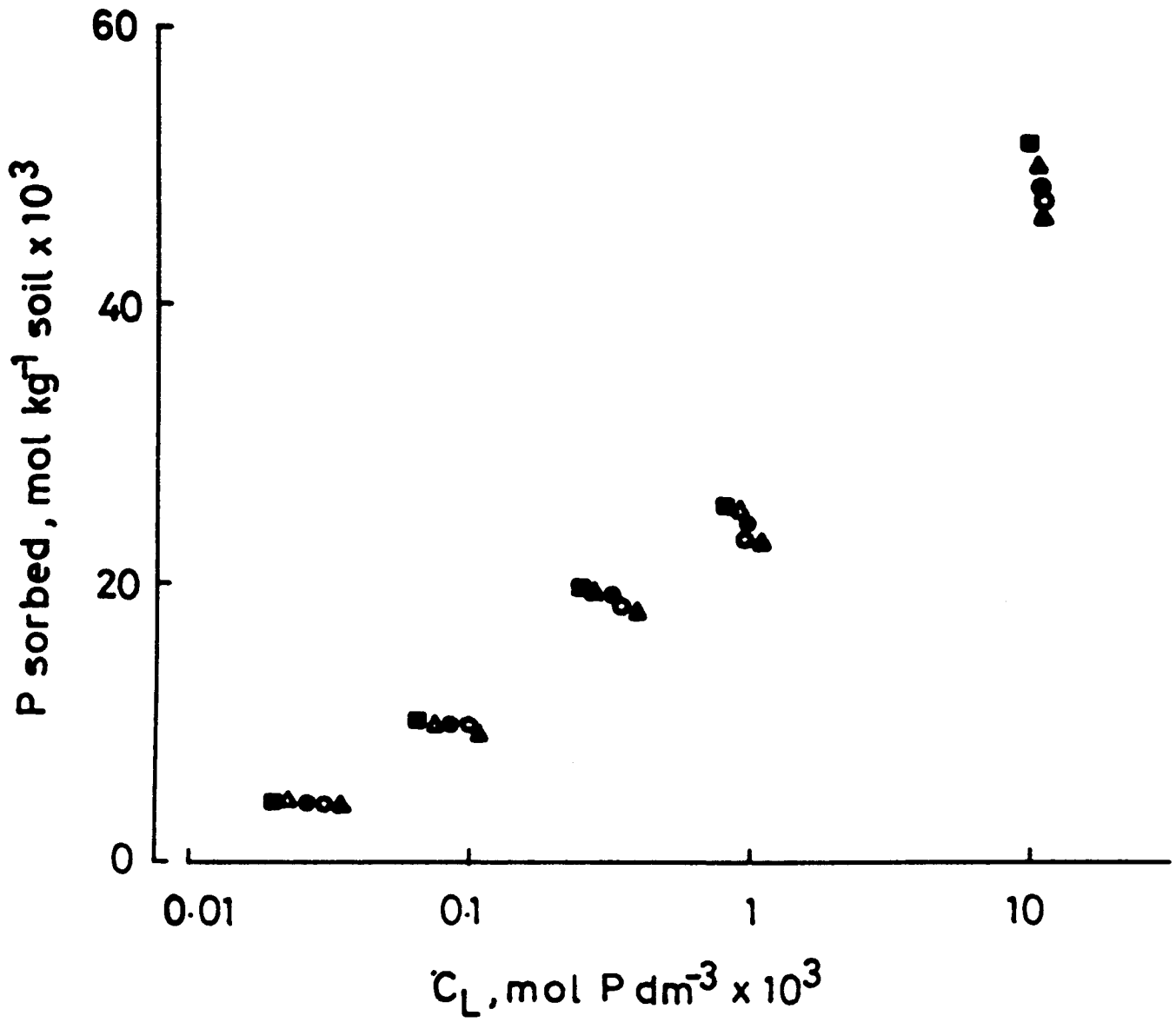


Fig. 3.4. Phosphate sorption isotherms after different reaction times: (▲) 5h, (o) 10h, (●) 30h, (Δ) 100h, (■) 200h.

equilibrium within 10h. Thereafter there is a small amount of slow reaction but less than 5% additional phosphate was sorbed after 8 days. The experimental conditions would favour an exaggerated rate of slow reaction because shaking tends to break down soil aggregates exposing less accessible reaction sites (Hope and Syers, 1976; Barrow and Shaw, 1979). The amount of additional DCPD dissolved as a result of slow reaction is therefore small, and does not warrant the complication of including kinetics in the model.

3.2 The Lime Potential Buffer Capacity

Method

2g portions of air dry soil were shaken with 10 cm^3 of 10^{-2} mol dm^{-3} $CaCl_2$ containing graded amounts of KOH. After 4h, little change in pH could be detected showing that equilibrium had been established.

Results

The lime potential buffer capacity was calculated from a linear regression of the change in soil base against lime potential (fig. 3.5). The change in soil base was found from the difference per kg of soil solid between base added and base in the equilibrium solution. A correction was made for H^+ desorbed from the soil into the measuring suspension whose volume was ten times that of the true pore solution (see below). The value obtained for the lime potential buffer capacity was 0.115 mol $kg^{-1}pH^{-1}$ (r^2=0.998).

For longer reaction times there was a small increase in b_{HS} due to slow equilibration of bases with the soil. The increase in b_{HS} was less than

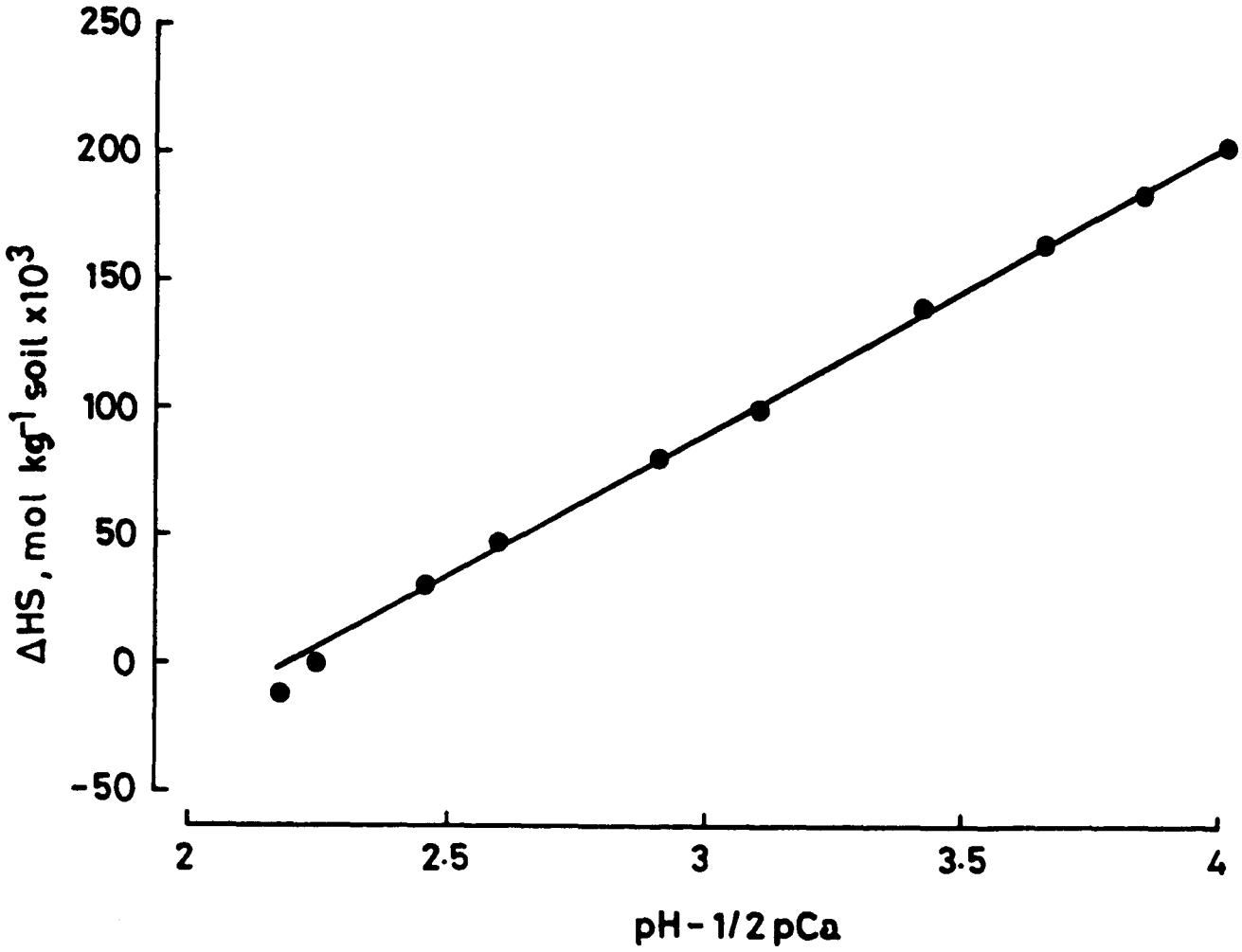


Fig. 3.5. The lime potential buffer curve.

5% (in agreement with Ramzan and Nye, 1978 and Ameloko, 1983), and so can be ignored.

Adjustment of the phosphate and lime potential buffer parameters to whole soil basis

The measured values of the Freundlich a coefficient and the lime potential buffer capacity are on a mol kg^{-1} of dry soil basis, but are required in the model on a mol dm^{-3} of whole soil basis.

$$w(\text{dry soil}) = w(\text{moist soil}) - w(\text{moisture})$$

$$= \rho V(\text{moist soil}) - V(\text{moisture})$$

thus $$w(\text{dry soil}) / V(\text{moist soil}) = \rho - \theta$$

The measured buffer terms must therefore be multiplied by $(\rho-\theta)$.

3.3 The Diffusion Impedance Factor

The method was based on the pulse labelling technique of Pinner and Nye (1982) with ^{36}Cl. Since Cl is non-adsorbed, there is no sorption term in the diffusion coefficient, and

$$D_{eff} = D_L f$$

Thus measurements of D_{eff} under the same conditions as the main experiment, can be used to obtain f. f is more or less constant for different ions (Rowell et al 1967).

Method

Moist soil was packed into perspex cells of 3.0 cm diameter to a bulk density of 1.0 kg dm^{-3}. A piece of filter paper moistened with 10^{-3}

mol dm^{-3} $CaCl_2$, was placed over one face of the column and left to equilibrate for 2h. Instantaneous labelling of the column was effected by removing the filter paper, dropping onto it a microvolume of $Ca^{36}Cl_2$ of appropriate activity, and then briefly bringing it back into contact with the face. No redistribution of moisture could be detected with this method.

After 2h, the column was sectioned into 10 cm^3 plastic centrifuge tubes and the activity of each slice determined by extraction in unlabelled $CaCl_2$ (soil:solution ratio of 1:10), and Cerenkov counting. The soil moisture content was determined on the unsliced remainder of the soil block.

Results

The linear diffusion of a solute, S, deposited instantaneously in a plane at the surface of a soil block is described by (Crank, 1975, eqn. 2.7)

$$S_L = \frac{M}{(\pi D_L ft)^{1/2}} \exp\left[\frac{-x^2}{4D_L ft}\right]$$

thus $$\ln S = \ln S_0 - x^2/(4D_L ft)$$

ie. a plot of $\ln[(counts)/(counts)_0]$ against $x^2/(4D_L t)$ (fig. 3.6) will be a straignt line with slope -1/f.

The value thus obtained for the impedance factor of the present soil at a bulk density of 1.0 kg dm^{-3} and volumetric moisture content of 0.28, was 0.15.

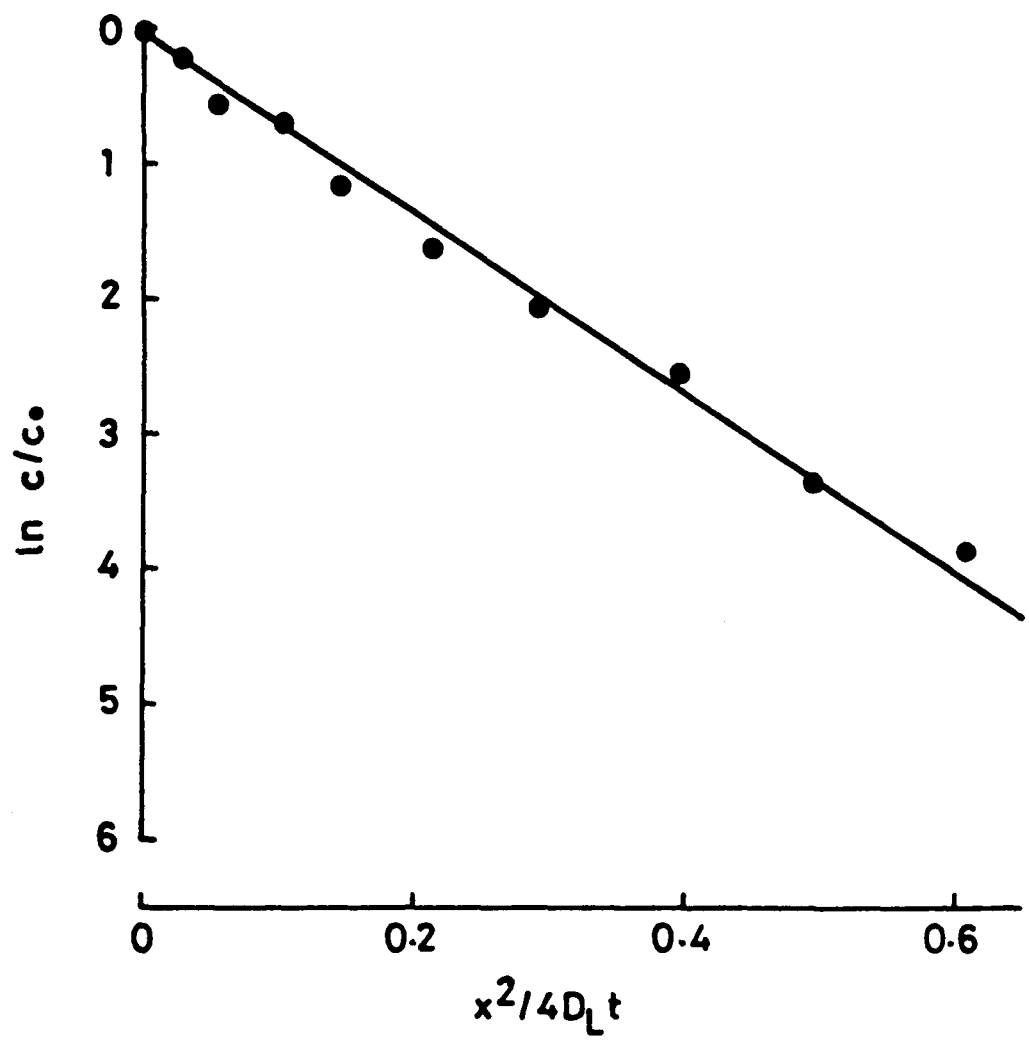


Fig. 3.6. ^{36}Cl concentration profile for calculation of the diffusion impedance factor (f=1/slope); θ=.28.

The Solute Concentration Profiles

3.4 Preparation of DCPD

Mineral DCPD is available from chemical suppliers, but in view of its instability with respect to dehydration and the importance of having consistent samples, I decided that it would be wise to prepare the mineral myself. The method is based on that of Moreno et al (1960a), in which precipitation of fine crystals of DCPD from a saturated calcium phosphate solution is brought about by gradually increasing the pH with ammonia gas. Precipitation commences at about pH 5.

Method

Sufficient $Ca(H_2PO_4)_2.2H_2O$ was shaken for one hour with 1 dm^3 of water to produce a saturated solution. The saturated solution was filtered into a large side-armed flask and this connected to an ammonia generator. Ammonia was slowly sucked through the solution so that the pH increased gradually. Vigorous mechanical stirring prevented agglomeration of the precipitate. After several hours, the suspension was filtered and the crystals washed repeatedly with distilled water until the pH rose to 6.5. Excess water was removed by careful washing with acetone under moderate suction.

The crystals produced were examined microscopically and found to be colourless and needle-shaped with approximate dimensions 30 x 10 x 10 microns, as expected. The Ca:P ratio was determined by dissolving a sample in dilute HCl and was found to be close to the theoretical 1:1 ratio of the pure salt. Other possible precipitates are MCP (1:2), OCP (4:3), TCP(3:2), and HAP(5:3).

The solubility product was determined by equilibrating a sample of the crystals with distilled water at 20°C, and analysing the filtered suspension for calcium, phosphate and pH. The value was calculated as follows

Phosphate measured, $P_T = [H_2PO_4^-]+[HPO_4^{2-}]+[CaH_2PO_4^+]$

$$= (1+\lambda_{II}\frac{[H^+]}{K_2}+\lambda_{II}K_3\frac{[Ca^{2+}][H^+]}{K_2})\lambda_{II}^{-2}\frac{K_{SP}}{[Ca^{2+}]}$$

where λ_{II} is the activity coefficient of divalent ions.

$$K_{SP} = \lambda_{II}K_2P_T[Ca^{2+}]/(K_2/\lambda_{II}+[H^+]+K_3[Ca^{2+}][H^+])$$

which may be solved by iterating on the ionic strength. The value thus obtained for K_{SP} was 2.00×10^{-7} which agrees with published values (Moreno et al, 1960a; Bates and Acree, 1943).

3.5 Measurement of the Concentration Profiles

Method

Samples of the air dry soil were wetted to a gravimetric moisture content of about 0.3 by applying a fine spray of 10^{-3} mol dm^{-3} $CaCl_2$ containing 50 mg dm^{-3} $HgCl_2$. The moist soil was packed into perspex cells, 8 cm internal diameter by 1 or 2 cm deep (depending on the run time), to a bulk density of 1.0 kg dm^{-3}. Thus a 0.2 mm section of soil contained approximately 1g of moist soil which is the minimum quantity required for accurate phosphate analysis. One surface of each soil column was covered with a moistened glass fibre filter paper and over this a

perspex plate was fixed. The other end of the column was covered with a perforated plate to permit gaseous exchange. The whole was then incubated for 24h in a moisture saturated atmosphere with a constant P_{CO_2} of 0.005 atm.

After incubation, fine crystals (<100 μm long axis) of DCPD were sprinkled over the filter paper to give a uniform covering. About 10 mg of crystals were sufficient to provide a continuous source for over one month. The perspex cover plate was bolted tightly over the crystals to ensure good contact at the crystal/filter paper and filter paper/soil interfaces. The springiness of the filter paper under tension ensured that good contact was maintained as the crystals dissolved. The assembled cells were then incubated as before.

At the end of runs, the filter paper holding the undissolved material was removed and the sample sectioned at 0.2 mm intervals using a microtome (fig. 3.7) and a heavy stainless steel blade. Finer slicing than 0.2 mm was not possible since the largest soil particles have diameters of about this size. In view of the thinness of the slices (0.2mm) and their large diameters (8 cm), an exact slicing technique was needed. To this end, the front of the microtome was faced with a brass plate through which the soil column was extruded, thus by resting the blade against the brass face and slicing down, the edge of the slice was always perpendicular to the axis of diffusion.

The exact slice thickness was calculated from the sample weights using the sample bulk density and the cross-sectional area. Sample moisture contents were obtained by drying the unsliced remainders of the soil blocks at 105°C overnight. The uniformity of packing and moisture distribution was checked by taking large slices (whose thickness was

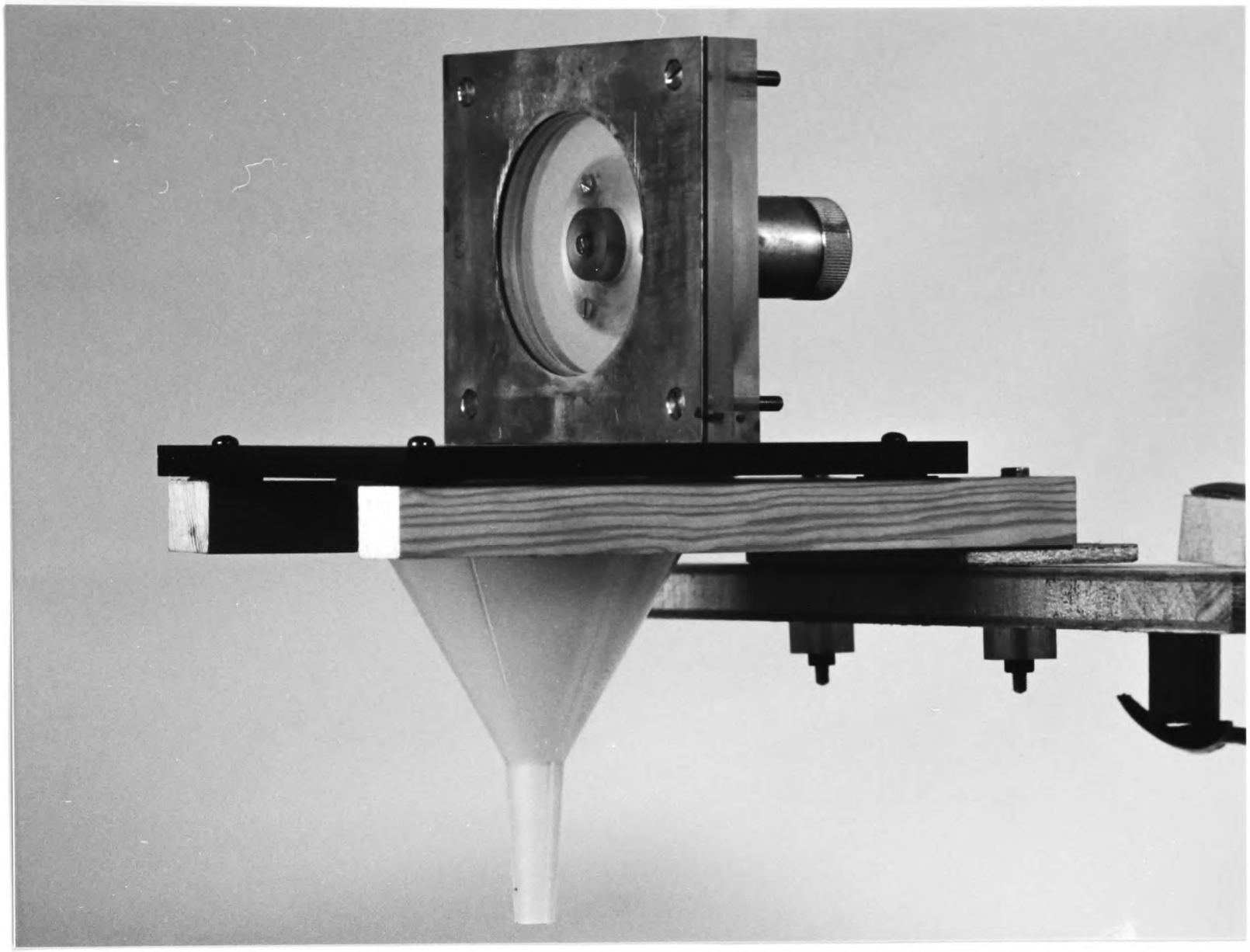


Fig. 3.7. Microtome for sectioning soil columns.

therefore known from the micrometer displacement) for a dummy run, weighing them and measuring their moisture contents.

Alternate slices were used for calcium determination and pH and phosphate determinatons. Calcium was determinedy by shaking the slices for 1h in 10 cm^3 of 1 mol dm^{-3} NH_4OAc and analysing by atomic adsorption spectroscopy. pH was determined in suspensions prepared by shaking the slices in $5cm^3$ of 10^{-2}mol dm^{-3} $CaCl_2$. The correction of the pH to that of the pore solution is described below. Total inorganic phosphate was measured by adding 35 cm^3 of 1 mol dm^{-3} HCl + 0.05 mol dm^{-3} NH_4F to these suspensions and shaking overnight. A high solution:soil ratio and addition of flouride ions reduced resorption of dissolved phosphate which was the main source of error in the assay. After shaking, the suspensions were filtered and the phosphate concentrations measured. By this method, the recovery of phosphate from soil incubated with known concentrations of phosphate for two months, was better than 95%. The variation in measured phosphate between replicate samples was less than 5%.

Adjustment of the Measured pH Values for differences between the Measuring Suspension and the True Pore Solution

The pH values measured on the slices must be adjusted for H^+ desorbed from the soil into the measuring suspension, and for the difference in calcium activity between the true soil solution and the solution in which the measurements were made.

The amount, M, of H^+ desorbed from the soil (mol kg^{-1} of dry soil) into the measuring suspension is given by

$$M = \frac{V \times 10^{-pH} / \lambda_{H^+}}{wt}$$

where V is the volume (dm^3) of solution added to the moist soil, λ_{H^+} the activity coefficient of H^+ in 10^{-2} mol dm^{-3} $CaCl_2$, and wt the weight (kg) of dry soil used. The pH in a soil pore containing 10^{-2} mol dm^{-3} $CaCl_2$ is less than in the measuring suspension by M divided by the buffer capacity in units mol $kg^{-1}pH^{-1}$. At pH 3.5 and a soil:solution ratio of 1:10, the amount desorbed is 7.3 mmol H^+ kg^{-1} of dry soil, corresponding to a reduction in pH of .06 units. This quantity is insignificant at higher pHs (lower concentration of H^+ in solution). It will be more significant for less strongly buffered soils.

Having corrected the measured pH for M, the true calcium concentration and hence true pH were calculated by successive approximation using (a) the balance of cations and anions:

$$[Ca^{2+}]_L = 1/2\ ([H_2PO_4^-]_L + [Cl^-]_L - [H^+]_L)$$

with the value of $[H_2PO_4^-]_L$ interpolated from the measured total phosphate using the sorption isotherm; and (b) the ratio law:

$$(H^+)_{L,1} = (H^+)_{L,2} \sqrt{\frac{(Ca^{2+})_{L,1}}{(Ca^{2+})_{L,2}}}$$

The terms in parentheses are ionic activities and subscripts 1 and 2 refer to the true pore solution and measuring suspension. Activity coefficients were calculated using the Davies equation.

Comparison of the Observed Concentration Profiles with the Model Predictions

Figs. 3.8, 3.9 and 3.10 show the total phosphate, pH and total calcium profiles developed after 48h.

Unfortunately it was not possible to take concentration measurements nearer to the interface because one is limited by the slicing thickness. I do not, therefore, have a direct measure of the interface boundary concentrations to compare with the predicted values. However, since the agreement between the observed and predicted profiles is good, and the predicted spread depends critically on the interface boundary concentrations, the calculated boundary concentrations appear to be correct.

Fig. 3.11 shows the total phosphate profiles for longer times.

For the longer runs, phosphate and pH measurements were taken in all the slices. Thus the total amounts of phosphate and base dissolved could be found by summing the amounts in individual slices, calculating the amount of base by multiplying the lime potential by b_{HS} (Table 3.2).

There is a small but increasing discrepancy between the amounts dissolved, phosphate being less than base. This may be due to the formation of non-acid-soluble forms of phosphate such as those in combination with organic matter, which were not recovered in the extraction. However, the agreement between the base and phosphate is reasonable, showing that the experimental methods are accurate.

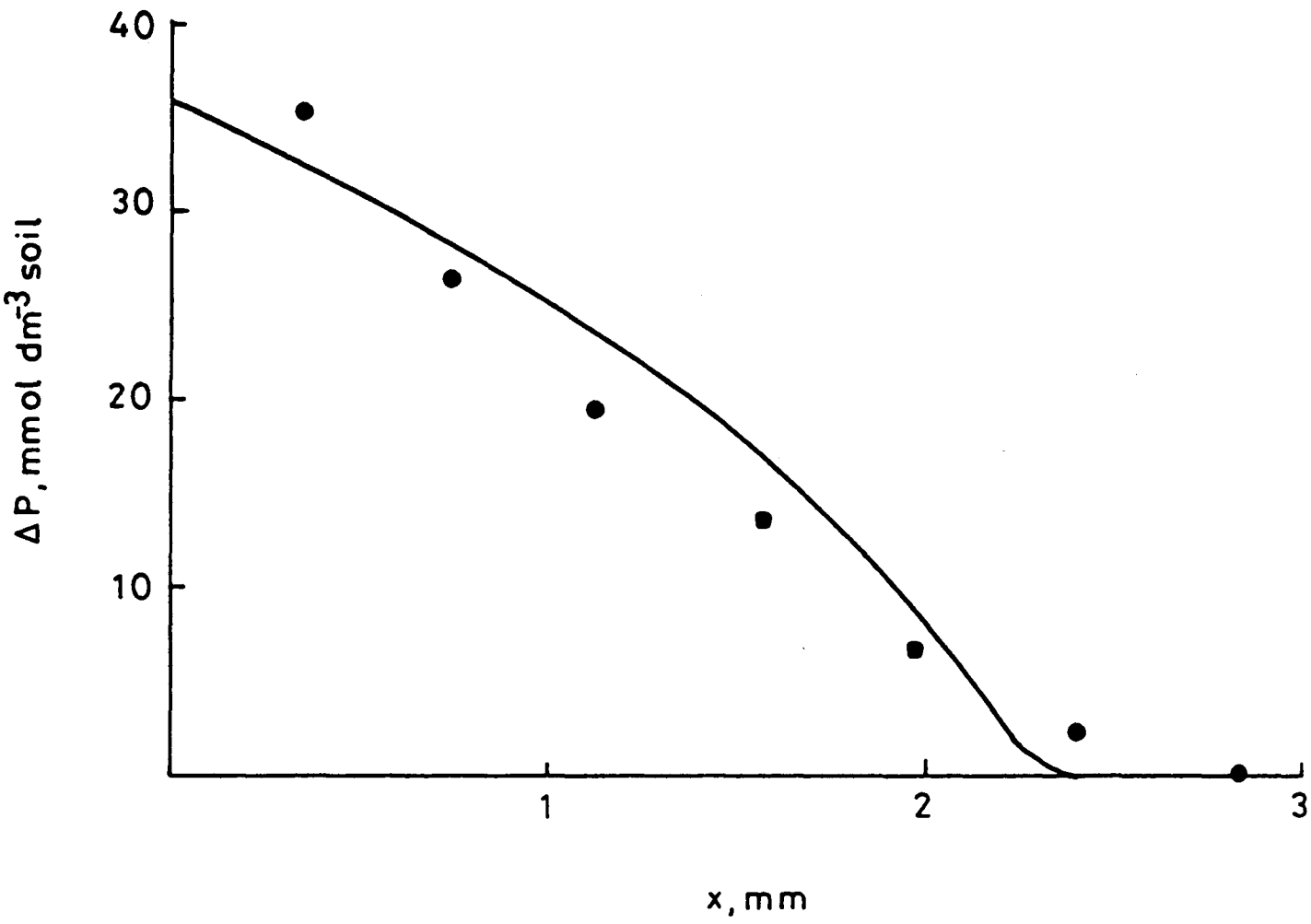


Fig. 3.8. Profiles of the change in total inorganic phosphate after 48h: (●) observed, (—) predicted. θ=0.28, ρ=1.0 kg dm^{-3}, f=0.15.

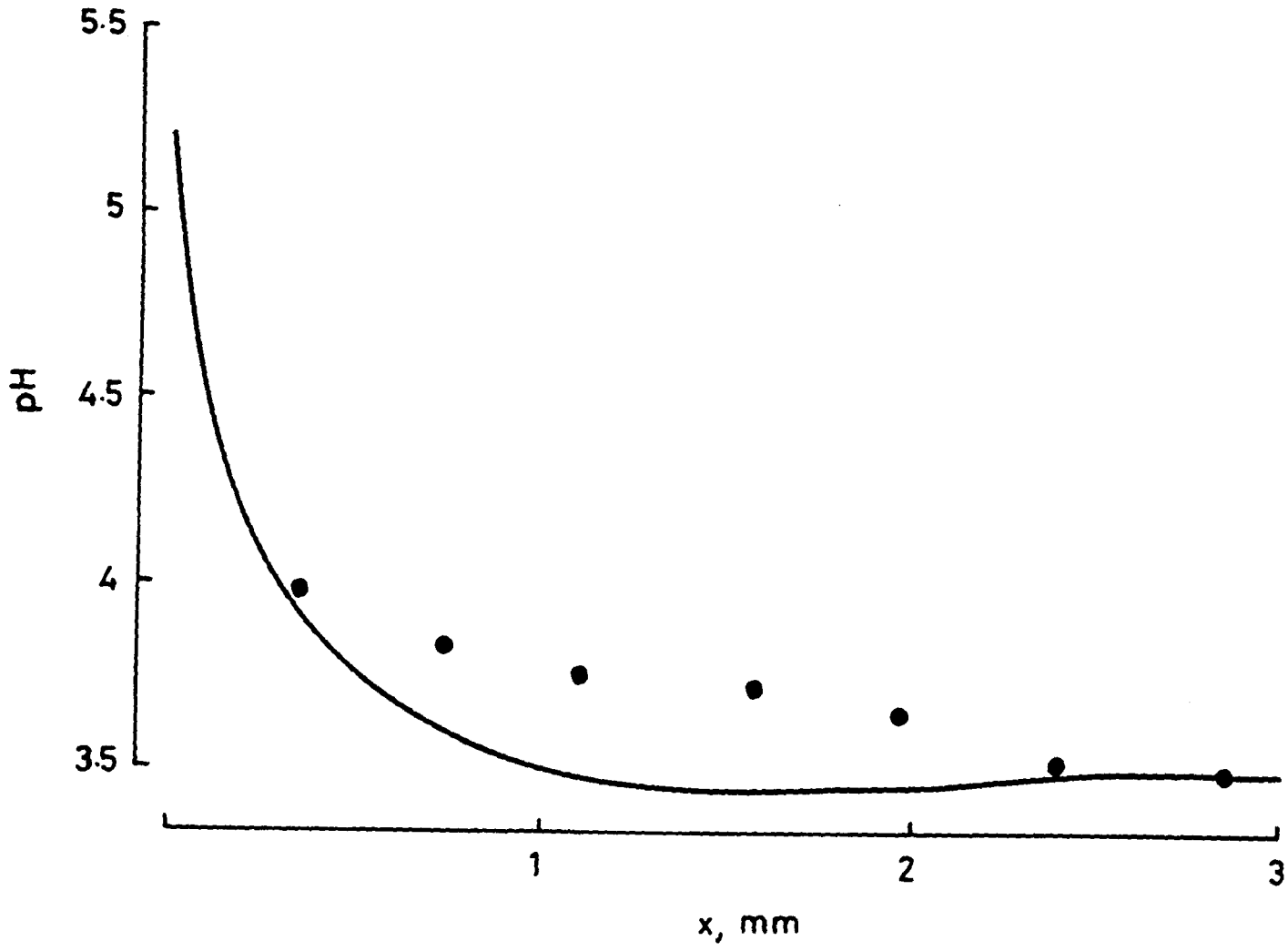


Fig. 3.9. pH profiles after 48h: (●) observed, (——) predicted. Values of soil variables as in Fig. 3.8. The pH is less than the native soil pH between x=1 and x=2 mm because the Ca gradient is steep there.

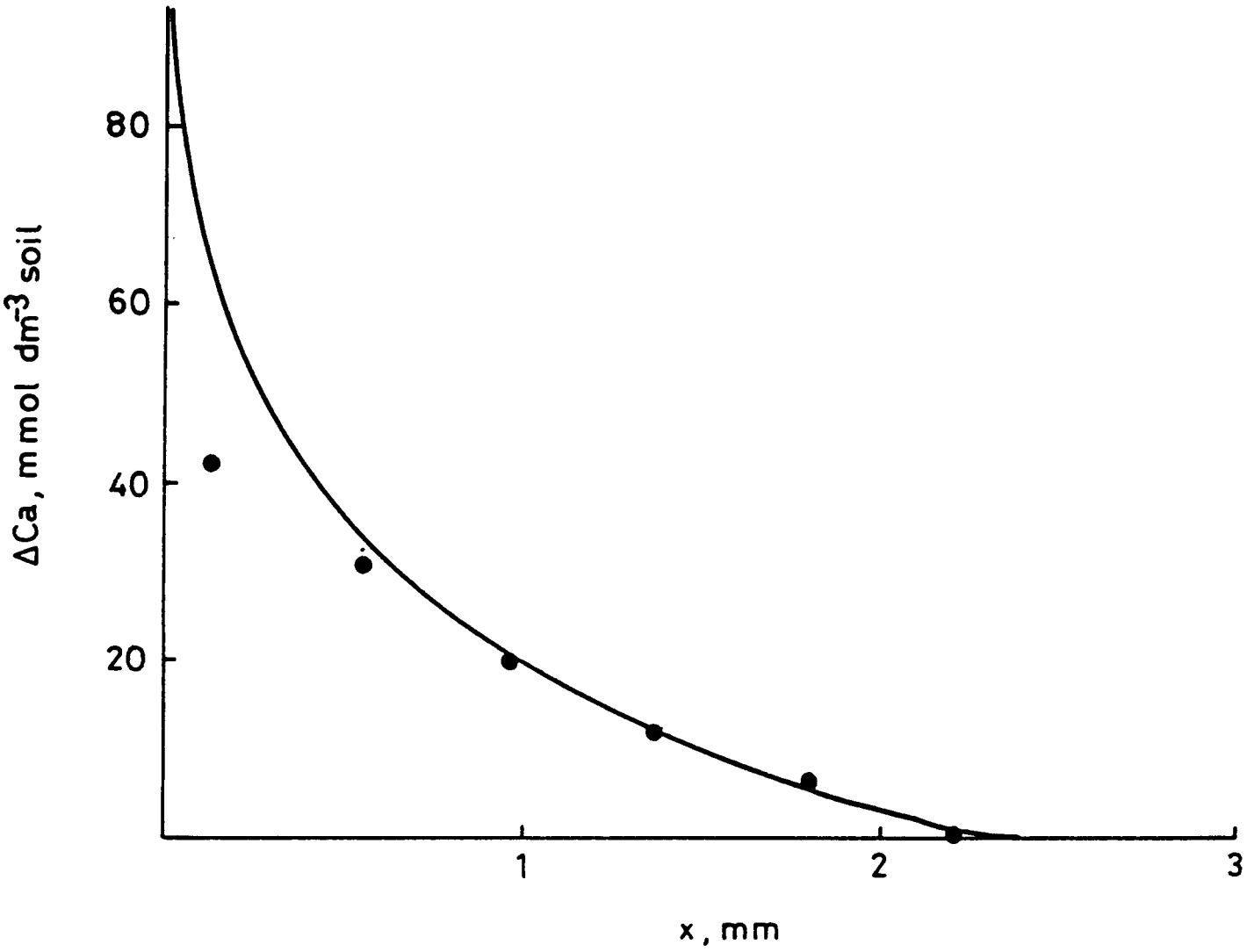


Fig. 3.10. Profiles of the change in total calcium concentration after 48h: (●) observed, (—) prediced. Values of soil variables as in Fig. 3.8.

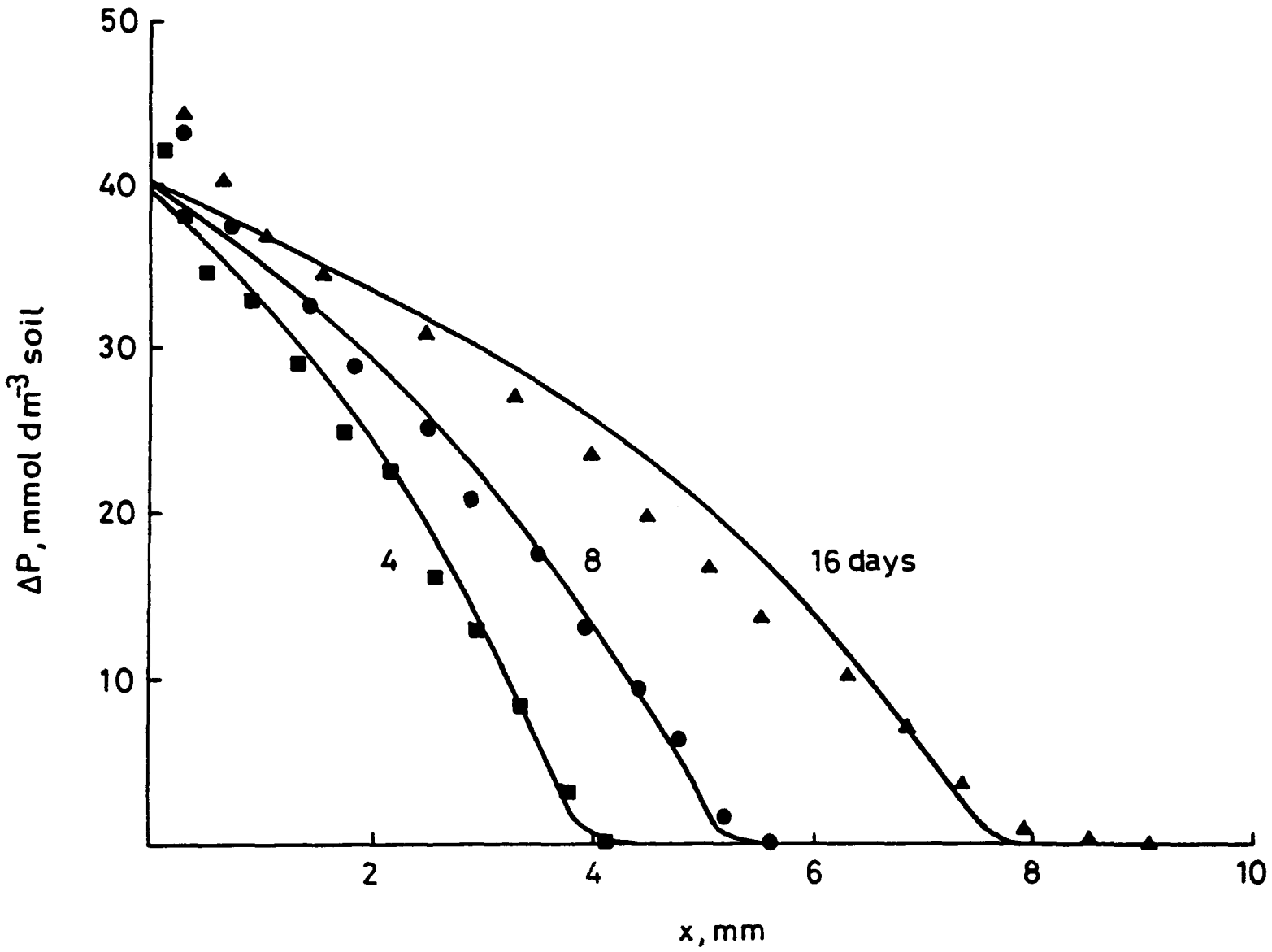


Fig. 3.11. Profiles of the change in total phosphate concentration after different times: (■ , ● , ▲) observed, (—) predicted. θ=0.31, ρ=1.0 kg dm^{-3}, f=0.17.

Table 3.2.

The experimentally determined total amounts of phosphate and base dissolved at different times, and the corresponding predicted amounts of DCPD dissolved.

	Experimental		Predicted
Time, h	Total P, mmol	Total base, mmol	Total DCPD, mmol
99	0.51	0.52	0.52
186	0.60	0.65	0.63
432	0.93	1.00	0.97

With regard to the model predictions, the amount of phosphate sorbed near the mineral at the longer run times is greater than predicted although the predicted spread is correct. This is probably due to the slow reaction of phosphate with internal soil surfaces, which has been ignored in the model. The rate of removal of phosphate by the slow reaction is small compared to the flux through the main pore network. Thus the concentration of phosphate in solution, and hence spread, are unaffected over the times considered in the present study. Slow reaction would, however, have to be taken into account in modelling the dissolution of less soluble phosphate minerals such as rock phosphate, whose dissolution in soil is very slow.

I conclude that all important processes have been accounted for in the model, and that it is the simplest model that satisfactorily characterises the system. The same principles should be applied in modelling the dissolution of granules of DCPD which is the subject of the next chapter.

4

A MODEL OF THE DISSOLUTION OF GRANULES OF DCPD IN SOIL

Chapters 2 and 3 have been concerned with the development and testing of a model of the dissolution of a planar source of DCPD in soils. This chapter is concerned with the extension of the model to the more practically relevant system of discreet particles of DCPD dissolving in soil. A number of complications arise in addition to the processes that were found to be important in the planar system. These are outlined below.

4.1 The Effect of Particle Size

It is obvious that the more finely divided a fertilizer is, the more rapidly it will dissolve. For a given total amount of material, and other factors being equal, the higher the surface area to volume ratio of the particles (ie. the lower their radii), the higher will be the net flux of material into the soil and hence the higher will be the rate of dissolution. Most simple models of mineral phosphate dissolution take account of this (eg. Bouldin and Sample, 1959; Mattingly, 1963; Olsen, 1975; Chien et al, 1980). Less obvious is the possibility of interactions between surface area and other factors that limit the rate of dissolution; if such interactions occur, simple relationships between size and rate are inadequate. We have seen that the concentrations of dissolved solutes at the mineral surface depend upon the relative fluxes of the component ions away from the surface, and that the net rate of dissolution is strongly dependent on these concentrations. Since the fluxes of phosphate and base are coupled (propagation of base in soils being in part due to the movement of phosphate ions), the effect of changes in particle radius

on the fluxes of phosphate and base at the surface, will not necessarily be the same. Thus the concentrations of phosphate and base in solution at the surface of a particle dissolving in a particular soil will not necessarily be the same as the concentrations at the surface of a planar layer of DCPD in the same soil. No analytical solutions of the relevant equations are available to indicate the magnitude of such interactions, but it is possible that the effects are quite significant.

Additional to the effect of the initial particle size on the rate of dissolution is the effect of the diminution of the particle as it dissolves. Thus the rate of dissolution tends to decrease as dissolution proceeds.

4.2 The Effect of the Rate of Application

The rate of application (ie. amount of material applied per unit volume of soil) for a particular granule size determines the mean distance between adjacent granules and hence the length of time before the spheres of influence of adjacent particles overlap. As these spheres overlap, material is reflected back from the point of overlap causing an apparent back-flux of material which decreases the rate of dissolution. Also, since the movement of the dissolved phosphate and base is coupled, there may be a more complex interaction between adjacent particles. Thus if the spread of phosphate away from the particle is more rapid than the spread of base, reflection of phosphate back from the point of overlap would cause a relative accumulation of phosphate near the surface. As the concentration of the acid-base pair $H_2PO_4^-$-HPO_4^{2-} rises, the soil base diffusion coefficient will rise and consequently the surface pH will fall and the surface C_L tend to rise further.

Description of the Model

4.3 The Continuity Equations for Phosphate and Base in Spherical Geometry

A granule of DCPD comprises agglomerates of small, plate-shaped crystals, so that, as a granule dissolves, the surface becomes pitted with pore openings corresponding to the edges of adjoining crystals. The solution in the pores will remain saturated with the mineral as it dissolves, because, as we have seen, the rate of dissolution of DCPD in soils is controlled by the diffusion of its components, phosphate, base and calcium, into the soil, and diffusion of these solutes in soils is very slow. Thus, if the particle is spherical, the effective surface is an infinitesimally thin spherical shell covering the exterior of the granule. The geometrical system to be considered, therefore, is a hollow sphere, and the continuity equations for phosphate and soil base in linear geometry (equations (2.43) and (2.410)) are replaced by a) for phosphate

$$\frac{\partial C_L}{\partial t} = \frac{D_{LP}\theta f}{\theta + abC_L^{\,b-1}} \left[\frac{\partial^2 C_L}{\partial r^2} + \frac{2}{r}\frac{\partial C_L}{\partial r}\right] \qquad (4.31)$$

and b) for soil base

$$\frac{b_{HS}}{2.3}\left(\frac{1}{[H^+]_L}\frac{\partial [H^+]_L}{\partial t} - \frac{1}{2[Ca^{2+}]_L}\frac{\partial [Ca^{2+}]_L}{\partial t}\right) =$$

$$\theta f\left\{\frac{\partial}{\partial r}\left(D_{LH}\frac{\partial [H^+]_L}{\partial r} - D_{LP}\frac{\partial [HPO_4^{\,2-}]_L}{\partial r} - D_{LC}\frac{\partial [HCO_3^{\,-}]_L}{\partial r}\right) + \right.$$

$$\left. \frac{2}{r}\left(D_{LH}\frac{\partial [H^+]_L}{\partial r} - D_{LP}\frac{\partial [HPO_4^{\,2-}]_L}{\partial r} - D_{LC}\frac{\partial [HCO_3^{\,-}]_L}{\partial r}\right)\right\} \qquad (4.32)$$

where r is the radial distance from the centre of the particle (after Crank, 1975, equation 6.1). The calcium profile is calculated, as in the planar model, by balancing the ionic charges for electroneutrality

(equations (2.412) and (2.413)).

4.4 The Boundary Conditions

The Interface Boundary

The concentrations of phosphate, base and calcium at the surface of a particle are fixed by the requirement that their fluxes across the surface boundary be equal, and that the concentrations of the component ions in solution are in agreement with the solubility product relationship (section 2.3).

As a particle dissolves, its size decreases and hence the particle surface retreats with time (Fig. 4.1 (a)). Depending on the pore size distribution of the soil and the initial particle radius, the space left by the dissolving particle may remain filled with solution, or may be partially drained. Thus, a 0.5 mm radius particle dissolving in a loamy clay soil, or finer, would probably leave a small air space. However, the film of solution around the particle will remain continuous with the solution in the soil pore network, and solute will continue to be radially transfered to the surrounding soil.

Since the volume of the region between the current and initial particle surfaces is very small compared to the volume of the soil bulk, over an interval of time, Δt, effectively all the material entering this region from the dissolving surface will be transfered to the soil bulk. Thus the rate of transfer of material will be the same at all points in this thin region and a steady state will exist.

If a_i is the initial radius of the particle and a_s the radius at a

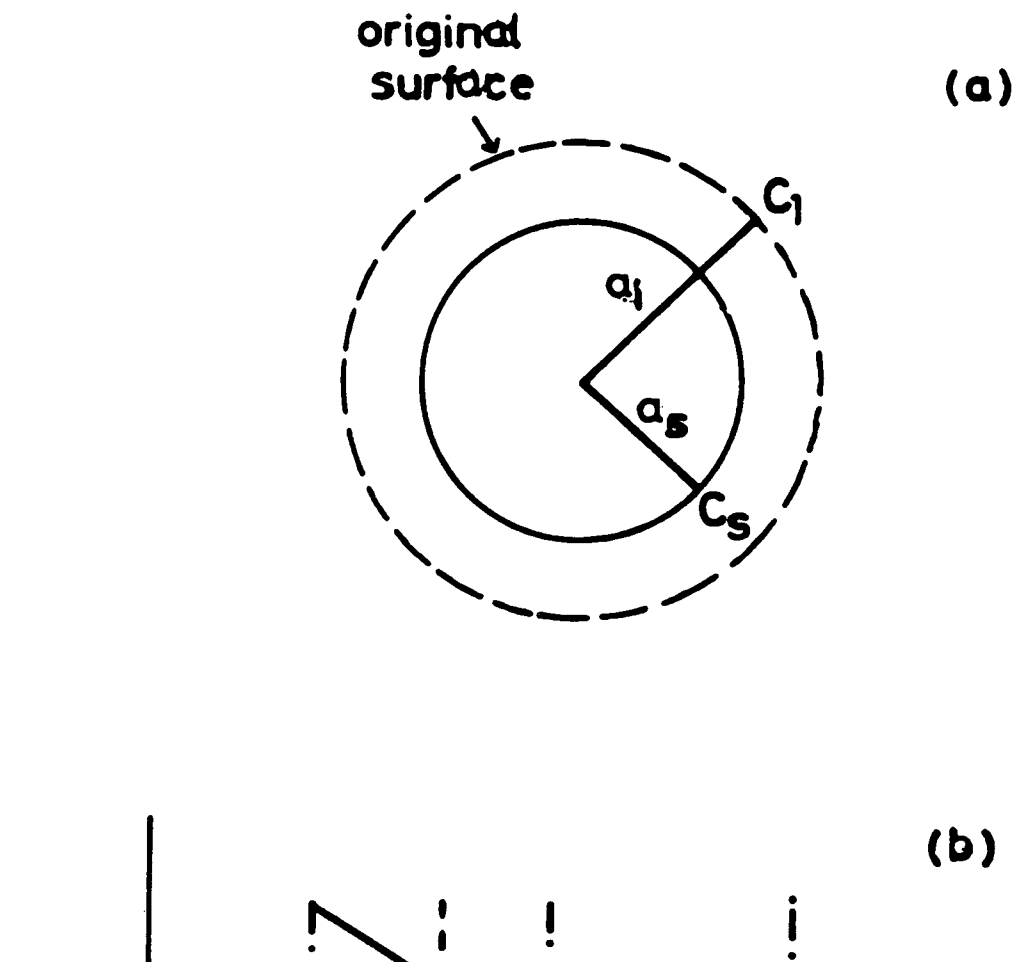


Fig. 4.1. (a) The soil/particle interface and (b) the concentration profile in the steady state region.

particular time, then the quantity of material, M_t, which passes through the spherical wall in the steady state in time Δt is given by

$$M_t = 4\pi D_{LP}\theta f \Delta t \frac{a_i a_s}{a_i - a_s}(C_{Ls} - C_{L1})$$

[Crank (1975), equation 6.7]. Thus the flux of phosphate at the particle surface is given by

$$F_P = \frac{dM_t/dt}{4\pi a_i^2} = -\frac{(a_i - \Delta a)/a_i}{\Delta a} D_{LP}\theta f(C_{L1} - C_{Ls}) \qquad (4.41)$$

and the flux of base by

$$F_B = \frac{(a_i - \Delta a)/a_i}{\Delta a} \theta f[D_{LH}([H^+]_{L1} - [H^+]_{Ls}) - D_{LC}([HCO_3^-]_{L1} - [HCO_3^-]_{Ls}) - D_{LP}([HPO_4^{2-}]_{L1} - [HPO_4^{2-}]_{Ls})] \qquad (4.42)$$

where Δa is the amount by which the radius has decreased ($=a_i - a_s$) and subscripts s and 1 refer to the current and initial positions of the particle surface. Δa, at a particular time, can be found from the amount of material left undissolved, n_t:

$$\Delta a = [3mw/(4\pi\rho)]^{1/3}(n_i^{1/3} - n_t^{1/3})$$

where n_i is the initial number of mol of DCPD per particle, mw is the molar weight of DCPD (=172) and ρ its density (=2.306 kg dm^{-3}). F_P and F_B can also be found from the concentrations at the initial surface and the (imaginary) first distance step inside the surface, of the numerical solutions of equations (4.31) and (4.32) (see fig. 4.1(b)). Thus the concentrations at the original surface can be expressed in terms of the concentrations at the current surface, and equations (4.31) and

(4.32) solved with respect to the concentrations at the original surface. The incorporation of equations (4.41) and (4.42) in the solutions of (4.31) and (4.32) is described in section 4.5.

The Boundary with Adjacent Particles

The zones of influence of neighbouring particles will eventually overlap. Diffusing material arriving at the point of overlap will effectively be reflected back. Formally this boundary condition is expressed

for equation (4.31) $dC_L/dx=0$ $r=R$ $t>0$

for equation (4.32) $d[H^+]_L/dx=0$ $r=R$ $t>0$

where R is the radial distance to the point of overlap. R is calculated from the number of particles per unit volume of soil, N. Thus,

$$1/N = (4/3)\pi R^3$$

But

$$N = \frac{w}{(4/3)\pi a_i^3 \rho}$$

where w is the weight of DCPD applied per unit volume of soil and ρ the density of DCPD. Thus

$$R = a_i(\rho/w)^{1/3}$$

Strictly the points of overlap will lie on a non-spherical surface corresponding to the mid-points between adjacent particles. However, the assumption that the surface is spherical is a reasonable approximation because the volume of the intervening spaces will be small compared to the overall volume, and this greatly simplifies the problem.

The Initial Conditions

for equation (4.31) $C_L = C_L'$ $a_i \leq r \leq R$ $t=0$

for equation (4.32) $[H^+]_L = [H^+]_L'$ $a_i \leq r \leq R$ $t=0$

where superscript ' refers to quantities in the native soil.

4.5 The Numerical Solutions of the Continuity Equations

The method of solution was the same as used for the planar system (section 2.6), based on equations (2.61) to (2.64). The relevant equations are given below. Subscript L has been omitted for clarity and $[H^+]_L$, $[Ca^{2+}]_L$, $[HPO_4^{2-}]_L$ and $[HCO_3^-]_L$ written H, Ca, P2 and HC respectively.

a) Phosphate

The Crank-Nicolson form of equation (4.31) is

$$C_j^t - C_j = \alpha^\circ[(1+\Delta r/r)(C_{j+1}^t + C_{j+1}) - 2C_j^t - 2C_j + (1-\Delta r/r)(C_{j-1}^t + C_{j-1})] \quad (4.51)$$

where $\alpha^\circ = D_{LP}\theta f \Delta t/(\theta + abC_0^{b-1})2\Delta r^2$.

If $W_{Pj}^\circ = \alpha^\circ(1+\Delta r/r)$, $X_{Pj}^\circ = (2\alpha^\circ+1)$ and $Y_{Pj}^\circ = \alpha^\circ(1-\Delta r/r)$, then

$$-W_{Pj}^\circ C_{j+1}^t + X_{Pj}^\circ C_j^t - Y_{Pj}^\circ C_{j-1}^t = W_{Pj}^\circ C_{j+1} + (2-X_{Pj}^\circ)C_j + Y_{Pj}^\circ C_{j-1} = Z_{Pj}^\circ \quad (4.52)$$

(cf. equation (2.66)).

The boundary conditions

(i) The interface boundary conditions are described in section 4.4. Equation (4.52) at j=1 (ie. the initial particle surface) becomes

$$-W_{P1}^\circ C_2^t + X_{P1}^\circ C_1^t - Y_{P1}^\circ C_0^t = W_{P1}^\circ C_2 + (2-X_{P1}^\circ)C_1 + Y_{P1}^\circ C_0 \quad (4.53)$$

where subscripts 0, 1, and 2 are the distance steps inside, at and outside the initial surface boundary.

The C_0 concentrations are imaginary but can be eliminated from (4.53)

using the steady state flux condition across the current/initial surface region. Thus, for the flux of phosphate at j=1,

$$F_P = \frac{(a_i-\Delta r)/a_i}{\Delta r} D_{LP}\theta f(C_1-C_o)$$

F_P is also given by equation (4.41), thus

$$\frac{(a_i-\Delta a)/a_i}{\Delta a} D_{LP}\theta f(C_1-C_s) = \frac{(a_i-\Delta r)/a_i}{\Delta r} D_{LP}\theta f(C_1-C_0)$$

or
$$C_0 = \frac{C_1(1-\Delta r/\Delta a) + C_s(\Delta r/\Delta a-\Delta r/a_i)}{(1-\Delta r/a_i)}$$

If $R_1=(1/\Delta a-1/a_i)/(1/\Delta r-1/a_i)$, then $C_0=C_1(1-R_1)+C_sR_1$.
Substituting for C_0 in equation (4.53) and rearranging

$$C_1^t = \frac{W_{P1}^\circ C_2^t+W_{P1}^\circ C_2+[2-X_{P1}^\circ+Y_{P1}^\circ(1-R_1)]C_1+Y_{P1}^\circ R_1(C_s^t+C_s)}{[X_{P1}^\circ-Y_{P1}^\circ(1-R_1)]}$$

Comparison with (2.62) gives

$$E_{P1}^\circ = W_{P1}^\circ/[X_{P1}^\circ-Y_{P1}^\circ(1-R_1)] \qquad (4.54)$$

$$F_{P1}^\circ = \frac{W_{P1}^\circ C_2+[2-X_{P1}^\circ+Y_{P1}^\circ(1-R_1)]C_1+Y_{P1}^\circ R_1(C_s^t+C_s)}{[X_{P1}^\circ-Y_{P1}^\circ(1-R_1)]} \qquad (4.55)$$

C_s^t is unknown. The flux balancing routine used for its calculation in the planar model is unsuitable for the spherical system because the volume of the saturated surface layer is much smaller, and therefore the

amount of material removed from the layer in Δt is large compared with the amount in it. However, at steady state, we may write from (4.41) and (4.42),

$$D_{LP}(C_1-C_s) = D_{LH}([H^+]_s-[H^+]_1) \qquad (4.56)$$
$$-D_{LP}([HCO_3^-]_s-[HCO_3^-]_1)-D_{LP}([HPO_4^{2-}]_s-[HPO_4^{2-}]_1)$$

Now, by assuming that, as a first approximation, $[H^+]_s^t-[H^+]_1^t = [H^+]_s-[H^+]_1$, and calculating the corresponding values for $[HCO_3^-]^t$ and $[HPO_4^{2-}]^t$, C_s^t and hence the whole phosphate concentration profile can be calculated. Thus $[H^+]_s^t$ can be found from the solubility product relationship, and hence the soil base concentration profile can be obtained (see below), whence the calculation can be iterated until the C_j^t and $[H^+]_j^t$ values accord.

(ii) At the boundary with adjacent particles,

$$\partial C/\partial r = 0 = C_{R+1}-C_R$$

ie.
$$C_{R+1} = C_R$$

Substituting for C_{R+1} in equation (2.62) and rearranging,

$$C_R^t = F_{PR}^\circ/(1-E_{PR}^\circ) \qquad (4.57)$$

Thus by evaluating E_{P1}° and F_{P1}° (as a first approximation) from (4.54) and (4.55), E_{Pj}° and F_{Pj}° can be found for j=(2 to R) using equations (2.63) and (2.64). Thence C_R^t can be found from (4.57) and C_j^t from (2.62) for j=(R-1 to 1).

b) Soil base

In the planar model, the soil base continuity equation was solved by evaluating the $[HPO_4^{2-}]_L$ and $[HCO_3^-]_L$ terms separate from $[H^+]_L$ to avoid having to deal with terms in $1/[H^+]_L$. This was done by calculating an approximate base profile assuming no change in $[HPO_4^{2-}]_L$ and $[HCO_3^-]_L$, and then repeating the calculation with the new values for $[H^+]_L$ and corresponding new $[HPO_4^{2-}]_L$ and $[HCO_3^-]_L$ values. This approach did not work for the spherical model because much steeper concentration gradients arise, and therefore, the changes in $[HPO_4^{2-}]_L$ and $[HCO_3^-]_L$ over a time interval near the start of runs are much greater. However, by rewriting equation (4.32) with pH as the working variable, all the terms can be solved simultaneously. Thus for the H_2O-H_3O^+ pair

$$\frac{\partial[H^+]_L}{\partial r} = \frac{d[H^+]_L}{dpH}.\frac{\partial pH}{\partial r} = -2.303[H^+]_L\frac{\partial pH}{\partial r} \qquad (4.58)$$

for the HCO_3^--H_2CO_3 pair

$$\frac{\partial[HCO_3^-]_L}{\partial r} = \frac{d(K^*/[H^+]_L)}{dpH}.\frac{\partial pH}{\partial r} = \frac{K^*2.303}{[H^+]_L}.\frac{\partial pH}{\partial r} \qquad (4.59)$$

and for the HPO_4^{2-}-$H_2PO_4^-$ pair

$$\frac{\partial[HPO_4^{2-}]_L}{\partial r} = \frac{\partial(K_2[H_2PO_4^-]_L/[H^+]_L)}{\partial r}$$

$$= K_2\left(\frac{1}{[H^+]_L}.\frac{\partial[H_2PO_4^-]_L}{\partial r}+[H_2PO_4^-]_L\frac{2.303}{[H^+]_L}.\frac{\partial pH}{\partial r}\right) \qquad (4.510)$$

Substituting equations (4.58), (4.59) and (4.510) in (4.32) gives the soil base continuity equation with pH as the working variable

$$-b_{HS}\frac{\partial(pH-1/2pCa)}{\partial t} = \theta f\ \frac{\partial}{\partial r}[-D_{LH}2.303H\frac{\partial pH}{\partial r}-D_{LC}\frac{K^{*}2.303}{H}\cdot\frac{\partial pH}{\partial r}$$

$$-D_{LP}K_2(\frac{1}{H}\cdot\frac{\partial C}{\partial r}+C\frac{2.303}{H}\cdot\frac{\partial pH}{\partial r})]$$

$$+\frac{2}{r}[-D_{LH}2.303H\cdot\frac{\partial pH}{\partial r}-D_{LC}\frac{K^{*}2.303}{H}\cdot\frac{\partial pH}{\partial r}$$

$$-D_{LP}K_2(\frac{1}{H}\cdot\frac{\partial C}{\partial r}+C\frac{2.303}{H}\cdot\frac{\partial pH}{\partial r})] \qquad (4.511)$$

Let $\ell=2.303(D_{LH}H+D_{LC}\frac{K^{*}}{H}+D_{LP}\frac{K_2C}{H})$; grouping terms in $\frac{\partial pH}{\partial r}$

$$b_{HS}\frac{\partial(pH-1/2pCa)}{\partial t} = \theta f\{\frac{\partial}{\partial r}(\ell\cdot\frac{\partial pH}{\partial r})+\frac{\partial}{\partial r}(D_{LP}\frac{K_2}{H}\cdot\frac{\partial C}{\partial r})$$

$$+\frac{2}{r}(\ell\frac{\partial pH}{\partial r}+D_{LP}\frac{K_2}{H}\cdot\frac{\partial C}{\partial r})\}$$

which gives

$$b_{HS}\frac{\partial(pH-1/2pCa)}{\partial t} = \theta f\{(\ell\frac{\partial^2 pH}{\partial r^2}+[\frac{\partial\ell}{\partial r}+\frac{2\ell}{r}+D_{LP}\frac{K_2}{H}\cdot\frac{\partial C}{\partial r}]\frac{\partial pH}{\partial r} \qquad (4.512)$$

$$+D_{LP}\frac{K_2}{H}(\frac{\partial^2 C}{\partial r^2}+\frac{2}{r}\cdot\frac{\partial C}{\partial r})\}$$

The Richtmyer form of the Crank-Nicolson form of equation (4.512) is

$$-W_{Bj}^{\circ}pH_{j+1}^{t}+X_{Bj}^{\circ}pH_{j}^{t}-Y_{Bj}^{\circ}pH_{j-1}^{t} = W_{Bj}^{\circ}pH_{j+1}+(2-X_{Bj}^{\circ})pH_j+Y_{Bj}^{\circ}pH_{j-1}$$

$$+\beta^{\circ}D_{LP}K_2/H_j[(1+\Delta r/r)(C_{j+1}^{t}+C_{j+1})-2(C_j^{t}-C_j)+(1-\Delta r/r)(C_{j-1}^{t}+C_{j-1})]$$

$$-1/2\log(Ca_j^{t}/Ca_j) \qquad (4.513)$$

where $\beta^{\circ}=\theta f\Delta t/(b_{HS}2\Delta r^2)$

$W_{Bj}^{\circ}=\beta^{\circ}[\bar{\ell}+\Delta r/2(\partial\bar{\ell}/\partial r+D_{LP}K_2/H\cdot\partial C/\partial r+2\bar{\ell}/r)]$

$$X_{Pj}^{\circ}=1+2\beta^{\circ}$$

and $$Y_{Bj}^{\circ}=\beta^{\circ}[\bar{\ell}-\Delta r/2(\partial\bar{\ell}/\partial r+D_{LP}K_2/H.\partial C/\partial r+2\bar{\ell}/r)]$$

In the course of a time step in the program, $\bar{\ell}$ (the average value of ℓ over the time step) must be iterated for. In practice iteration is only necessary near the start of the run, and then the value of ℓ converges after a single iteration.

The boundary conditions

(i) at the interface (as for phosphate)

$$F_B = \frac{(a_i-\Delta a)/a_i}{\Delta a}\,\bar{D_{HB}}(pH_1-pH_s) = \frac{(a_i-\Delta r)/a_i}{\Delta r}\,\bar{D_{HB}}(pH_1-pH_0)$$

where $\bar{D_{HB}}$ is the average value of the "soil base diffusion coefficient" in the steady state region. $\bar{D_{HB}}$ between s and 1, and 0 and 1, will be approximately constant as the particle dissolves because the pH gradient in the steady state region will be approximately constant. Thus

$$\frac{(a_i-\Delta a)}{\Delta a}(pH_1-pH_s) = \frac{(a_i-\Delta r)}{\Delta r}(pH_1-pH_0)$$

or $$pH_0 = pH_1(1-R_1)+pH_sR_1$$

where R_1 has the same meaning as above. Thus, as for phosphate

$$E_{B1}^{\circ} = W_{B1}^{\circ}/[X_{B1}^{\circ}+Y_{B1}^{\circ}(1-R_1)] \tag{4.514}$$

$$F_{B1}^{\circ} = \{W_{B1}^{\circ}pH_2+[2-X_{B1}-Y_{B1}^{\circ}(1-R_1)]pH_1+R_1Y_{B1}^{\circ}pH_s^t+ \tag{4.515}$$

$$\beta^{\circ}D_{LH}K_2/H_1(1+\Delta r/r)(C_2^t+C_2)-2(C_1^t+C_1)+(1-\Delta r/r)(C_0^t+C_0)]$$

$$-1/2\log(Ca_1{}^t/Ca_1)\}/[X_{B1}^{\circ}-Y_{B1}^{\circ}(1-R_1)]$$

and (ii) at the boundary with adjacent particles

$$H_R^t = F_{BR}^{\circ}/(1-E_{BR}^{\circ}) \tag{4.516}$$

4.6 The Method of Programing

The program, written in FORTRAN, is reproduced in appendix B.

In the course of a time step, the following series of operations is performed:

(1) The phosphate profile is calculated assuming $C_{Ls}{}^{t}=C_{Ls}$.

(2) The soil base profile is calculated using the new set of values for C_L and $[Ca^{2+}]_L$, and assuming $pH_s{}^{t}=pH_s$.

(3) Step (2) is repeated with the new values for $\bar{\ell}_j$ until the values are constant.

(4) The true values of $C_{Ls}{}^{t}$ and $pH_s{}^{t}$ are found from equation (4.56) and the solubility product relationship, and the process repeated from stage (1) if the values are different from those used originally in stage (1).

In practice iterations in the calculation are only necessary for the first few time steps.

Initially, Δa is extremely small so that very large and very small numbers would be generated in calculating the boundary concentrations and the program would fail. This can be avoided by assuming $\Delta a=0$ until an appreciable amount of material has dissolved, so that $C_{L1}=C_{Ls}$ et cetera.

The total quantity dissolved after a particular time is found by keeping a running total of the amounts dissolved in individual time steps. Thus

$$M_t = \sum_{0}^{t} [4\pi D_{LP}\theta f a_i(a_i-\Delta a)/\Delta a(C_{Ls}-C_{L1})]\Delta t$$

For the numerical solutions to be stable, the model needed smaller

distance and, consequently, time steps than the planar model, owing to the intricacy of the surface boundary condition. This was, however, acceptable because the spread of material was smaller. Optimal values were 10^{-4}dm for the distance steps and time steps of 10^{2}s increasing to 10^{3}s after 0.1% of the particle had dissolved. Halving these values made no difference to the results showing that the finite-differencing was satisfactory.

As a check on the program, the total amount, M_t, of phosphate dissolved after a particular time with the surface concentration and the effective phosphate diffusion coefficient held constant, was compared with the value obtained using an analytical solution of equation (4.31), with these constraints:

$$M_t = \sum_{0}^{t} b_P (C_{Ls}-C_L')4\pi(a_i-\Delta a)^3 \left[\left(\frac{D_{LP}\theta f/b_P}{\pi(a_i-\Delta a)^2 t}\right)^{1/2} + \frac{D_{LP}\theta f/b_P}{(a_i-\Delta a)^2}\right]\Delta t \qquad (4.61)$$

where b_P is the phosphate buffer power and C_L' the concentration of $H_2PO_4^-$ in the native soil solution (derivation given in appendix C). The values agreed to within 0.1%. A similar check could not be made on the soil base profile, but the amounts of phosphate and base dissolved, as calculated using Simpson's rule, were equal, showing that the solution of equation (4.32) was also accurate.

The program requires 10 minutes of CPU time to simulate 32 days of dissolution.

The Predicted Concentration Profiles

Fig. 4.2 shows the predicted pH and total calcium and phosphate profiles after 96 hours of dissolution. The total amounts of calcium and phosphate dissolved are given by the integrals, with respect to distance, of concentration x $4\pi r^2$. The total amount of base dissolved is given by the distance integral of $b_{HS}(pH-1/2pCa)4\pi r^2$. Although the concentration of calcium in the soil near the surface is very much greater than the concentration of phosphate, the total amounts of each component dissolved are in the ratio 1:1:1, in accord with equations (2.31) and (2.32).

The phosphate profile is less stunted than in the planar system because the solution concentration gradients are much steeper (compare Figs. 2.7 and 4.4): with increasing r, the volume of a section of soil increases in proportion to r^3 so that, compared to the planar system, a greater flux of material between adjacent sections of soil is required to maintain continuity. Thus the spherical profiles are steeper and have longer tails.

Fig. 4.3 shows the effect of the receding surface boundary on the phosphate profiles. At the rate of application used (which corresponds to a uniform field application of 120 kg of DCPD per ha - see section 6.0), the spheres of influence of adjacent particles overlap within 4 days. After this time, reflection of material back from the point of overlap greatly effects the shape of the profiles.

A higher pH was used for the experiments with granules of DCPD than for the planar experiments (see chapter 5). The increased role of HCO_3^- in the propagation of base at the higher pH can be seen in Fig. 4.4. The

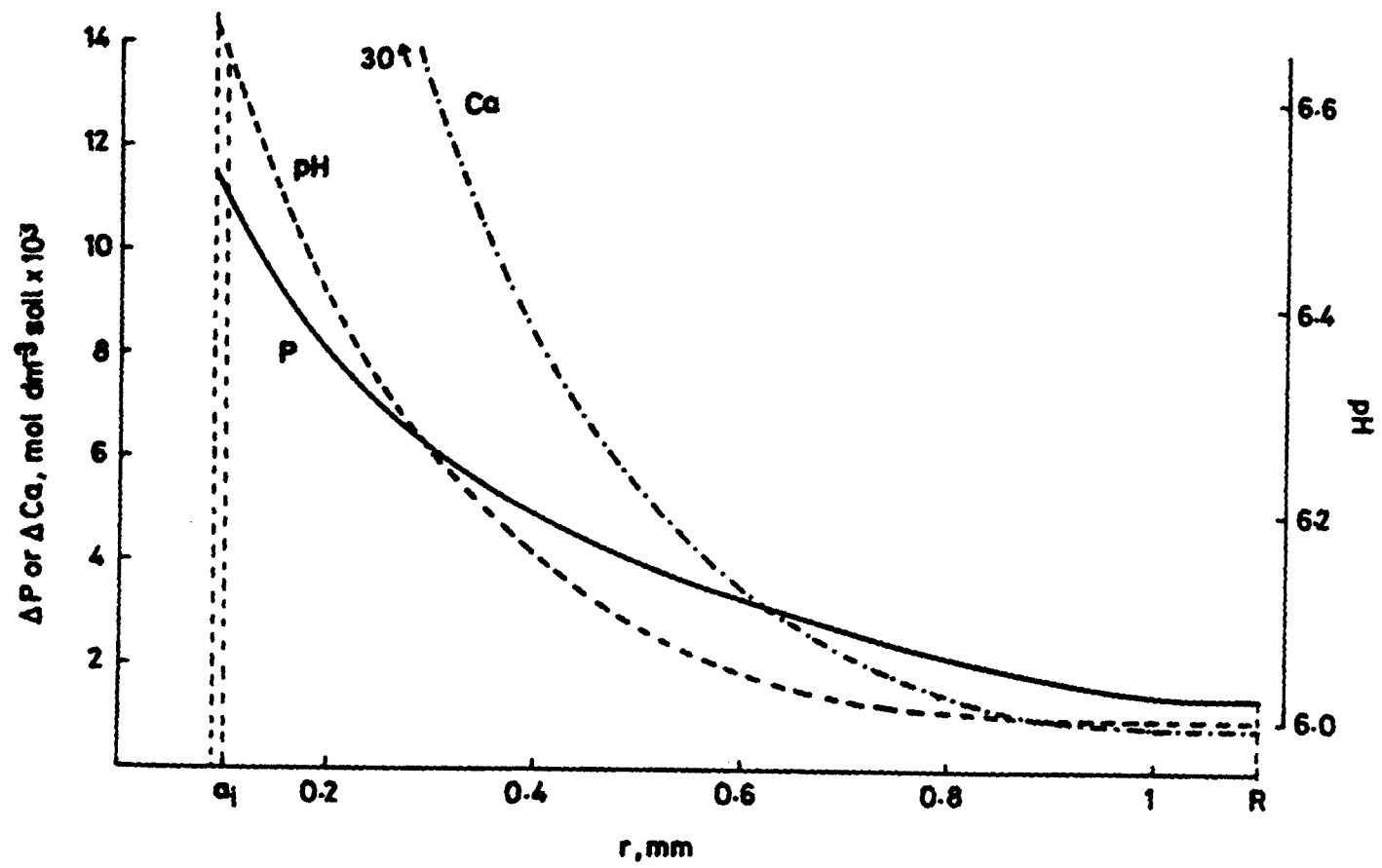


Fig. 4.2. Profiles of pH and changes in total concentrations of phosphate and calcium after 96h. $\theta f=.05$, $a=.2$, $b=.3$, $b_{HS}=.1$, native soil pH=6.0, $a_i=10^{-3}$dm, $R=10^{-2}$dm.

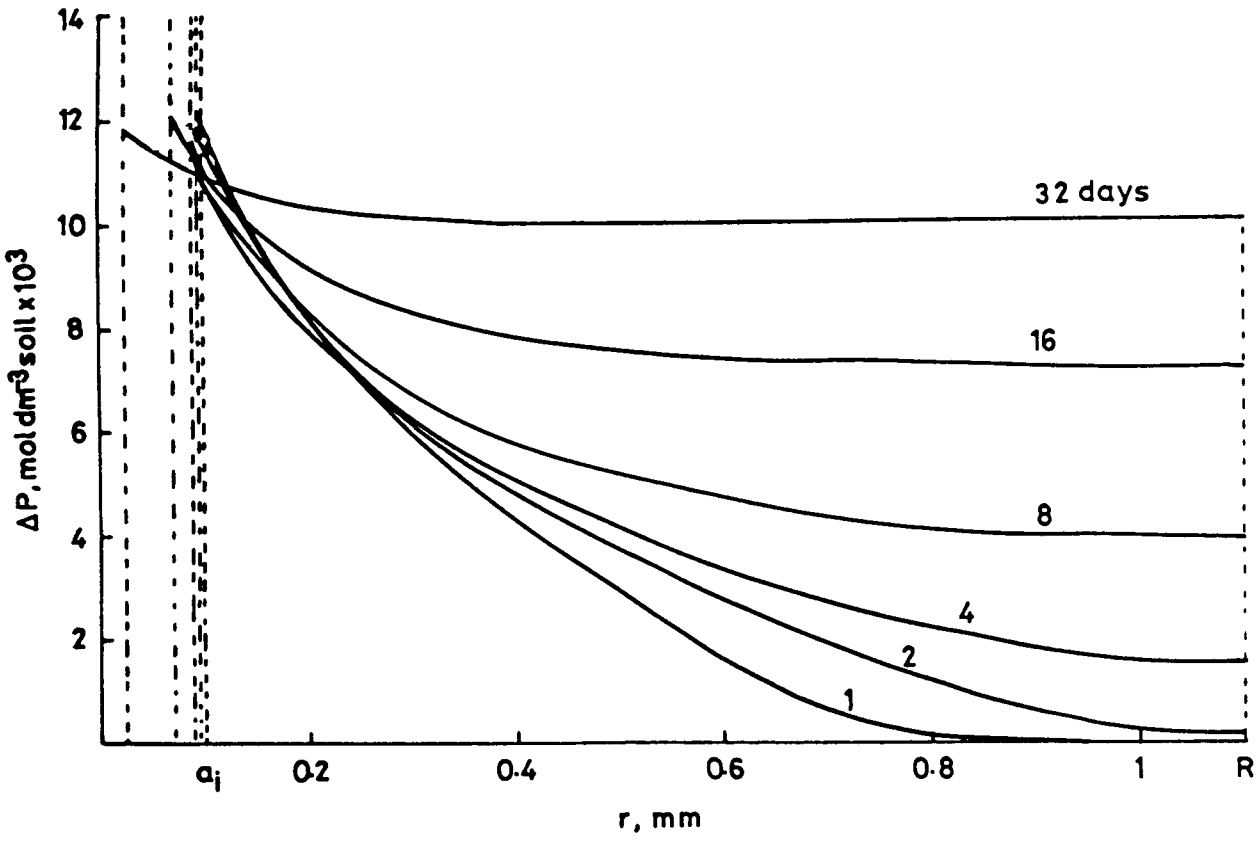


Fig. 4.3. Total phosphate profiles at different times showing the effect of the receding boundary. Values of soil and particle variables as in Fig. 4.2

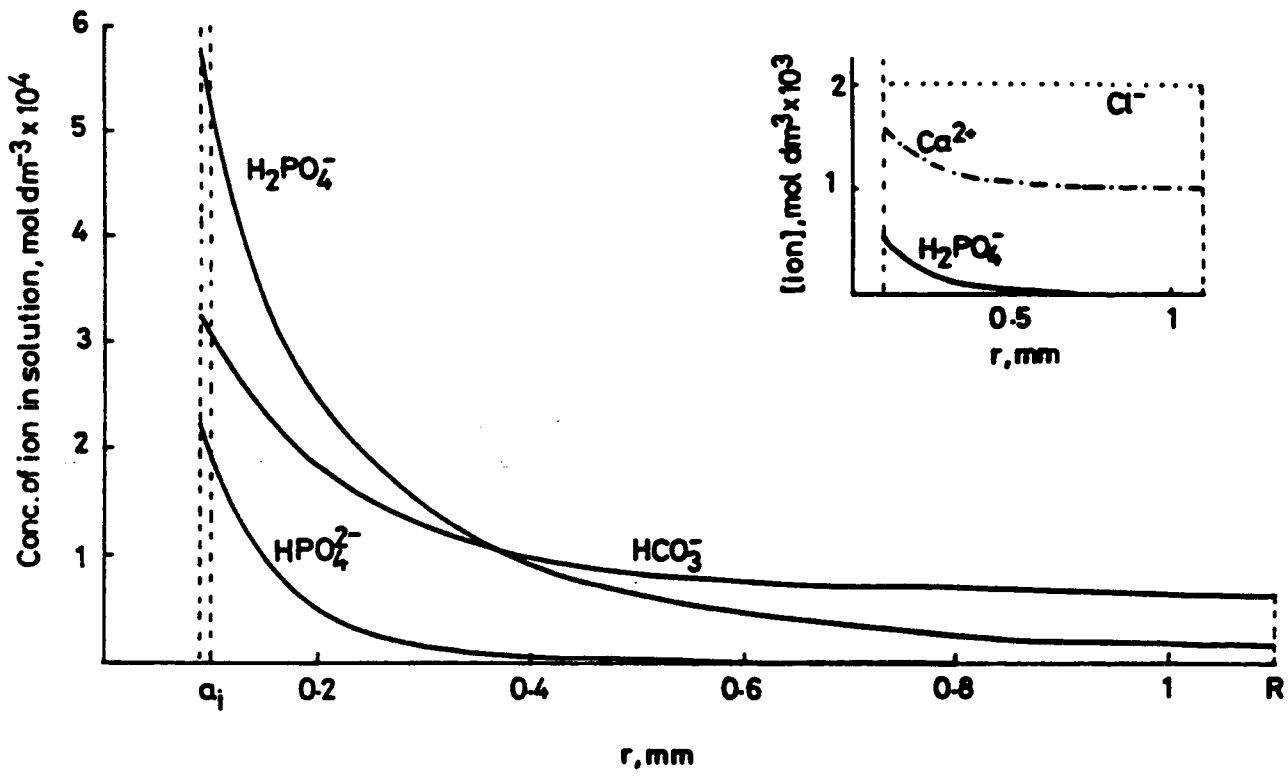


Fig. 4.4. Profiles of major ions in solution after 96h. Values of soil and particle variables as in Fig. 4.2.

increase in HPO_4^{2-} relative to $H_2PO_4^-$ should also be noted. The H_2O-H_3O^+ pair is relatively unimportant at this pH.

A full sensitivity analysis of the model is given in chapter 6.

5

EXPERIMENTAL ASSESSMENT OF THE GRANULAR MODEL

This chapter is concerned with the experimental assessment of the model of the dissolution of granules of DCPD in soil. It is not feasible to measure the solute concentration gradients near the dissolving surface, as for the planar system, but one can measure the net rate of dissolution, either by recovering the undissolved material or by measuring the amount of dissolved material in the soil.

A commonly used method (Muller, 1977) for separating mixtures of minerals is to shake the mixture with a heavy liquid whose density is intermediate between the densities of the mineral to be separated and the other components of the mixture; thus the wanted mineral either sinks or floats in the liquid whilst the unwanted material reacts in the reverse manner. The same principle may be applied to the present problem, the density of DCPD (2.306) being lower than that of most soil components. Accordingly I attempted to separate fine particles of DCPD from moist soil by air drying the mixture and shaking it in tetrabromoethane (ρ=2.964) diluted with ethanol to ρ=2.4. However, it was not possible to obtain a complete separation of the undissolved material from the soil, largely because the DCPD was so fine that it became trapped under the larger, denser soil particles. The material that did float to the surface was mixed with fine organic matter. [This method did, however, work well for the separation of 100 μm particles of Gafsa rock phosphate (ρ=3.20) from moist soil]

The final method used was based on that of Abdou and Larsen (1964) who measured the rates of dissolution of an assortment of sparingly soluble phosphates by labelling their samples with ^{32}P and extracting the

dissolved ^{32}P in phosphate solutions saturated with the mineral. The basis of the method is that if there is no pH change on extraction, no additional material will dissolve in the saturated extractant, but effectively all the exchangeable, dissolved ^{32}P will be recovered from the soil. However, an increasing proportion of the dissolved ^{32}P will become non-exchangeable as it is fixed by the soil, and thus it is necessary to assess a correction factor for the extraction which introduces a degree of uncertainty. This problem can be avoided if one is only interested in calcium phosphates and can therefore use ^{45}Ca as the label in place of ^{32}P, because Ca does not become non-exchangeable. Thus the assessment of the rate of dissolution is direct.

5.1 Preparation of the Soil

Soil at pH 3.5 was used in the planar system so that a measureable spread of solutes would be obtained in a reasonable time. But individual particles of DCPD will dissolve too rapidly at this pH for the rate to be measured. So for the particle experiments, Bagley Wood soil was limed to about pH 6, as described below. It is assumed that the lime potential and phosphate buffer capacities of the soil are unaffected by the treatment, as expected from the results given in chapter 3.

Method

30g of Analar $CaCO_3$ (corresponding to 0.6 mol of OH^-) was added to 2kg of air dry soil and mixed in well. From the lime potential buffer capacity (fig. 3.5), this was known to be sufficient lime to raise the pH by about two units. The soil was then moistened to θ_g=0.3 and incubated at 20°C for 10 days. From the work of Ameloko (1983), this was known to be long enough to ensure complete dissolution of the lime. The incubated

soil was air dried and resieved to <212 μm, breaking up any clods so that all the material passed through the sieve.

5.2 Preparation of Labelled DCPD

Large spherical granules of DCPD are required, so the method used in Chapter 3 is not suitable. In the method described below, a low rate of precipitation with no stirring produces large agglomerates of crystals.

Method

200 cm^3 of a solution saturated with NaH_2PO_4 were poured onto 50 cm^3 of 0.68 mol dm^{-3} $CaCl_2$ labelled with ^{45}Ca, in a wide bottomed flask. An activity of 0.1 mCi per g of Ca is sufficient for the present purposes (see below), corresponding to 500 μCi in 200 cm^3 of 0.68 mol dm^{-3} $CaCl_2$. The mixture was seeded with a small quantity of fine crystals of DCPD and allowed to stand for two days, whereupon a mat of crystal agglomerates formed at the bottom of the flask. This was separated from the reaction mixture by filtration, washed several times with water and acetone, and dried gently. The Ca:P ratio of the product was 1:1 as expected, and K_{SP} 2.00 x 10^{-7} (see section 3.4). The yield was about 20% on a moles of calcium basis.

The dried product was gently ground to give variously shaped particles ranging in size from <30 μm to 700 μm. These were rendered approximately spherical using the device shown in fig. 5.1. In this procedure, a stream of compressed air entering tangentially at the side of the chamber causes the particles to be dashed against the glass-paper lined walls. Within a few minutes they are chipped into rough spherical form. Three size fractions of particles were prepared by sieving the spherical material so

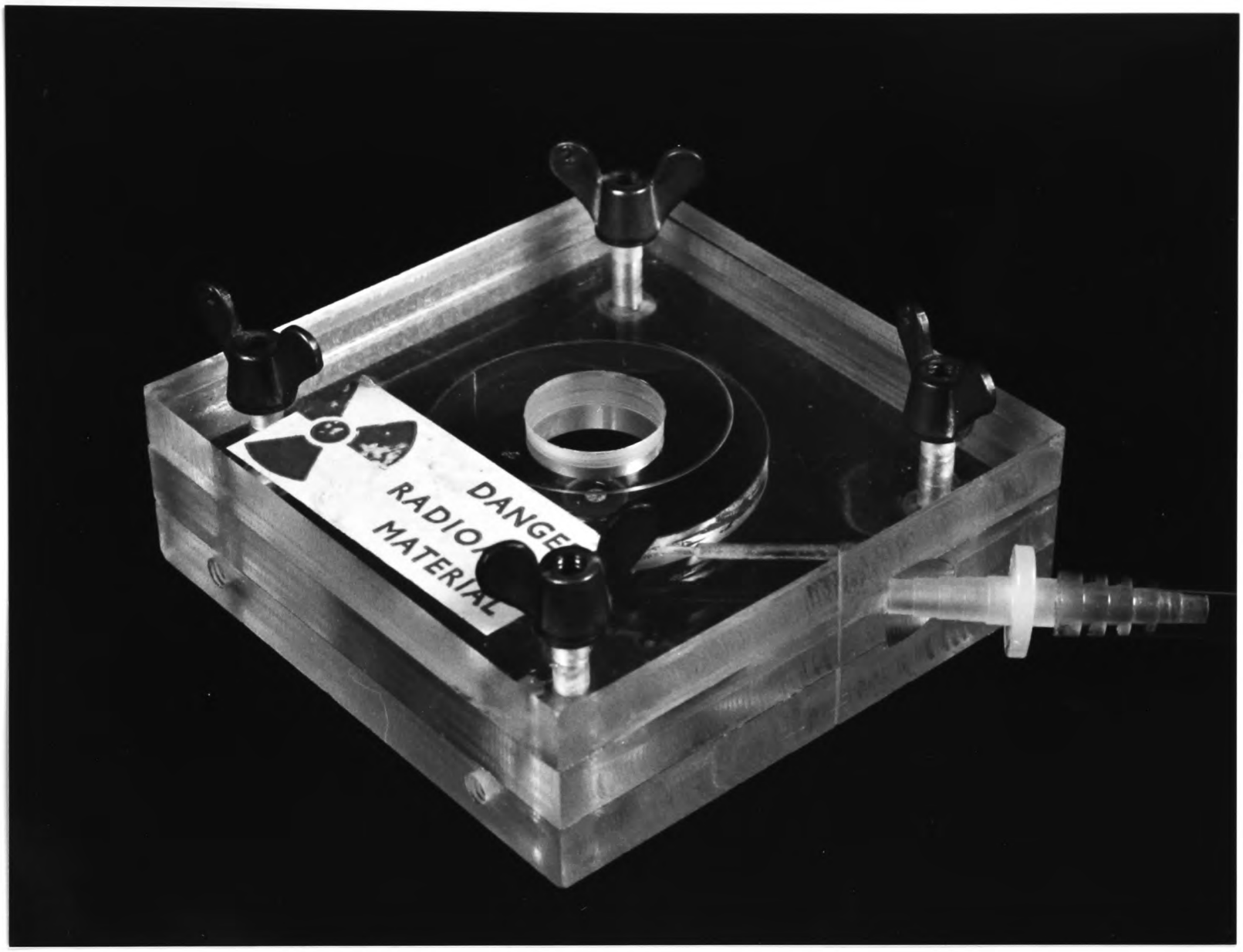


Fig. 5.1. Device for rendering particles spherical.

produced - 38-45 μm, 105-150 μm and 425-500 μm (diameters).

The stereo-photograph of 425-500 μm diameter particles (fig. 5.2) shows that their gross dimensions are approximately equal in all directions but that the surfaces are irregular. The maximum depth of the irregularities is about 100 μm. But the soil solution in the irregularities will quickly be filled with dissolved material : the spread of material in time t is approximately equal to $(D_{eff}t)^{1/2}$, thus if $D_{eff}=1x10^{-10} dm^2 s^{-1}$, $(D_{eff}t)^{1/2}=100$ μm in 10^4s, ie. less than 3h. Thus the particles are effectively spherical.

5.3 Incubation of Particles with Soil

Method

Particles of DCPD were uniformly mixed with air dry soil at a rate of 100 mg of DCPD per 50g of soil. Samples were mixed in duplicate for the three particle size fractions. The mixtures were moistened to $\theta_g=0.3$ with 10^{-3} mol dm^{-3} $CaCl_2$ + 50 mg dm^{-3} $HgCl_2$, and packed to $\rho=1.4$ in perspex cells, 3.5 cm deep by 1.5 cm internal radius. The cells were incubated at 20°C in a moisture saturated atmosphere with a constant P_{CO_2} of 0.005 atm. The ends of the cells were left open to allow gaseous exchange. Runs were conducted for 1, 2, 4, 8 and 16 days.

5.4 Extraction of the Dissolved Calcium

The amount of Ca in the extractant must be large compared to the amount of exchangeable ^{45}Ca on the soil so that isotopic exchange is effectively complete; but if the Ca concentration in the extractant is too high, the lime potential of the suspension will be raised, precipitating DCPD. For

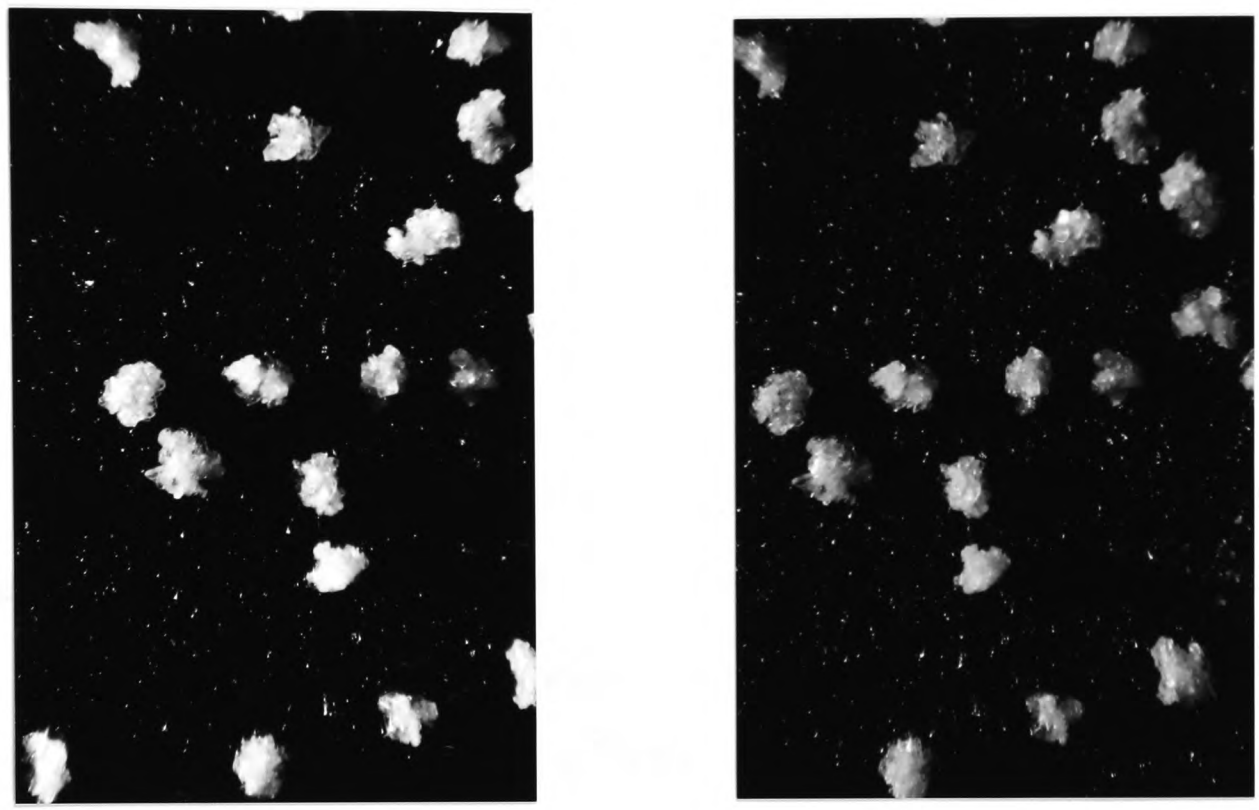


Fig. 5.2. Stereo-photograph of spherical particles of DCPD, prepared by the method described in section 5.2 (a_i=2.3x10^{-3}dm).

this reason, a high solution:soil ratio is desirable, but the ratio must not be so high that the extracted ^{45}Ca is excessively diluted.

Method

The extractant composition was 0.01 mol dm^{-3} with respect to $CaCl_2$ and 0.002 mol dm^{-3} with respect to NaH_2PO_4 at pH 6.0. From equations 2.31 and 2.32 and calculating activity coefficients with equation 2.416, this was known to be a saturated solution. A solution:soil ratio of 20:1 (ie. approximately one quarter of the contents of a cell in 100 cm^3 of extractant) and shaking time of 2h were optimal. This gave complete recovery of ^{45}Ca incubated with soil as $CaCl_2$. No ^{45}Ca was recovered from dry mixtures of $D^{45}CPD$ and soil extracted immediately, showing that none of the mineral dissolved in the extraction.

For counting, the extractant/soil suspensions were centrifuged at 5000 rpm for 10 minutes and filtered. 1.5 cm^3 aliquots were added to 15 cm^3 of scintillant in disposable plastic vials, and counted on a Beckman 1650 Liquid Scintillation System. The scintillant was Butyl PBD in a 4:6 mixture of "Triton" and toluene. Standards were obtained from extracts of soil in which a known quantity of $D^{45}CPD$ had dissolved. This was prepared by incubating soil with 10^{-3} mol dm^{-3} $CaCl_2$ containing $D^{45}CPD$ dissolved in the minimum of acid. Thus the colouration of the extractant by dissolved organic matter was accounted for. The quantity of ^{45}Ca extracted if 5% of the added DCPD dissolved, corresponded to about 200 counts per minute.

Results and Comparison with the Model Predictions

Fig. 5.3 shows the experimental results and the model predictions. There are a number of possible sources of error : a) the particles may not be perfectly spherical; b) each particle size group contains a range of sizes whereas the model assumes a single particle size; c) the particles may be partially broken-up on mixing with the dry soil; d) non-uniform distribution of particles in the soil would result in slowed dissolution where particles are clumped. In view of these possible errors, the agreement between the observed and predicted results is very good and therefore the model works well under these conditions. To obtain data at a lower soil pH, the method was used to measure the rate of dissolution of particles in soil limed to only pH 4.5. However the results were spurious because an excessively concentrated extractant was needed for saturation at the lower pH, and the high phosphate concentration caused excessive dissolution of soil organic matter which interfered with the ^{45}Ca assay. But since the model worked well for the planar system at a lower pH (3.5), one may conclude that the spherical model will be effective over the range of acid pHs.

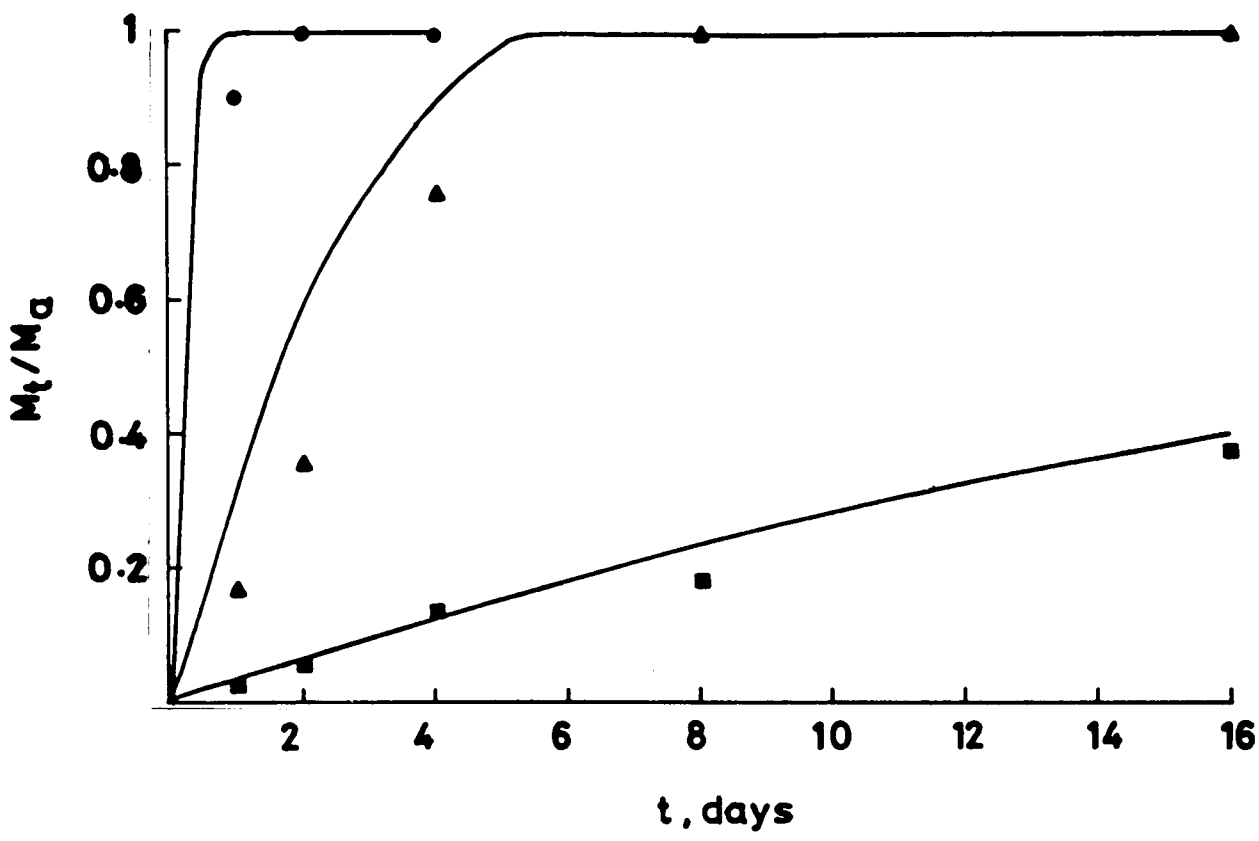


Fig. 5.3. The observed rates of dissolution of (●) 38-45 μm, (▲) 105-150 μm, and (■) 425-500 μm diameter partcles, and (——) the corresponding model predictions. Native soil pH 6.0, θ=.42, ρ=1.4, f=0.28

6

APPLICATIONS OF THE MODEL

The model satisfactorily describes the experimental data for a range of soil conditions (planar at pH 3.5 and granular at pH 6) and particle sizes. Thus all important processes have been accounted for. Since the model parameters were measured by independent experiment and no arbitrary assumptions were made, the model predictions are absolute.

This chapter is concerned with the sensitivity of the model to its input parameters, and identifying any interactions between them.

Sensitivity Analysis

a) Soil Variables

Fig. 6.1 shows how the rate of dissolution depends on the various soil variables in the model. The standard inputs were chosen to represent the mid point of the range of soil conditions found in practice; the extreme values were chosen to represent realistic extremes. The values of the standard inputs are: Freundlich a=0.2, Freundlich b=0.3, b_{HS}=0.1 mol kg^{-1} soil $(pH-1/2pCa)^{-1}$, θf=0.05, pH'=6.0, P_{CO_2}=0.005 atm, $[Ca^{2+}]_L'=1x10^{-3}$mol dm^{-3}, $C_L'=5x10^{-6}$mol dm^{-3}, $a_i=1x10^{-3}$ dm, $R=1.1x10^{-2}$dm. The effects of the individual variables are now discussed in turn.

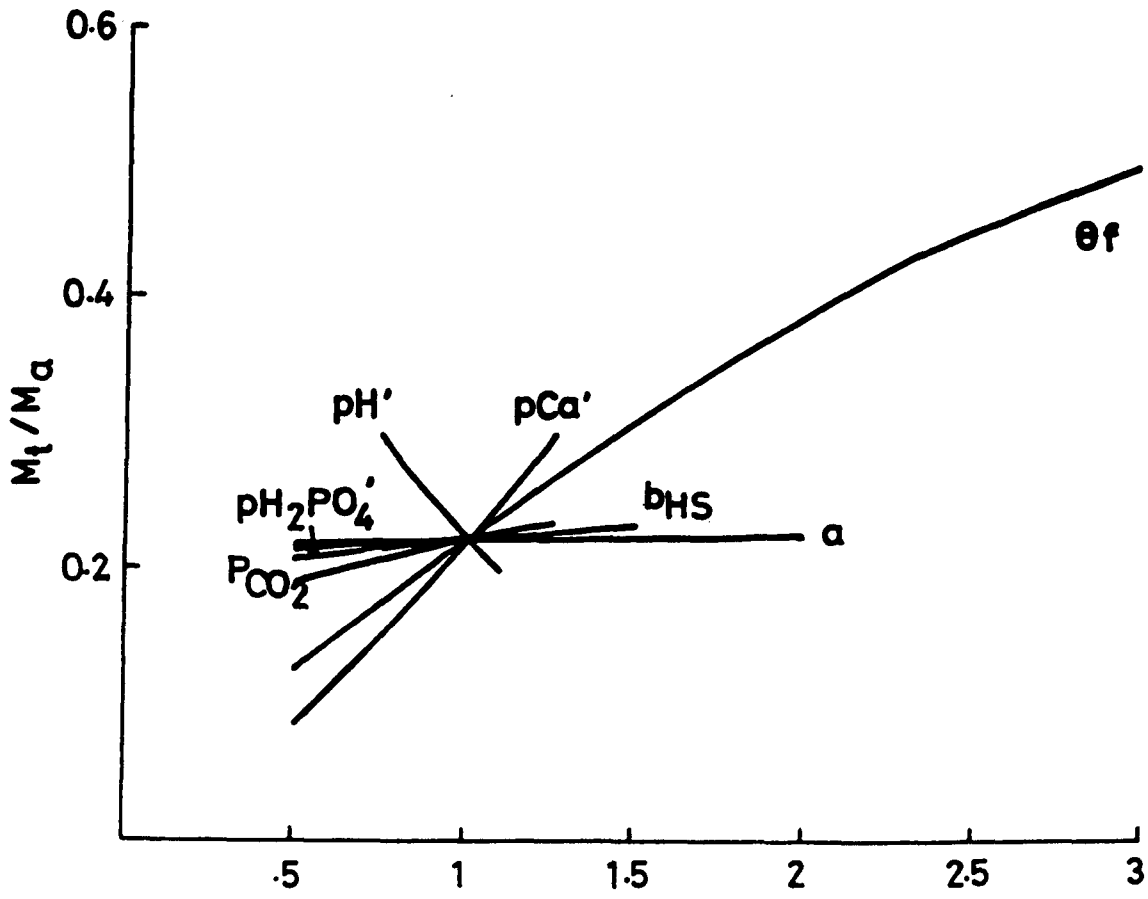


Fig. 6.1. Effect of soil variables on the fraction of DCPD dissolved after 4 days. M_a is the amount of DCPD added.

Standard values are: Freundlich a=0.2, Freundlich b=0.3, b_{HS}=0.1 mol kg^{-1} soil $(pH-1/2pCa)^{-1}$, θf=0.05, pH'=6.0, P_{CO_2}=0.005 atm, $[Ca^{2+}]_L'=10^{-3}$ mol dm^{-3}, $C_L'=5\times10^{-6}$ mol dm^{-3}, $a_i=10^{-3}$ dm, $R=1.1\times10^{-2}$ dm.

6.1. The phosphate sorption parameters

A characteristic of the spherical geometry is that the region close to the granule surface quickly approaches a steady state in which the rate of dissolution is controlled by more or less constant concentration gradients in this region. This can be appreciated by noting that, from one time step to the next, the diffusion front is reaching increasingly large volumes of soil and thus increasingly large amounts of solute are required to maintain a given concentration in solution. Thus most of the material dissolved in a time step is used to "feed" the diffusion front and the rate of dissolution is controlled by the rate of diffusion through the solution to the front. The rate is therefore not greatly sensitive to changes in the soil buffer terms which determine the concentration of solute on the soil solid for a particular concentration in solution (fig. 6.2 at times less than 4 days and figs. 6.3 (a) and (c)). This steady state is disrupted once adjacent particles have begun to influence each other and solute is being reflected back from the point of overlap. The concentration gradients in solution are therefore no longer constant at a given value of r, and so the effect of the buffer capacities is apparent (fig. 6.2 at times exceeding 4 days and figs. 6.3 (b) and (d)).

This finding is practically important because, in circumstances where overlap occurs only after a very long time (see section 6.9), the rate of dissolution can be accurately predicted without very precise measurements of the buffer terms.

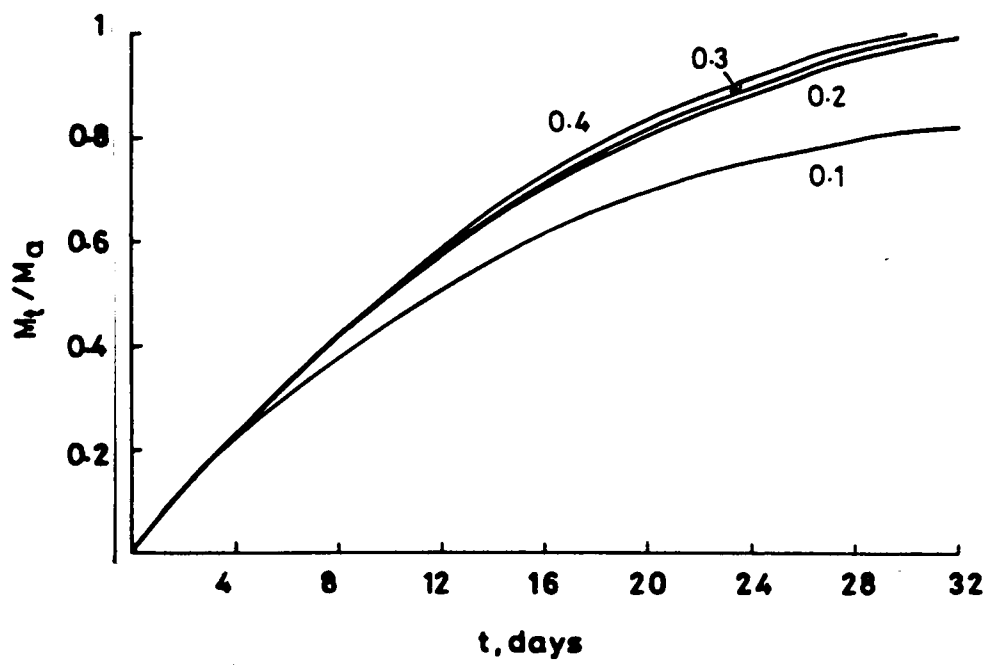


Fig. 6.2. Effect of Freundlich a parameter on the rate of dissolution. Other variables as standards in Fig. 6.1.

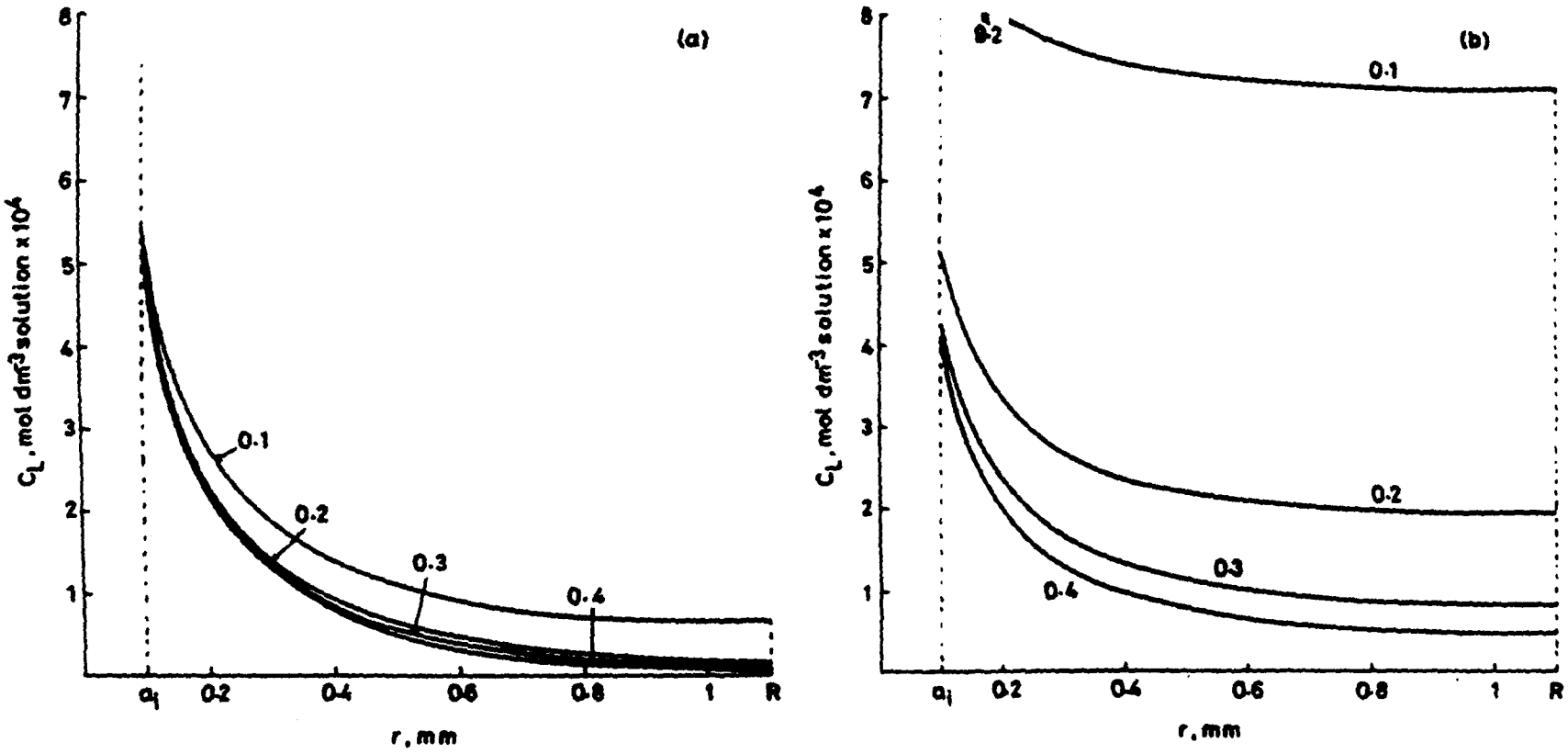


Fig. 6.3. Effect of Freundlich a parameter on the concentration profiles of phosphate in solution after (a) 4 days and (b) 16 days, and on the concentartion profiles of phosphate in the whole soil after (c) 4 days and (d) 16 days. Other variables as standards in Fig. 6.1.

6.2. The lime potential buffer capacity

The effect of varying the lime potential buffer capacity can be seen in fig. 6.1. As with the phosphate buffer capacity, the rate of dissolution is not very sensitive to b_{HS} in the early stages because it is controlled by approximately steady state concentration gradients near the granule surface. With the standard input values, the spread of base is slower than the spread of phosphate and therefore, overlap of neighbouring base profiles occurs after overlap of phosphate profiles (see figs. 6.10 (a) and (b)). Thus the effect of b_{HS} becomes apparent later than the effect of the phosphate buffer terms.

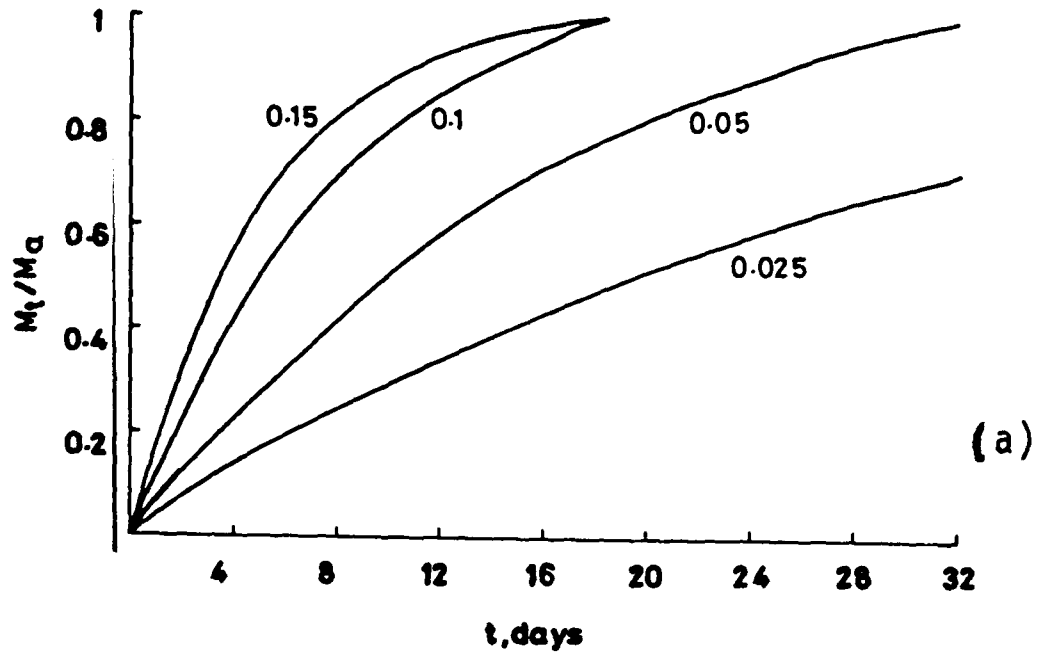
6.3 The soil moisture content and impedance factor

The impedance factor increases approximately linearly with the soil moisture content (Nye, 1979) - for the present soil the relationship $f=0.9\theta-0.1$ is approximately correct. Over the field moisture range the product θf varies from 0.1 to 0.001 (Nye, 1979).

Because I have assumed the moist soil bulk density, ρ, to be constant with varying θ, the dry bulk density varies with θ and, consequently, so do the buffer terms (see section 3.2). Thus the total solute concentrations in the soil at a given soil solution concentration change as a fuction of θf. This would not be the case if the dry bulk density remained constant on wetting the soil, whence ρ would vary. For most soils, the true situation would be between these two extremes.

An increase in θf results in increased fluxes of phosphate and base into the soil and consequently a greater rate of dissolution and spread of solutes (fig. 6.4(b)). The solute concentrations in solution at the particle surface are not influenced by θf because the fluxes of phosphate, base and calcium are affected equally.

Once overlap has occured, the rate of dissolution decreases as material is reflected back from the point of overlap, reducing the concentration gradients in solution. This occurs most rapidly at high values of θf because the solute fluxes are higher. At higher values of θ, the buffer terms are smaller and thus a given volume of soil can accomodate less dissolved material, and the reduction in rate caused by overlap occurs when less DCPD has dissolved. Indeed the time taken for particles to dissolve completely at $\theta f=0.15$ was greater than at $\theta f=0.10$ (fig. 6.4(a)).



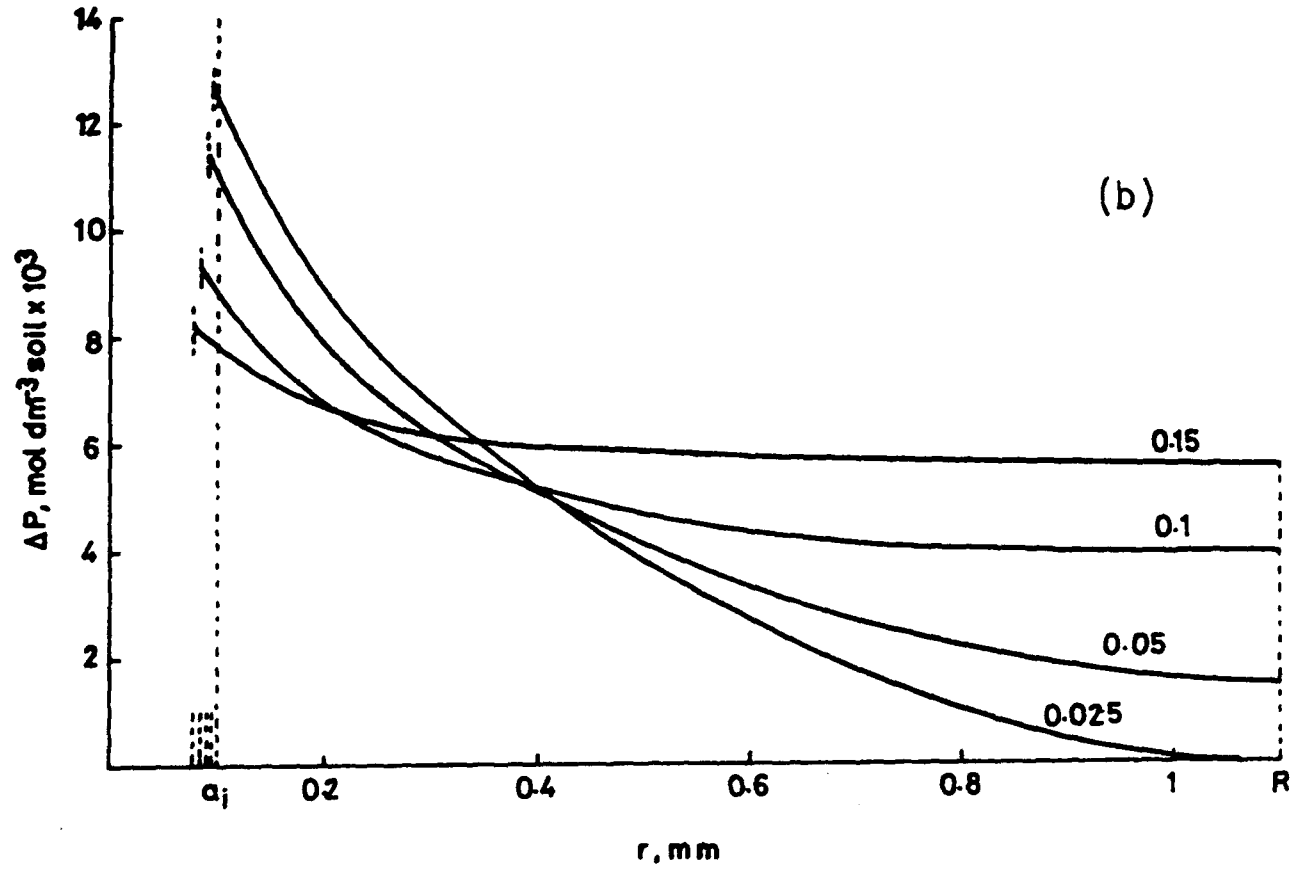
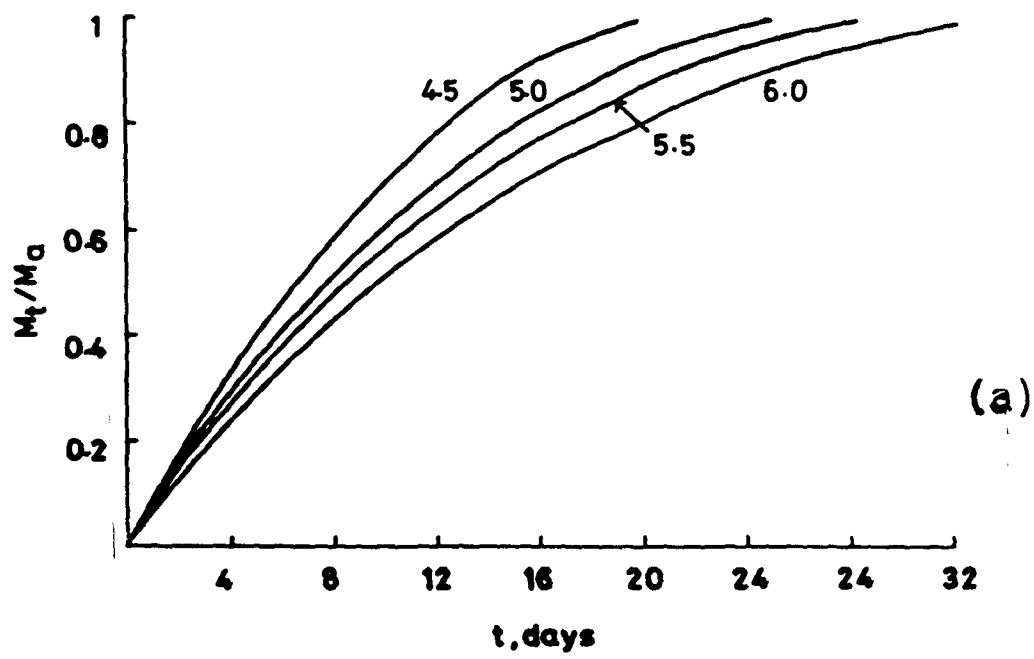


Fig. 6.4. Effect of θf on (a) the rate of dissolution and (b) the phosphate concentration profiles in the whole soil after 4 days. Other variables as standards in Fig. 6.1.

6.4 The initial soil pH

pH' has two separate effects on the rate of propagation of base into the soil. First it affects the amount of base already in the soil and hence the concentration gradients controlling the diffusion of basic ions. Secondly it affects the value of the apparent soil base diffusion coefficient (D_{HB}) which has a minimum value at about pH 5 where the contributions of the pairs H_2O-H_3O^+ and HCO_3^--H_2CO_3 are minimal. D_{HB} increases markedly either side of this pH. Thus the pH at the surface falls only slightly as the native soil pH changes from 6.0 to 4.5 (fig. 6.5 (a)). In consequence, over the range of pH's of practical interest (4.5 to 6.5), the rate of dissolution of DCPD is less sensitive to pH than might be expected.

A comparison of fig. 6.5 (b) with fig. 2.10 shows that the pH rise at the mineral surface is slightly higher in the granular system than for the corresponding conditions in the planar system. This is a consequence of the greater fluxes of material near the surface in the spherical system (section 4.3) : a high flux of phosphate results in a low concentration of $H_2PO_4^-$-HPO_4^{2-} resulting in a low D_{HB} which in turn results in a high pH.



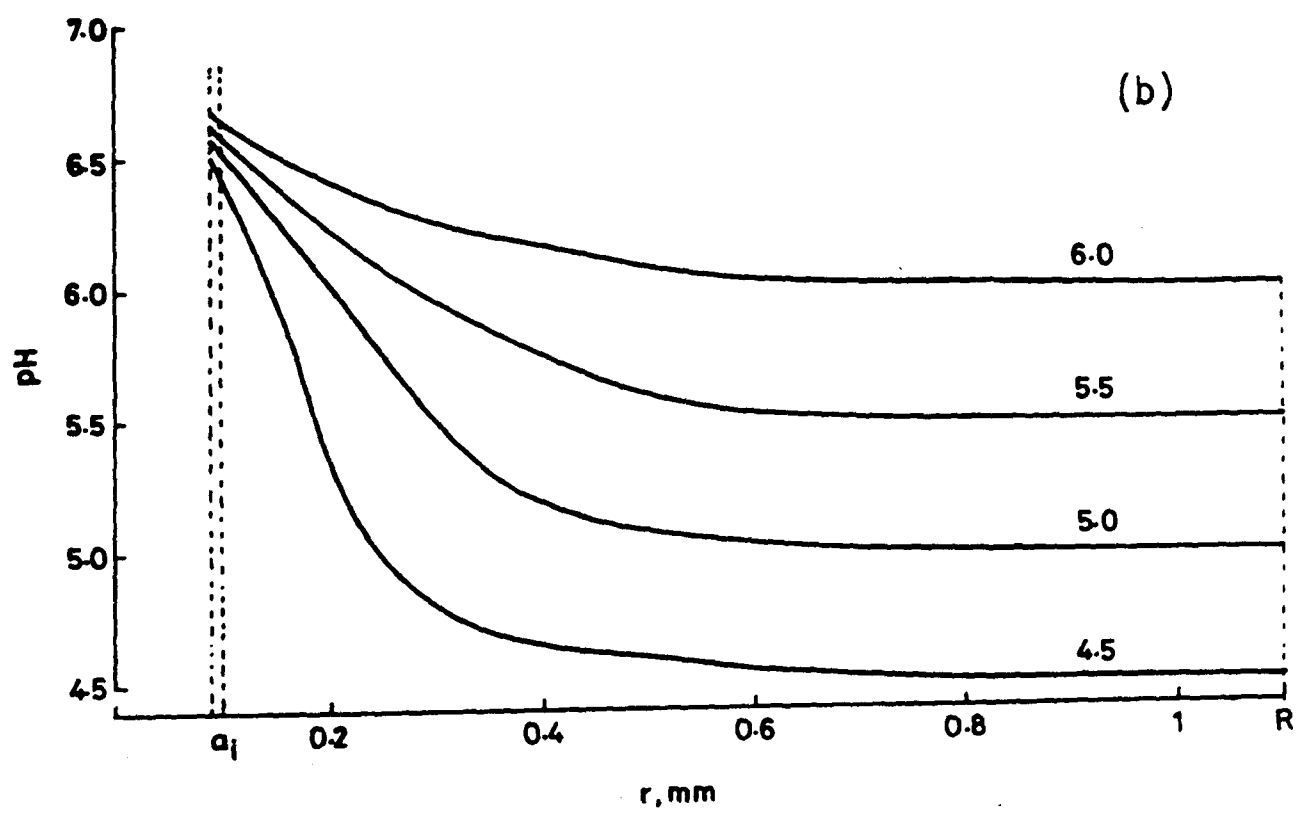


Fig. 6.5. Effect of initial soil pH on (a) the rate of dissolution and (b) the pH profiles after 4 days. Other variables as standards in Fig. 6.1.

6.5 The pressure of carbon dioxide

Since $[HCO_3^-]_L$ is directly proportional to the pressure of CO_2, at pH's greater than 5 the soil base diffusion coefficient is very sensitive to P_{CO_2}. At lower P_{CO_2} values, D_{HB} will be lower thus the pH rise at the surface will be higher and the rate of dissolution less. This will be to some extent offset by the effect of the reduction in $[HCO_3^-]_L$ on $[Ca^{2+}]_L$ which would tend to increase the rate of dissolution. But since $[HCO_3^-]_L$ is small compared with the concentrations of the other anions in solution (especially Cl^- and $H_2PO_4^-$), this effect will be small.

Typically P_{CO_2} varies in the range 0.002 to 0.005 atm in arable top soils. At P_{CO_2}=0.002 and with the other inputs as standard, 15% less DCPD was dissolved after 4 days than at P_{CO_2}=0.005 (fig. 6.1).

6.6 The initial calcium concentration in solution

Fig. 6.6 shows the effect of $[Ca^{2+}]_L'$ on the rate of dissolution. High $[Ca^{2+}]_L$ at the DCPD surface results in a low concentration of phosphate in accord with the solubility product, and hence a low rate of dissolution. Additionally, $[Ca^{2+}]_L'$ influences the propagation of base into the soil - a low value increases the gradient in lime potential and hence the flux of base. A high flux of base leads to a high flux of phosphate.

In opposition to these effects is the affect of $[Ca^{2+}]_L'$ on the ionic strength of the surface solution. The ionic strength controls the activities of all the ions in equilibrium with the DCPD and so strongly influences the rate of dissolution. A high value of $[Ca^{2+}]_L'$ gives a high ionic strength and thus low ionic activities. Hence an increase in $[Ca^{2+}]_L$ at the surface from 10^{-3} to 10^{-2} mol dm^{-3} (ie. ten-fold), at pH 6.0, produces only a seven-fold reduction in C_L.

6.7 The initial phosphate concentration in solution

$[H_2PO_4^-]_L'$ has no significant effect on the rate of dissolution below 10^{-4} mol dm^{-3} since it is small compared to the surface concentration. In all practical situations, $[H_2PO_4^-]_L'$ will be less than 10^{-4} mol dm^{-3} and therefore will not greatly influence the rate of dissolution.

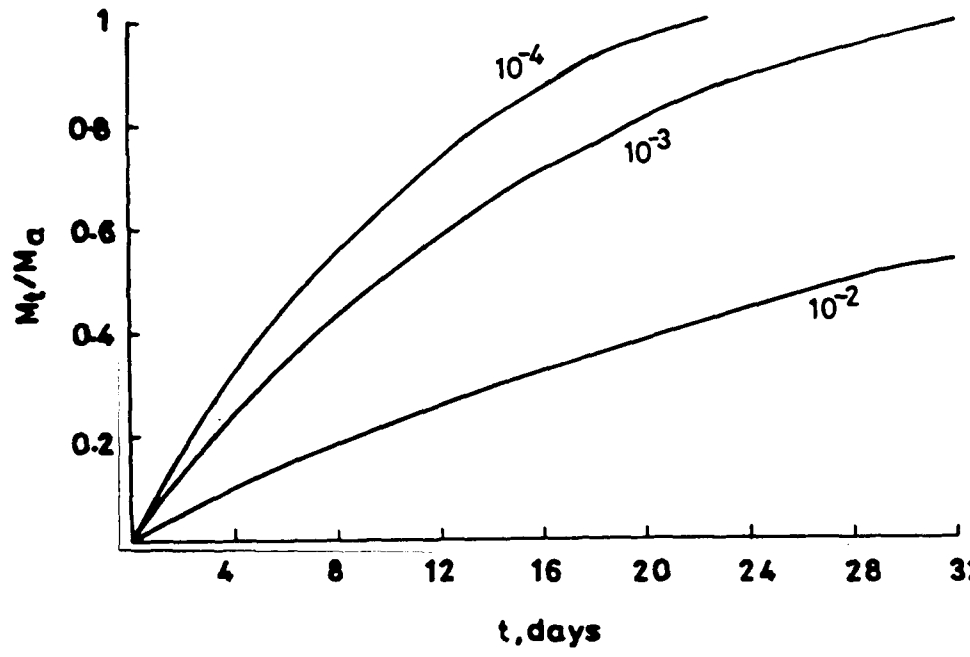


Fig. 6.6. Effect of the initial calcium concentration in the soil solution on the rate of dissolution. Other variables as standards in Fig. 6.1.

b) Management Variables

The effect of management variables (ie. particle size and rate of application) on the rate of dissolution is summarised in fig. 6.7. Sections 6.8 and 6.9 are concerned with the individual effects of particle size and rate of application, and the interactions between them.

6.8 Particle size

The effect of particle size on the rate of dissolution can be appreciated from equation (4.61) which approximately describes the system when the particles do not overlap. After a short time period

$$(D_{eff}t/\pi a_i^2)^{1/2} << D_{eff}t/a_i^2$$

where $D_{eff}=D_{LP}\theta f/b_p$. Thus equation (4.61) reduces to

$$M_t = b_p(C_{L1}-C_L')4\pi a_i D_{eff}t = (C_{L1}-C_L')4\pi a_i D_{LP}\theta f t$$

[nb. the rate is now independent of the buffer term, as was found in section 6.1.] Thus the net rate of dissolution of a given number of particles is proportional to their radius. But for a given rate of application of DCPD, w (ie. weight of DCPD applied per unit volume of soil), the number of particles per unit volume of soil, N increases as a_i is reduced. Thus the total amount of DCPD dissolved at t is

$$NM_t = \frac{w}{(4/3)\pi a_i^3 \rho}(C_L'-C_{L1})4\pi a_i D_{LP}\theta f t$$

ie.

$$M_t(\text{total}) = \frac{3w}{a_i^2 \rho}(C_L'-C_{L1})\pi D_{LP}\theta f t \qquad (6.81)$$

(ρ is the density of DCPD). The net rate of dissolution is therefore inversely proportional to the square of the radius of the particles.

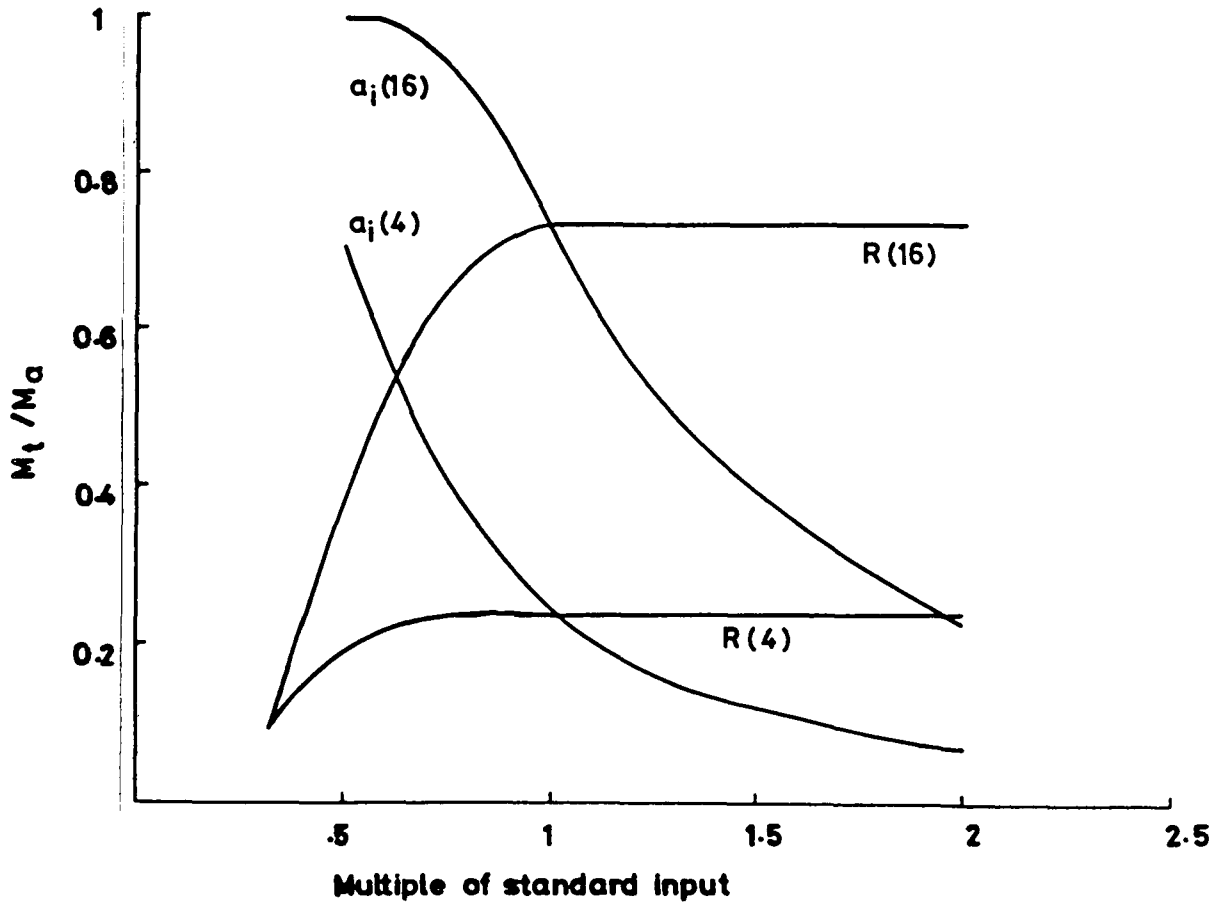


Fig. 6.7. Effect of management variables on the fraction of DCPD dissolved after 4 and 16 days. Numbers in parentheses are times. Other variables as standards in Fig. 6.1.

However, at normal rates of application, adjacent particles are likely to influence each other and so the system is more complicated than indicated by equation (6.81). For a given rate of application, the smaller the particle size the smaller will be the distance between adjacent particles. Thus smaller particles should tend to overlap with each other sooner. The relationship between rate of application (normally expressed as kg of P_2O_5 per ha of soil), particle radius and the distance between neighbouring particles can be obtained as follows:

$$R = a_i(\rho/w)^{1/3}$$

(section 4.4). Suppose the particles are uniformly mixed to 15 cm depth in the field:

Volume of 1ha of soil 15 cm deep = $1.5\text{x}10^6$ dm^3

If w_w be the weight in kg of P_2O_5 (= 1.1kg of DCPD) applied per ha

$$R = a_i\left(\frac{3.15\text{x}10^6}{w_w}\right)^{1/3}$$

Table 6.1 shows the variation in particle separation over the typical range of application rates and particle sizes.

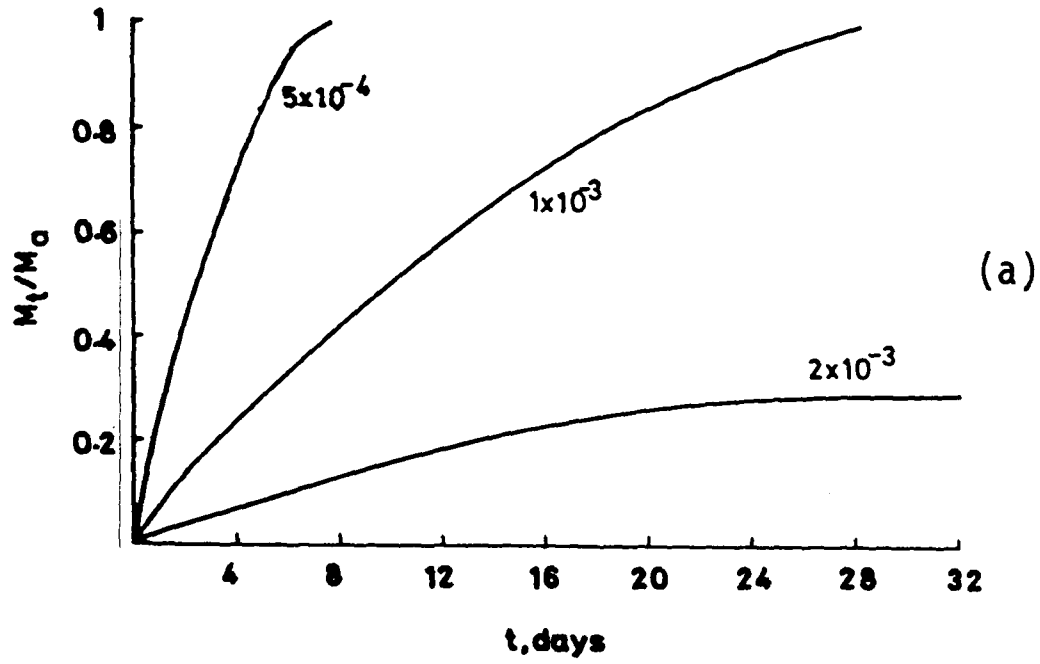
Table 6.1

The distance, R between uniformly mixed particles at different rates of application and particle sizes, a_i.

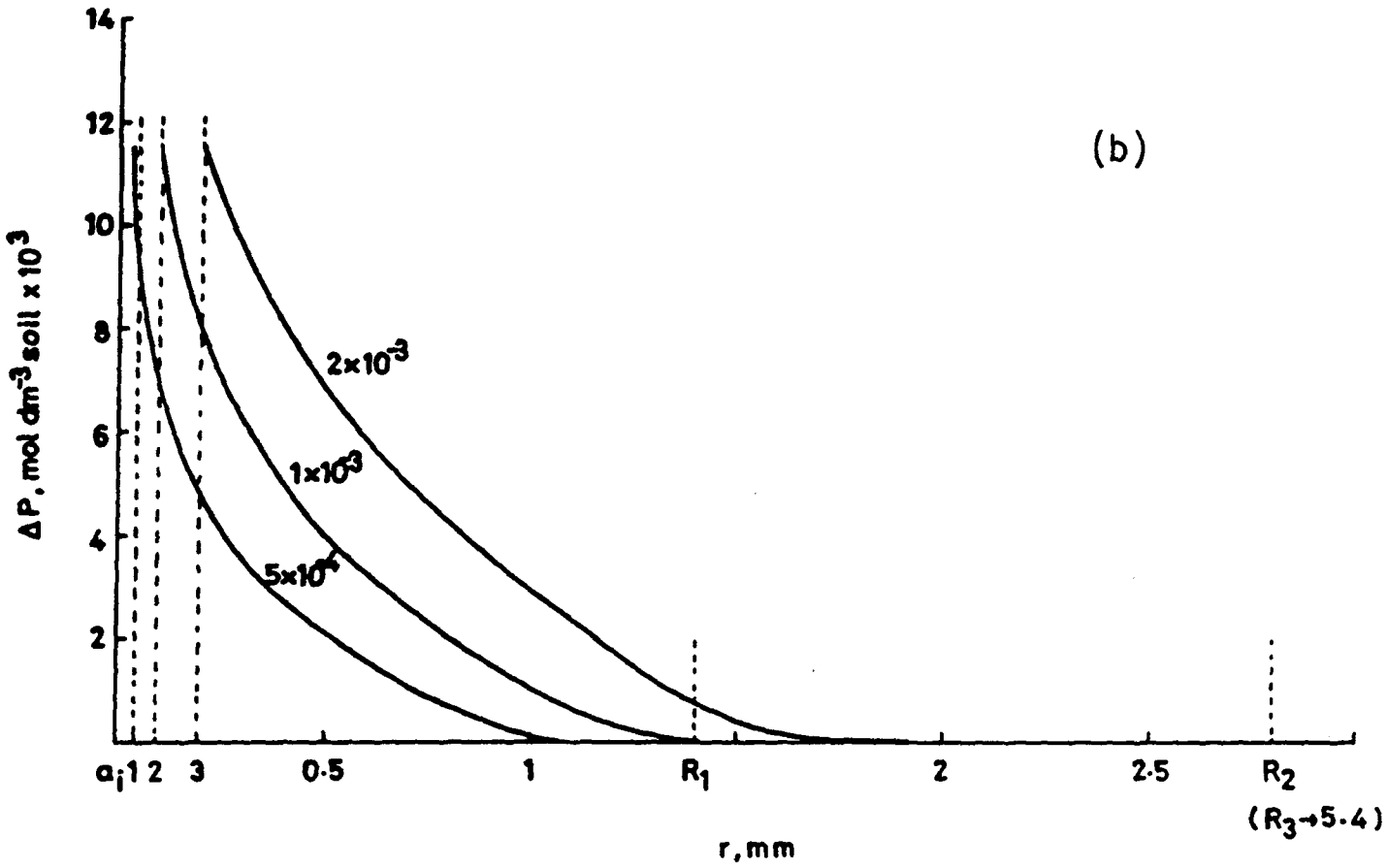
a_i (dm)	Rate of application ($kg\ P_2O_5\ ha^{-1}$)	R (dm)
$2x10^{-4}$	50	$8.0x10^{-3}$
$1x10^{-3}$	50	$4.0x10^{-2}$
$5x10^{-3}$	50	$2.0x10^{-1}$
$2x10^{-4}$	100	$5.5x10^{-3}$
$1x10^{-3}$	100	$2.8x10^{-2}$
$5x10^{-3}$	100	$1.4x10^{-1}$

These are the maximum expected values of R - placement practices will reduce the values considerably.

The model predictions shown in fig. 6.8 are for a rate of application of 100 kg P_2O_5 ha^{-1}, uniformly mixed to 15 cm; the separation of the particles varies as shown in the legend. The initial rate of dissolution and particle size follow an approximate inverse square relationship as expected from equation (6.81) for each particle size. The effect of overlap becomes evident at longer times whence the rate declines more sharply than expected from the reduction in particle radius alone.



(a)



(b)

Fig. 6.8. Effect of particle size on (a) the rate of dissolution and (b) the phosphate concentration profiles after 4 days. Rate of application = 100 kg P_2O_5 ha^{-1}. Numbers on curves are values of a_i. $R_1=1.4x10^{-2}$ ($a_i=5x10^{-4}$); $R_2=2.8x10^{-2}$ ($a_i=1x10^{-3}$); $R_3=5.4x10^{-2}$ ($a_i=2x10^{-3}$). All values are in dm.

Other variables as standards in Fig. 6.1.

6.9 Rate of application

Fig. 6.9 shows the effect of the rate of application on the rate of dissolution and the consequent effect on the separation of particles. The value of a_i is constant.

When particles are very close together, overlap occurs very quickly and the soil more rapidly becomes saturated with respect to the DCPD, whereafter no more DCPD will dissolve. Saturation occurs within 12 days at a separation of less than $R=7.5\times10^{-3}$ dm, with the other inputs as standard.

At the largest separation shown in fig. 6.9 ($R=2.1\times10^{-2}$dm), the particles dissolved completely before they overlapped with each other. Thus one should expect that at low rates of application (<50 kg P_2O_5 ha^{-1}), uniformly mixed, particles larger than $a_i=10^{-3}$dm (ie. anything coarser than a dust) would never influence each other. Also, small particles ($a_i<5\times10^{-4}$dm) may dissolve completely before overlap occurs, although the separation of the particles is less than the separation of larger particles at the same rate of application. However, the effect of overlap is clearly very significant in all other circumstances.

Fig. 6.10 shows that overlap results in changes in the composition of the saturated solution near the particle surface. With the soil variables at the standard values, the rate of propagation of phosphate is greater than that of base, so overlap results in an increase in surface C_L in response to the reflection of phosphate. Consequently the surface pH is reduced in accord with the solubility product. Additionally, D_{HB} will

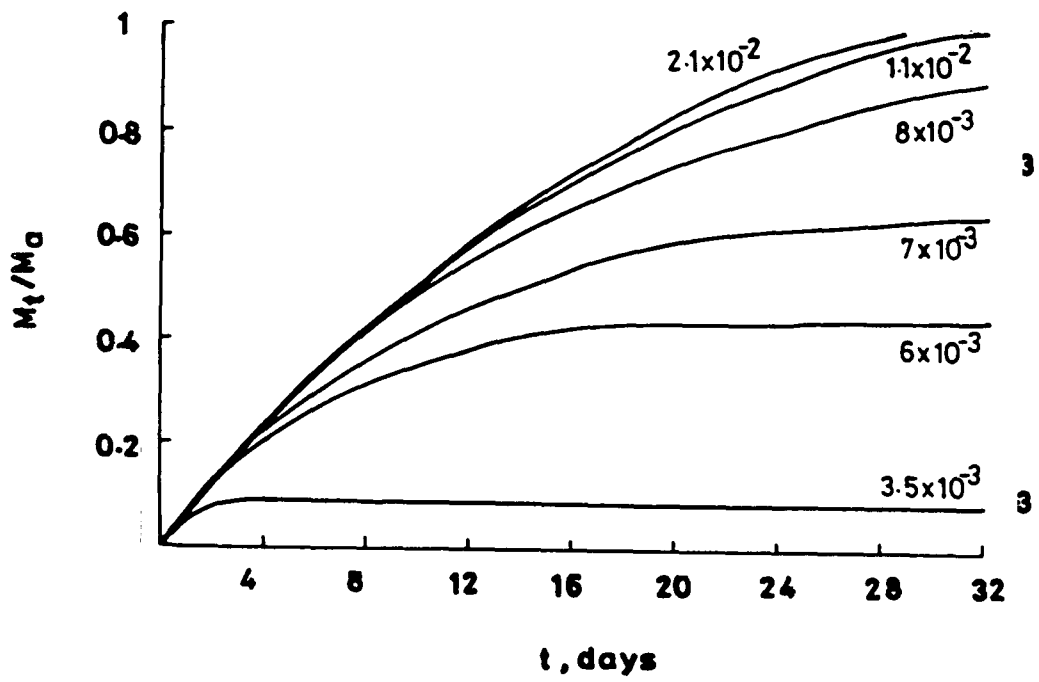
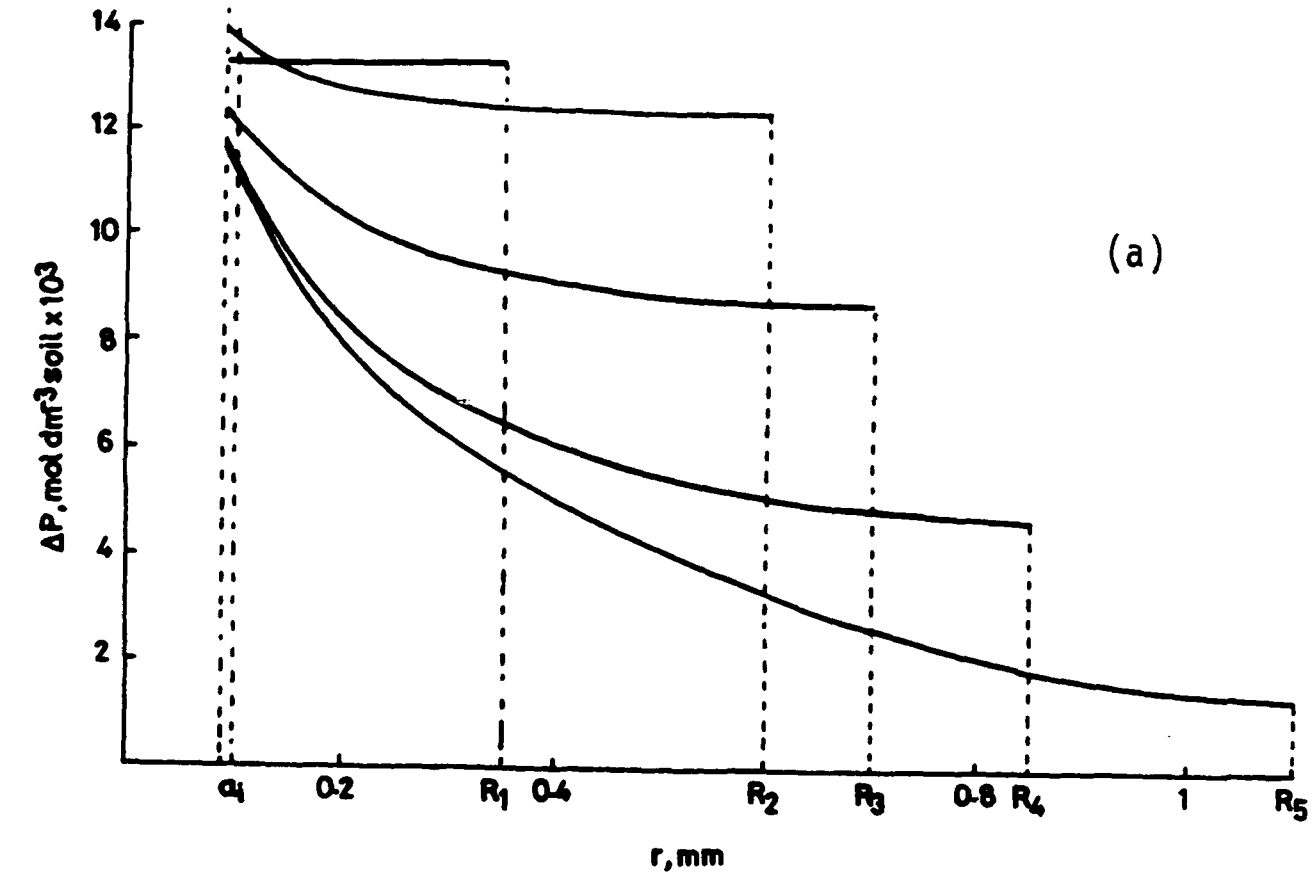


Fig. 6.9. Effect of the rate of application on the rate of dissolution.

Numbers on curves are values of R in dm.

Other variables as standards in Fig. 6.1.

increase as the concentration of the $H_2PO_4^-$-HPO_4^{2-} pair increases. Thus the gradient of basic ions must be reduced to maintain the balance of fluxes, and the pH at the surface is further reduced. The effect of these changes in surface concentrations on the rate of dissolution is significant, and so it is important that the model is capable of taking account of the effect.



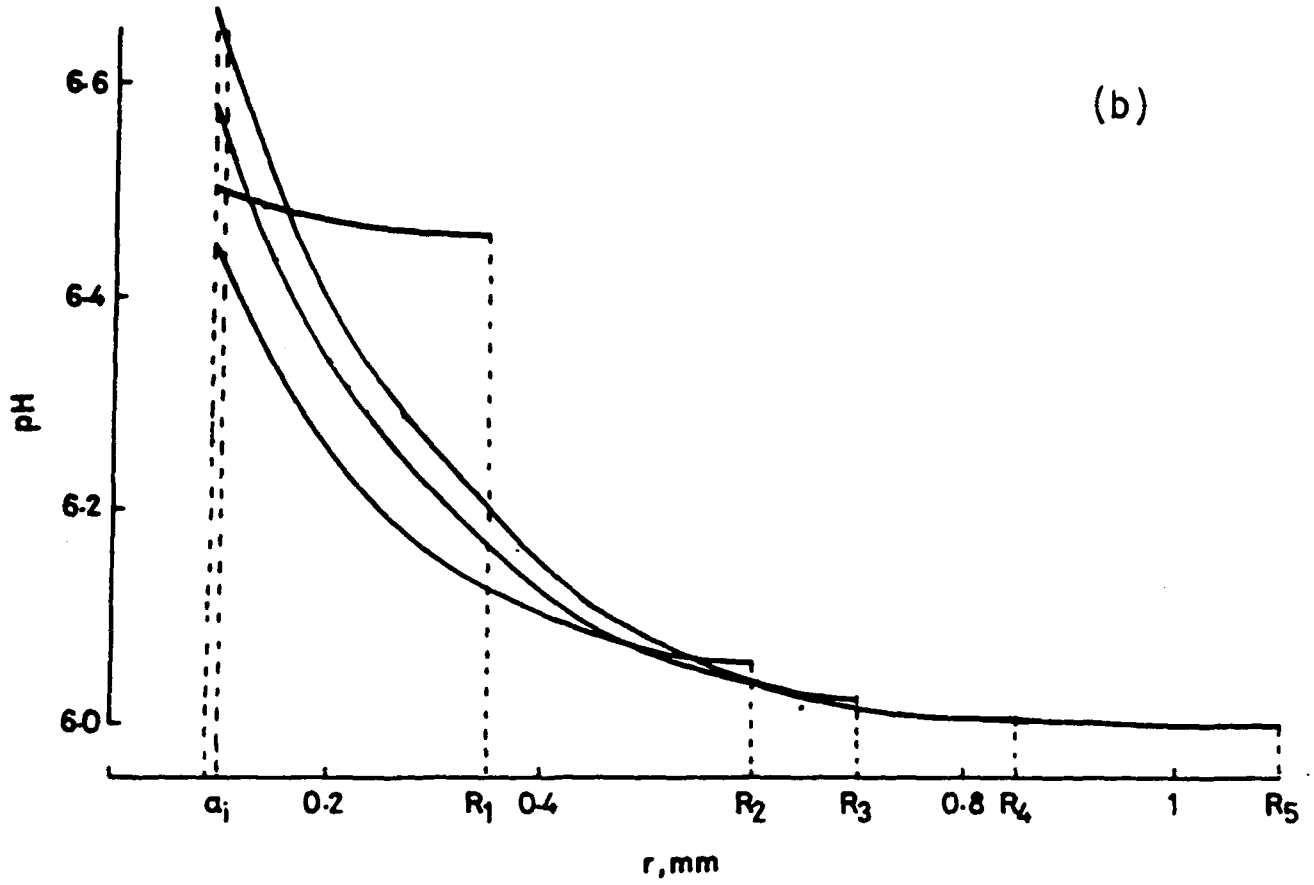


Fig. 6.10. Effect of the rate of application on (a) the phosphate concentration profiles and (b) the pH profiles after 4 days. $R_1=3.5\times10^{-3}$dm, $R_2=6\times10^{-3}$dm, $R_3=7\times10^{-3}$dm, $R_4=8.5\times10^{-3}$dm, $R_5=1.1\times10^{-2}$dm. Other variables as standards in Fig. 6.1.

Further Developments of the Model

6.10 The Effect of Placement

Localised placement of slowly dissolving phosphates with the aim of increasing their efficiency has been widely promoted; it is not entirely without drawbacks (Fox and Kang, 1978). Placement enables nutrients to be concentrated in zones which emergent rootlets can reach rapidly. Thus the phosphate supply to crops in the crucial initial stages of growth can be made optimal. None of the fertilizer is applied to regions that the root system never taps. However, phosphate may be wasted if it is being concentrated above the level at which root uptake is maximal. This occurs below 10^{-4} mol dm^{-3} for most plants (Brewster et al, 1976; Keay et al, 1970; Loneragan and Asher, 1967), indeed concentrations greater than this appear to inhibit plant growth (Brewster et al, 1976). Also, root exploration of the soil for water and nutrients other than phosphate will be discouraged by placement so the crop's stress resistance may be reduced.

The effect of placement is to reduce the distance between neighbouring particles. In terms of the model, placement effectively increases the rate of application in localised zones. Thus the value of placement practices could be investigated by varying the value of R.

6.11 The effect of temperature

One might expect a greater rate of dissolution at higher temperatures because of temperature effects on the equilibrium constants and D_L values. Probert and Larsen (1970) found a slight increase in the rate of dissolution of DCPD in soil, on raising the temperature from 15 to 35°C.

Modelling the effect of temperature would simply require substitution in the model of revised values of the solution diffusion coefficients and equilibrium constants. The change in equilibrium constants with temperature can be calculated using the appropriate thermodynamic constants for the dissolution of DCPD in aqueous solution. Gregory et al (1970) give the following expression for the temperature dependence of K_{SP}

$$pK_{SP} = 3648.9/T - 18.178 + 0.04202T$$

where T is the temperature in kelvin. Bates and Acree (1943) give for K_2

$$pK_2 = 1979.5/T - 5.3541 + 0.01984T$$

The change in D_L values can be found from equation (2.414). Table 6.2 gives the variation in K_{SP}, K_2 and D_L values thus calculated for a range of temperatures.

Table 6.2

Effect of temperature on K_{SP}, K_2 and D_L values ($dm^2s^{-1}x10^7$).

T,°C	pK_{SP}	pK_2	D_{LP}	D_{LH}	D_{LC}
15	6.60	7.23	0.875	8.26	1.06
20	6.59	7.21	0.890	8.40	1.08
25	6.59	7.20	0.905	8.54	1.10
35	6.61	7.18	0.936	8.83	1.14

The changes in K_{SP} and K_2 with temperature are not sufficient to cause much change in the rate of dissolution. K_2 increases with temperature and this would tend to reduce the concentration of $H_2PO_4^-$ in equilibrium with the solid DCPD, reducing the rate of dissolution. KSP

has a minimum value at around 20°C. D_L values increase marginally between 15 and 35°C and this would favour a higher rate of dissolution. Phosphate sorption by soils tends to be exothermic (Barrow and Shaw, 1975) so the phosphate buffer capacity will decrease with temperature, lowering the rate of dissolution.

The net effect of temperature on the rate of dissolution of DCPD is therefore not expected to be marked. The solubility product of other calcium phosphates may of course be more strongly temperature dependent.

6.12 The effect of other additives

The possibilty of increasing the effectiveness of sparingly soluble calcium phosphates fertilizers by mixing them with acid-forming fertilizer materials has been widely suggested (Khasawneh and Doll, 1978). The proposed additives include N sources such as ammonium sulphate and urea nitrate whose reaction products acidify the soil, elemental sulphur which is oxidized to H_2SO_4 by soil micro-organisms, and farmyard manure. In principle, it would be possible to adapt the model to evaluate the usefulness of such additives. On the basis that phosphate diffuses much more slowly than the components of these acidifying agents, one should expect the acidifying agent to be uniformly dispersed in the soil before an appreciable amount of the calcium phosphate had dissolved. An estimate of the effect could therefore be made by calculating the adjusted native soil pH and using the value in the model directly.

Non-acidifying additives may also influence the rate of dissolution. KCl might be expected to reduce the rate of dissolution because K^+ would displace Ca^{2+} from exchange sites, increasing $[Ca^{2+}]_L$. This could be accounted for in the model by incorporating a cation exchange equation

in the calculation of the balance of cations and anions.

6.13 Plant uptake

Removal of phosphate from the soil solution by plant roots will enhance the rate of dissolution. The distance between particles and neighbouring roots will not of course be constant, and the geometry of the particle-root system will be extremely complex so a precise simulation of the effect of roots would be difficult. However, the magnitude of the effect could be seen by assuming a uniform distribution of roots over the soil. The effect of roots could therefore be incorporated in the model as sink terms in the continuity equations:

$$\partial C/\partial t = [\text{diffusion terms}] - S$$

where S is the rate of uptake by roots per unit volume. S could be described by a Michaelis-Menten type equation:

$$S = S_{max} C_L / (K_M + C_L)$$

(see Nye and Tinker, 1977, chapter 5).

The effect of plant uptake on the rate of dissolution of calcium phosphates will depend on the difference between the flux of phosphate into the roots and the flux from the fertilizer particle into the soil. In practice a wide range of values for these fluxes are possible.

Extension of the Model to Other Calcium Phosphates.

Rock phosphates used for direct application largely comprise fluor-apatites substituted to varying degrees with carbonate. Their general formula is

$$Ca_{10-a-b}Na_aMg_b(PO_4)_{6-x}(CO_3)_xF_{2+y}$$

(McClellan and Lehr, 1969). The limit on the extent of substitution, x, is that $x/(6-x)<.3$. On average, $y=0.4x$, $a=1.327x/(6-x)$ and $b=0.515x/(6-x)$. A particular rock phosphate will contain a range of carbonate-apatites of this type. The range in composition is from pure fluor-apatite ($Ca_5(PO_4)_3F$) to the most highly substituted form for which $x=1.5$ (giving a net positive charge on the mineral). Increasing substitution of CO_3^{2-} increasingly disrupts the apatitic structure, increasing the solubility of the mineral. Chien and Black (1976) found for a range of carbonate-apatites

$$pK_{SP} = 122.2 - 6.3x$$

where K_{SP} is given by

$$(Ca^{2+})^{10-a-b}(Na^+)^a(Mg^{2+})^b(PO_4^{3-})^{6-x}(CO_3)^xF^{2+y}$$

The dissolution of these minerals in acid soils is controlled by the same mechanisms that control the dissolution of DCPD. The dissolution reaction of fluor-apatite in acid conditions is

$$Ca_5(PO_4)_3F + 6H_2O = 5Ca^{2+} + 3H_2PO_4^- + F^- + OH^-$$

and that of the maximally substituted carbonate-apatite is

$$[Ca_{9.4}Na_{0.4}Mg_{0.2}(PO_4)_{4.5}(CO_3)_{1.5}F_{2.6}]^{0.5+} + 12H_2O =$$

$$9.4Ca^{2+} + 0.4Na^+ + 0.2Mg^{2+} + 4.5H_2PO_4^- + 1.5H_2CO_3 + 2.6F^- + 12OH^-$$

In principle, therefore, adapting the model to describe the dissolution of individual carbonate-apatites would be a matter of substituting the appropriate value for K_{SP} and adjusting the Ca:P:base ratio in the

interface boundary condition. Na^+, Mg^{2+} and F^- ions will alter the balance of ionic charges in solution, but their concentrations will be small compared to those of the ions already accounted for.

The rate of dissolution of carbonate-apatites will be much smaller than that of DCPD because the K_{SP} values are smaller, and thus much larger times are involved. In these circumstances slow reaction of phosphate with the soil may have to be allowed for.

Conclusion

A model which makes no arbitrary assuptions has been developed, which accurately predicts the rates of dissolution of calcium phosphates in soils. The model is somewhat complex but all the processes accounted for by it have been shown to be important and so could not be omitted to simplify the model.

The major use of the model is that it may be extended to the more practically important, but more complex, carbonate-apatites which comprise rock phosphate fertilizers. With the extended model it would be possible to predict the rates of dissolution of a particular rock phosphate in a particular soil, from a knowledge of the solubility product of the rock phosphate and its ionic compositon, and routinely measured soil parameters. Thereby one could short-cut the usual practice of running extensive field trials to establish the responses over a wide range of field conditions and management practices.

Appendix A : The planar model

```
(0001)C.DCAL1.FOR
(0002)       REAL IS,L,LPI,NT,NTB,FA,FB,KSP,K2,K3,KH
(0003)       DIMENSION A(101),B(101),C(101),D(101),E(101),F(101)
(0004)      +,X(101),PT(101),PH(101),BP(101)
(0005)      +,DP(101),EP(101),FP(101),BT(101),H(101)
(0006)      +,TC(101),P2(101),TP2(101),CA(101),CAT(101)
(0007)      +,THC(101),CP(101),ACT(101),HC(101)
(0008)      +,TH(101),HT(101),TCA(101),VH(101),VCA(101)
(0009)       TT1=1.5E6
(0010)       TT2=1.6E6
(0011)       TT3=1.7E6
(0012)       NT=0
(0013)       NTB=0
(0014)C.Diffusion Coefficients
(0015)       D1=8.9E-8
(0016)       D2=8.4E-7
(0017)       D3=1.08E-7
(0018)       DC=D1/D2
(0019)       DH=D3/D2
(0020)C.Equilibrium Constants
(0021)       KSP=2.E-7
(0022)       K2=10**-7.213
(0023)       K3=8.2
(0024)       KH=8.172E-11
(0025)       Q=1.E-3
(0026)       F1=.17
(0027)       L=.31
(0028)       PD=1.1
(0029)       Q1=5.E-4
(0030)C.Initial Concentrations
(0031)       C(1)=1.E-2
(0032)       PH(1)=5.
(0033)       H(1)=10**-PH(1)
(0034)       TP2(1)=C(1)/(1/K2*H(1))
(0035)       P2(1)=TP2(1)
(0036)       THC(1)=KH/H(1)
(0037)       HC(1)=THC(1)
(0038)       PHI=3.5
(0039)       CL=2.E-3+10**-PHI
(0040)       CA(1)=TP2(1)+.5*(C(1)+THC(1)+CL-H(1))
(0041)       CP(1)=0
(0042)       IS=SQRT(2*(CA(1)+TP2(1))+.5*(C(1)+H(1)+THC(1)+CL))
(0043)       ACT(1)=.524*(IS/(1+IS)-.3*IS**2)
(0044)       H(1)=10**(ACT(1)-PH(1))
(0045)       VC=C(1)
(0046)       TC(1)=C(1)
(0047)       TH(1)=H(1)
(0048)       TCA(1)=CA(1)
(0049)       DO 3 J=2,101
(0050)       C(J)=1.84E-6
```

```
(0051)        PH(J)=PHI
(0052)        H(J)=10**-PH(J)
(0053)        TP2(J)=C(J)/(1/K2*H(J))
(0054)        P2(J)=TP2(2)
(0055)        THC(J)=KH/H(J)
(0056)        HC(J)=THC(J)
(0057)        CA(J)=TP2(J)+.5*(C(J)+THC(J)+CL-H(J))
(0058)        CP(J)=0
(0059)        IS=SQRT(2*(CA(J)+TP2(J))+.5*(C(J)+H(J)+THC(J)+CL))
(0060)        ACT(J)=.524*(IS/(1+IS)-.3*IS**2)
(0061)        H(J)=10**(ACT(2)-PH(2))
(0062)3       CONTINUE
(0063)        CAI=CA(2)
(0064)        LPI=PH(2)-2*ACT(2)+.5*LOG10(CA(2))
(0065)C.Sorption Parameters
(0066)        FAI=.235
(0067)        FB=.317
(0068)        BHSI=.115
(0069)        FA=FAI*(PD-L)
(0070)        PO=FA*C(2)**FB
(0071)        BHS=BHSI*(PD-L)
(0072)C.Start of Time Loops
(0073)        TT=0.0
(0074)        DO 50 I=1,5000
(0075)C.Time Steps
(0076)C.   The length of the time steps is increased gradually once the
(0077)C.   initial concentration profiles have been established
(0078)        IF(I.GT.100)GOTO 12
(0079)        P=1.E2
(0080)        GOTO 14
(0081)12      CONTINUE
(0082)        IF(P.GT.1.E3)GOTO 14
(0083)        P=1.E2+(TT-1.E4)/25
(0084)14      CONTINUE
(0085)        TT=TT+P
(0086)        AA=F1*L*P/(2*Q**2)
(0087)C.Richtmyer Algorithm
(0088)C.Phosphate
(0089)C.   The numerical solution of equation (2.43)
(0090)        DO 20 J=1,101
(0091)        A(J)=D1*AA/(FA*FB*C(J)**(FB-1)+L)
(0092)        B(J)=1+2*A(J)
(0093)20      CONTINUE
(0094)        E(100)=2*A(100)/B(100)
(0095)        F(100)=(2*A(100)*C(101)+(2-B(100))*C(100))/B(100)
(0096)        DO 30 JR=2,100
(0097)        J=102-JR
(0098)        D(J)=A(J)*C(J+1)+(2-B(J))*C(J)+A(J)*C(J-1)
(0099)        E(J-1)=(B(J)-A(J)/E(J))/A(J)
(0100)        F(J-1)=(F(J)*(B(J)-A(J)*E(J-1))-D(J))/A(J)
(0101)30      CONTINUE
(0102)C.Concentrations in Soil Bulk
(0103)C.   The numerical solution of equation (2.410)
(0104)        DO 40 J=2,101
(0105)        TC(J)=C(J)
```

```
(0106)          C(J)=(C(J-1)-F(J-1))/E(J-1)
(0107)          TH(J)=H(J)
(0108)          TCA(J)=CA(J)
(0109)          CA(J)=P2(J)+.5*(C(J)+HC(J)+CL-H(J))
(0110)          TP2(J)=P2(J)
(0111)          P2(J)=C(J)*K2*10**(4*ACT(J))/H(J)
(0112)          THC(J)=HC(J)
(0113)          HC(J) :KH*10**(-2*ACT(J))/H(J)
(0114)40        CONTINUE
(0115)C.Soil Base
(0116)          AP=AA*2.303*D2/BHS
(0117)          DO 70 J=1,101
(0118)          VH(J)=(TH(J)+H(J))/2
(0119)          VCA(J)=(TCA(J)+CA(J))/2
(0120)          BP(J)=2*AP+1/VH(J)+1/(4*VCA(J))
(0121)70        CONTINUE
(0122)46        CONTINUE
(0123)          EP(100)=2*AP/BP(100)
(0124)          FP(100)=(2*AP*H(101)-(4*AP-BP(100))*H(100)-
(0125)         +2*DH*AP*(HC(101)+THC(101)-HC(100)-THC(100))-
(0126)         +2*DC*AP*(P2(101)+TP2(101)-P2(100)-TP2(100))+
(0127)         +(C(100)-TC(100))/(4*VCA(100)))/BP(100)
(0128)          DO 80 JR=2,100
(0129)          J=102-JR
(0130)          DP(J)=AP*H(J+1)-(4*AP-BP(J))*H(J)+AP*H(J-1)-
(0131)         +DH*AP*(HC(J+1)+THC(J+1)-2*(HC(J)+THC(J))+HC(J-1)+THC(J-1))-
(0132)         +DC*AP*(P2(J+1)+TP2(J+1)-2*(P2(J)+TP2(J))+P2(J-1)+TP2(J-1))+
(0133)         +(C(J)-TC(J))/(4*VCA(J))
(0134)          EP(J-1)=(BP(J)-AP/EP(J))/AP
(0135)          FP(J-1)=(FP(J)*(BP(J)-AP*EP(J-1))-DP(J))/AP
(0136)80        CONTINUE
(0137)C.Concentrations in Soil Bulk
(0138)          DO 90 J=2,101
(0139)          H(J)=(H(J-1)-FP(J-1))/EP(J-1)
(0140)          P2(J)=C(J)*K2*10**(4*ACT(J))/H(J)
(0141)          HC(J)=KH*10**(-2*ACT(J))/H(J)
(0142)          CA(J)=P2(J)+.5*(C(J)+HC(J)+CL-CP(J)-H(J))
(0143)          CP(J)=K3*10**(-4*ACT(J))*CA(J)*C(J)
(0144)          IS=SQRT(2*(CA(J)+P2(J))+.5*(C(J)+HC(J)+CL-CP(J)-H(J)))
(0145)          ACT(J)=.524*(IS/(1+IS)-.3*IS**2)
(0146)90        CONTINUE
(0147)          DO 33 J=2,101
(0148)          G=(HT(J)-H(J))/H(J)
(0149)          IF(G.LE.-1.E-3.OR.G.GE.1.E-3)GOTO 47
(0150)33        CONTINUE
(0151)          GOTO 48
(0152)47        CONTINUE
(0153)          DO 44 J=2,101
(0154)          VH(J)=(TH(J)+H(J))/2
(0155)          VCA(J)=(TCA(J)+CA(J))/2
(0156)          BP(J)=2*AP+1/VH(J)+1/(4*VCA(J))
(0157)          HT(J)=H(J)
(0158)          H(J)=TH(J)
(0159)44        CONTINUE
(0160)          GOTO 46
```

```
(0161)48     CONTINUE
(0162)C.LH Boundary Concentrations
(0163)C.   These are adjusted at the begining of each time step so that
(0164)C.   The equation for H(1) coorresponds to (2.54).
(0165)       PF=L*F1*D1*(C(1)-C(2))/Q
(0166)       HF=L*F1*(D2*(H(2)-H(1))+D3*(HC(1)-HC(2))+D1*(P2(1)-P2(2)))/Q
(0167)       NT=NT+PF*P*5.027
(0168)       NTB=NTB+HF*P*5.027
(0169)       TC(1)=C(1)
(0170)       TH(1)=H(1)
(0171)       TCA(1)=CA(1)
(0172)       TP2(1)=P2(1)
(0173)       THC(1)=HC(1)
(0174)       N=0
(0175)45     CONTINUE
(0176)       N=N+1
(0177)       PB=FA*FB*C(1)**(FB-1)
(0178)       HB=BHS/(2.303*H(1))
(0179)       H(1)=TH(1)+((HF-PF)*P+BHS/(4.606*VCA(1))*Q1*(CA(1)-TCA(1)))/
(0180)      +(((L+PB)*KSP/K2*10**(4*ACT(1))/VCA(1)+HB)*Q1)
(0181)       C(1)=KSP/K2*10**(4*ACT(1))*H(1)/CA(1)
(0182)       PH(1)=-LOG10(H(1))
(0183)       P2(1)=KSP*10**(8*ACT(1))/CA(1)
(0184)       CP(1)=K3*10**(-4*ACT(1))*CA(1)*C(1)
(0185)       HC(1)=KH*10**(-2*ACT(1))/H(1)
(0186)       IS=SQRT(2*(CA(1)+P2(1))+.5*(C(1)+CP(1)+HC(1)+H(1)+CL))
(0187)       ACT(1)=.524*(IS/(1+IS)-.3*IS**2)
(0188)       CAB=CA(1)
(0189)       CA(1)=P2(1)+.5*(C(1)+HC(1)+CL-CP(1)-H(1))
(0190)       VCA(1)=(TCA(1)+CA(1))/2
(0191)       VH(1)=(TH(1)+H(1))/2
(0192)       VC=(TC(1)+C(1))/2
(0193)       IF(N.GT.1)GOTO 45
(0194)C.End of Time Loops
(0195)       IF(TT.LE.TT1)GOTO 41
(0196)       IF(TT.GE.TT1+1.1E3)GOTO 42
(0197)       GOTO 49
(0198)42     CONTINUE
(0199)       IF(TT.LE.TT2)GOTO 41
(0200)       IF(TT.GE.TT2+1.1E3)GOTO 43
(0201)       GOTO 49
(0202)43     CONTINUE
(0203)       IF(TT.LE.TT3)GOTO 41
(0204)       IF(TT.GE.TT3+1.1E3)STOP
(0205)49     CONTINUE
(0206)C.The Predicted Total Soil Concentration Profiles and Total
(0207)C.  Amounts Dissolved by Simpson's Rule
(0208)       DO 112 J=1,101
(0209)       X(J)=(J-1)*Q
(0210)       PT(J)=L*C(J)+FA*C(J)**FB-PO
(0211)       PH(J)=ACT(J)-LOG10(H(J))
(0212)       BT(J)=BHS*(PH(J)+.5*LOG10(CA(J))-LPI)
(0213)       CAT(J)=.5*(PT(J)+BT(J)-L*(C(J)+H(J)))+L*CA(J)
(0214)112    CONTINUE
(0215)       ASP=0
```

```
(0216)          ASH=0
(0217)          ASC=0
(0218)          BSP=0
(0219)          BSH=0
(0220)          BSC=0
(0221)          SP=0
(0222)          SH=0
(0223)          SC=0
(0224)          DO 95 J=2,100,2
(0225)          ASP=ASP+PT(J)
(0226)          ASH=ASH+BT(J)
(0227)          ASC=ASC+CAT(J)
(0228)95        CONTINUE
(0229)          DO 100 J=3,99,2
(0230)          BSP=BSP+PT(J)
(0231)          BSH=BSH+BT(J)
(0232)          BSC=BSC+CAT(J)
(0233)100       CONTINUE
(0234)          SP=Q/3*(PT(1)+PT(101)+4*ASP+2*BSP)*5.027
(0235)          SH=Q/3*(BT(1)+BT(101)+4*ASH+2*BSH)*5.027
(0236)          SC=Q/3*(CAT(1)+CAT(101)+4*ASC+2*BSC)*5.027
(0237)          WRITE(6,166)TT,NT,SP,NTB,SH,SC
(0238)          DO 120 J=1,101
(0239)          WRITE(6,150)X(J),PT(J),PH(J),BT(J),CAT(J)
(0240)120       CONTINUE
(0241)41        CONTINUE
(0242)50        CONTINUE
(0243)150       FORMAT(1X,5E10.3)
(0244)155       FORMAT(5E10.3)
(0245)166       FORMAT(1X,6E10.3)
(0246)          STOP
(0247)          END
(0248)**END**
```

Appendix B : The granular model

```
(0001)C.DCAL2.FOR
(0002)        REAL  IS,K2,KH,KSP,FB,FA,NO,NT,NTB,L,LPI
(0003)        DIMENSION A(222),B(222),C(222),D(222),E(222),F(222)
(0004)       +,G(222),X(222),YG(222),DE(222),PT(222),CP(222)
(0005)       +,AP(222),BP(222),TH(222),H(222),GP(222),DP(222),EP(222)
(0006)       +,FP(222),CA(222),TCA(222),P2(222),TP2(222),TC(222),PH(222)
(0007)       +,HC(222),THC(222),BT(222),CAT(222),WG(222),ACT(222),TPH(222
(0008)       +,U(222),Z(222),TZ(222),AZ(222)
(0009)C.  Initial values
(0010)        READ(5,444)Q,R,RL,PP
(0011)        READ(5,333)L,F1,PD
(0012)        READ(5,222)PH(1),PHI
(0013)        READ(5,222)CI,CL
(0014)        READ(5,333)FAI,FB,BHSI
(0015)        FA=FAI*(PD-L)
(0016)        BHS=BHSI*(PD-L)
(0017)        K=RL/Q
(0018)        NO=R**3*56.16
(0019)        NT=0.0
(0020)        D1=8.9E-8
(0021)        D2=8.4E-7
(0022)        D3=1.08E-7
(0023)        DC=D1/D2
(0024)        DH=D3/D2
(0025)        KSP=2.E-7
(0026)        K2=10**(-7.213)
(0027)        KH=8.172E-11
(0028)        K3=8.2
(0029)        H(1)=10**(-PH(1))
(0030)        C(1)=(SQRT((CL-H(1))**2+8*KSP/K2*H(1))-CL+H(1))/2
(0031)        P2(1)=C(1)*K2/H(1)
(0032)        HC(1)=KH/H(1)
(0033)        CA(1)=P2(1)+.5*(C(1)+CL+HC(1)-H(1))
(0034)        CP(1)=K3*CA(1)*C(1)
(0035)        X(1)=R
(0036)        Z(1)=2.303*(D2*H(1)+(D3*KH+D1*K2*C(1))/H(1))
(0037)        AZ(1)=Z(1)
(0038)        C(2)=CI
(0039)        PH(2)=PHI
(0040)        H(2)=10**(-PHI)
(0041)        P2(2)=C(2)*K2/H(2)
(0042)        HC(2)=KH/H(2)
(0043)        CA(2)=P2(2)+.5*(C(2)+HC(2)+CL-H(2))
(0044)        CP(2)=K3*CA(2)*C(2)
(0045)        X(2)=R+Q
(0046)        Z(2)=2.303*(D2*H(2)+(D3*KH+D1*K2*C(2))/H(2))
(0047)        AZ(2)=Z(2)
(0048)        IS=SQRT(2*(CA(2)+P2(2))+.5*(C(2)+H(2)+HC(2)+CL))
(0049)        ACT(2)=.524*(IS/(IS+1)-.3*IS**2)
(0050)        DO 3 J=2,K+1
```

```
(0051)        C(J)=C(2)
(0052)        PH(J)=PH(2)
(0053)        H(J)=H(2)
(0054)        HC(J)=HC(2)
(0055)        CA(J)=CA(2)
(0056)        X(J)=R+(J-1)*Q
(0057)        Z(J)=Z(2)
(0058)        AZ(J)=Z(2)
(0059)        ACT(J)=ACT(2)
(0060)3       CONTINUE
(0061)        PO=FA*C(2)**FB+L*C(2)
(0062)        LPI=PHI+.5*LOG10(CA(2))
(0063)        TT=0.0
(0064)C.  Start of time loops
(0065)        TT1=8.6E4
(0066)        TT2=1.73E5
(0067)        TT3=3.46E5
(0068)        TT4=6.91E5
(0069)        TT5=1.38E6
(0070)        TT6=2.76E6
(0071)        I=0
(0072)        IN=0
(0073)        P=10
(0074)50      CONTINUE
(0075)        I=I+1
(0076)        II=0
(0077)        III=0
(0078)        IF(I.LE.100)GOTO 15
(0079)        IF(P.GE.PP)GOTO 15
(0080)        P=P+10
(0081)15      CONTINUE
(0082)        TT=TT+P
(0083)        AA=D1*F1*L*P/(2*Q**2)
(0084)        DEP=F1*L*P/(2*Q**2*BHS)
(0085)        TCS=CS
(0086)        TPHS=PHS
(0087)        THS=HS
(0088)        TP2S=P2S
(0089)        THCS=HCS
(0090)        TCX=CX
(0091)        TZX=ZX
(0092)        TNT=NT
(0093)        TNTB=NTB
(0094)        DO 309 J=1,K+1
(0095)        TC(J)=C(J)
(0096)        TPH(J)=PH(J)
(0097)        TH(J)=H(J)
(0098)        TCA(J)=CA(J)
(0099)        THC(J)=HC(J)
(0100)        TP2(J)=P2(J)
(0101)        TZ(J)=Z(J)
(0102)309     CONTINUE
(0103)C.PHOSPHATE
(0104)310     CONTINUE
(0105)        DO 20 J=1,K+1
```

```
(0106)        DE(J)=AA/(FA*FB*C(J)**(FB-1)+L)
(0107)        A(J)=(1+Q/X(J))*DE(J)
(0108)        B(J)=1+2*DE(J)
(0109)        G(J)=(1-Q/X(J))*DE(J)
(0110)20      CONTINUE
(0111)C.  Initial distribution
(0112)        IF(IN.GT.1)GOTO 45
(0113)        E(K)=A(K)/(B(K)-G(K))
(0114)        F(K)=(A(K)*C(K+1)+(G(K)+2-B(K))*C(K))/(B(K)-G(K))
(0115)        DO 30 JR=2,K
(0116)        J=K+2-JR
(0117)        D(J)=A(J)*C(J+1)+(2-B(J))*C(J)+G(J)*C(J-1)
(0118)        E(J-1)=(B(J)-A(J)/E(J))/G(J)
(0119)        F(J-1)=(F(J)*(B(J)-G(J)*E(J-1))-D(J))/G(J)
(0120)30      CONTINUE
(0121)        DO 40 J=2,K
(0122)        C(J)=(C(J-1)-F(J-1))/E(J-1)
(0123)40      CONTINUE
(0124)        C(K+1)=C(K)
(0125)        GOTO 65
(0126)45      CONTINUE
(0127)C.  Actual distribution
(0128)23      CONTINUE
(0129)        E(1)=A(1)/(B(1)-G(1)*(1-R1))
(0130)        F(1)=(A(1)*C(2)+G(1)*(CS+TCS)*R1+(2-B(1)+G(1)*(1-R1))
(0131)       +*C(1))/(B(1)-G(1)*(1-R1))
(0132)        DO 51 J=2,K
(0133)        D(J)=A(J)*C(J+1)+(2-B(J))*C(J)+G(J)*C(J-1)
(0134)        E(J)=A(J)/(B(J)-G(J)*E(J-1))
(0135)        F(J)=(D(J)+G(J)*F(J-1))/(B(J)-G(J)*E(J-1))
(0136)51      CONTINUE
(0137)54      CONTINUE
(0138)        C(K+1)=F(K)/(1-E(K))
(0139)        DO 61 JR=2,K+1
(0140)        J=K+2-JR
(0141)        C(J)=E(J)*C(J+1)+F(J)
(0142)61      CONTINUE
(0143)65      CONTINUE
(0144)        DO 302 J=1,K+1
(0145)        P2(J)=C(J)*K2*10**(4*ACT(J))/H(J)
(0146)        CA(J)=P2(J)+.5*(C(J)+HC(J)+CL-CP(J)-H(J))
(0147)        IS=SQRT(2*(CA(J)+P2(J))+.5*(C(J)+HC(J)+CL+CP(J)+H(J)))
(0148)        ACT(J)=.524*(IS/(1+IS)-.3*IS**2)
(0149)        CP(J)=K3*10**(-4*ACT(J))*C(J)*CA(J)
(0150)302     CONTINUE
(0151)46      CONTINUE
(0152)C.BASE
(0153)        DO 301 J=2,K
(0154)        U(J)=Q*AZ(J)/X(J)+(D1*K2*10**(4*ACT(J))*2.303/H(J)*
(0155)       +(C(J+1)+TC(J+1)-C(J-1)-TC(J-1))/2+AZ(J+1)-AZ(J-1))/4
(0156)        AP(J)=DEP*(AZ(J)+U(J))
(0157)        BP(J)=1+2*DEP*AZ(J)
(0158)        GP(J)=DEP*(AZ(J)-U(J))
(0159)301     CONTINUE
(0160)C.  Initial distribution
```

```
(0161)        IF(IN.GT.1)GOTO 47
(0162)        EP(K)=AP(K)/(BP(K)-GP(K))
(0163)        FP(K)=(AP(K)*PH(K+1)+(GP(K)+2-BP(K))*PH(K)+
(0164)       +DEP*D1*K2*10**(4*ACT(K))/H(K)*((1+Q/X(K))*(C(K+1)+TC(K+1))-
(0165)       +2*(C(K)+TC(K))+(1-Q/X(K))*(C(K-1)+TC(K-1)))-
(0166)       +.5*LOG10(CA(K)/TCA(K)))/(BP(K)-GP(K))
(0167)        DO 75 JR=2,K
(0168)        J=K+2-JR
(0169)        DP(J)=AP(J)*PH(J+1)+(2-BP(J))*PH(J)+GP(J)*PH(J-1)+
(0170)       +DEP*D1*K2*10**(4*ACT(J))/H(J)*((1+Q/X(J))*(C(J+1)+TC(J+1))-
(0171)       +2*(C(J)+TC(J))+(1-Q/X(J))*(C(J-1)+TC(J-1)))-
(0172)       +.5*LOG10(CA(J)/TCA(J))
(0173)        EP(J-1)=(BP(J)-AP(J)/EP(J))/GP(J)
(0174)        FP(J-1)=(FP(J)*(BP(J)-GP(J)*EP(J-1))-DP(J))/GP(J)
(0175)75      CONTINUE
(0176)        DO 76 J=2,K
(0177)        PH(J)=(PH(J-1)-FP(J-1))/EP(J-1)
(0178)76      CONTINUE
(0179)        PH(K+1)=PH(K)
(0180)        GOTO 48
(0181)47      CONTINUE
(0182)C.  Actual distribution
(0183)        ZX=2.303*(D2*HX+(D3*KH*10**(-2*ACTS)+D1*K2*10**(4*ACTS)*CX)/HX
(0184)        AZX=(TZX+ZX)/2
(0185)        U(1)=Q*AZ(1)/X(1)+(D1*K2*10**(4*ACT(1))*2.303/H(1)*
(0186)       +(C(2)+TC(2)-CX-TCX)/2+AZ(2)-AZX)/4
(0187)        AP(1)=DEP*(AZ(1)+U(1))
(0188)        BP(1)=1+2*DEP*AZ(1)
(0189)        GP(1)=DEP*(AZ(1)-U(1))
(0190)        EP(1)=AP(1)/(BP(1)-GP(1)*(1-R1))
(0191)        FP(1)=(AP(1)*PH(2)+GP(1)*R1*(PHS+TPHS)+
(0192)       +(2-BP(1)+GP(1)*(1-R1))*PH(1)+
(0193)       +DEP*D1*K2*10**(4*ACT(1))/H(1)*((1+Q/X(1))*(C(2)+TC(2))-
(0194)       +2*(C(1)+TC(1))+(1-Q/X(1))*(CX+TCX))-
(0195)       +.5*LOG10(CA(1)/TCA(1)))/(BP(1)-GP(1)*(1-R1))
(0196)        DO 80 J=2,K
(0197)        DP(J)=AP(J)*PH(J+1)+(2-BP(J))*PH(J)+GP(J)*PH(J-1)+
(0198)       +DEP*D1*K2*10**(4*ACT(J))/H(J)*((1+Q/X(J))*(C(J+1)+TC(J+1))-
(0199)       +2*(C(J)+TC(J))+(1-Q/X(J))*(C(J-1)+TC(J-1)))-.5*LOG10
(0200)       +(CA(J)/TCA(J))
(0201)        EP(J)=AP(J)/(BP(J)-GP(J)*EP(J-1))
(0202)        FP(J)=(DP(J)+GP(J)*FP(J-1))/(BP(J)-GP(J)*EP(J-1))
(0203)80      CONTINUE
(0204)        PH(K+1)=FP(K)/(1-EP(K))
(0205)        DO 81 JR=2,K+1
(0206)        J=K+2-JR
(0207)        PH(J)=EP(J)*PH(J+1)+FP(J)
(0208)81      CONTINUE
(0209)48      CONTINUE
(0210)        DO 85 J=1,K+1
(0211)        H(J)=10**(-PH(J))
(0212)        HC(J)=KH*10**(-2*ACT(J))/H(J)
(0213)        Z(J)=2.303*(D2*H(J)+(D3*KH*10**(-2*ACT(J))+D1*
(0214)       +K2*10**(4*ACT(J))*C(J))/H(J))
(0215)        AZ(J)=(TZ(J)+Z(J))/2
```

```
(0216)85     CONTINUE
(0217)       IF(II.EQ.1)GOTO 49
(0218)       II=1
(0219)       DO 308 J=2,K+1
(0220)       PH(J)=TPH(J)
(0221)       H(J)=TH(J)
(0222)308    CONTINUE
(0223)       GOTO 46
(0224)49     CONTINUE
(0225)C.PARTICLE RADIUS & SURFACE CONCS.
(0226)       IF(IN.NE.1)GOTO 41
(0227)       IN=2
(0228)41     CONTINUE
(0229)       IF(IN.GT.1)GOTO 67
(0230)       IS=SQRT(2*(CA(1)+P2(1))+.5*(C(1)+HC(1)+CL+H(1)+CP(1)))
(0231)       ACT(1)=.524*(IS/(1+IS)-.3*IS**2)
(0232)       CII=C(1)
(0233)127    CONTINUE
(0234)       TCC=C(1)
(0235)       C(1)=C(2)*(1-K2*10**(4*ACT(2))/H(2))+P2(1)+
(0236)      +(D2*(H(2)-H(1))-D3*(HC(2)-HC(1)))/D1
(0237)       P2(1)=KSP*10**(8*ACT(1))/CA(1)
(0238)       CA(1)=P2(1)+.5*(C(1)+HC(1)+CL-CP(1)-H(1))
(0239)       H(1)=K2*10**(4*ACT(1))/P2(1)*C(1)
(0240)       HC(1)=KH*10**(-2*ACT(1))/H(1)
(0241)       CP(1)=K3*10**(-4*ACT(1))*CA(1)*C(1)
(0242)       GG=(TCC-C(1))/TCC
(0243)       IF(GG.GE.1.E-2.OR.GG.LE.-1.E-2)GOTO 127
(0244)       GG=(CII-C(1))/CII
(0245)       IF(GG.LE.1.E-2.AND.GG.GE.-1.E-2)GOTO 312
(0246)       PH(1)=-LOG10(H(1))
(0247)       Z(1)=2.303*(D2*H(1)+(D3*KH*10**(-2*ACT(1))+
(0248)      +D1*K2*10**(4*ACT(1))*C(1))/H(1))
(0249)       AZ(1)=(TZ(1)+Z(1))/2
(0250)       II=0
(0251)       III=III+1
(0252)       DO 311 J=2,K+1
(0253)       C(J)=TC(J)
(0254)       PH(J)=TPH(J)
(0255)       H(J)=TH(J)
(0256)       CA(J)=TCA(J)
(0257)       HC(J)=THC(J)
(0258)       P2(J)=TP2(J)
(0259)311    CONTINUE
(0260)       GOTO 310
(0261)312    CONTINUE
(0262)       NT=NT+12.566*D1*F1*L*P*R*(R+Q)/Q*(C(1)-C(2))
(0263)       NTB=NTB+12.566*F1*L*P*R*(R+Q)/Q*
(0264)      +(D2*(H(2)-H(1))+D1*(P2(1)-P2(2))+D3*(HC(1)-HC(2)))
(0265)       GG=NT/NO
(0266)       IF(GG.LT.1.E-2)GOTO 68
(0267)       IN=1
(0268)       HS=H(1)
(0269)       P2S=P2(1)
(0270)       HCS=HC(1)
```

```
(0271)          GOTO 68
(0272)67        CONTINUE
(0273)          NT=NT+12.566*D1*F1*L*P*R*(R-S)/S*(CS-C(1))
(0274)          NTB=NTB+12.566*F1*L*P*R*(R-S)/S*(D2*(H(1)-HS)+D1*(P2S-P2(1))·
(0275)         +D3*(HCS-HC(1)))
(0276)68        CONTINUE
(0277)          IF(IN.EQ.0)GOTO 42
(0278)          IF(NT.GE.NO)GOTO 60
(0279)          S=R-(((NO-NT)/56.16)**.3333333)
(0280)          R1=(1/S-1/R)/(1/Q-1/R)
(0281)          GGCS=CS
(0282)44        CONTINUE
(0283)          GCS=CS
(0284)          CS=C(1)*(1-K2*10**(4*ACTS)/H(1))+P2S+
(0285)         +(D2*(H(1)-HS)-D3*(HC(1)-HCS))/D1
(0286)          GG=(GCS-CS)/CS
(0287)          CAS=P2S+.5*(CS+HCS+CL-CPS-HS)
(0288)          IS=SQRT(2*(CAS+P2S)+.5*(CS+CL+HCS+CPS+HS))
(0289)          ACTS=.524*(IS/(1+IS)-.3*IS**2)
(0290)          P2S=KSP*10**(8*ACTS)/CAS
(0291)          HS=K2*10**(4*ACTS)/P2S*CS
(0292)          HCS=KH*10**(-2*ACTS)/HS
(0293)          PHS=-LOG10(HS)
(0294)          CPS=K3*10**(-4*ACTS)*CAS*CS
(0295)          IF(GG.GE.2.E-2.OR.GG.LE.-2.E-2)GOTO 44
(0296)          CX=C(1)*(1-R1)+CS*R1
(0297)          PHX=PH(1)*(1-R1)+PHS*R1
(0298)          HX=10**(-PHX)
(0299)          IF(IN.EQ.1)GOTO 42
(0300)          GG=(GGCS-CS)/CS
(0301)          IF(GG.LE.2.E-2.AND.GG.GE.-2.E-2)GOTO 42
(0302)          NT=TNT
(0303)          NTB=TNTB
(0304)          DO 22 J=1,222
(0305)          C(J)=TC(J)
(0306)          PH(J)=TPH(J)
(0307)          H(J)=TH(J)
(0308)          CA(J)=TCA(J)
(0309)          HC(J)=THC(J)
(0310)          P2(J)=TP2(J)
(0311)22        CONTINUE
(0312)          GOTO 23
(0313)42        CONTINUE
(0314)C.  End of time loops
(0315)          IF(TT.GE.TT1.AND.TT.LT.TT1+P)GOTO 56
(0316)          IF(TT.GE.TT2.AND.TT.LT.TT2+P)GOTO 56
(0317)          IF(TT.GE.TT3.AND.TT.LT.TT3+P)GOTO 56
(0318)          IF(TT.GE.TT4.AND.TT.LT.TT4+P)GOTO 56
(0319)          IF(TT.GE.TT5.AND.TT.LT.TT5+P)GOTO 56
(0320)          IF(TT.GE.TT6.AND.TT.LT.TT6+P)GOTO 56
(0321)          GOTO 50
(0322)56        CONTINUE
(0323)60        CONTINUE
(0324)C.  Conc. profiles & total amts. dissolved
(0325)          DO 130 J=1,K+1
```

```
(0326)          PT(J)=L*C(J)+FA*C(J)**FB-PO
(0327)          YG(J)=12.566*X(J)**2*PT(J)
(0328)          BT(J)=BHS*(PH(J)+.5*LOG10(CA(J))-LPI)
(0329)          WG(J)=12.566*X(J)**2*BT(J)
(0330)          CAT(J)=.5*(PT(J)+BT(J))
(0331)130       CONTINUE
(0332)          AS=0.0
(0333)          BS=0.0
(0334)          APS=0
(0335)          BPS=0
(0336)          DO 90 J=2,K,2
(0337)          AS=AS+YG(J)
(0338)          APS=APS+WG(J)
(0339)90        CONTINUE
(0340)          DO 100 J=3,K-1,2
(0341)          BS=BS+YG(J)
(0342)          BPS=BPS+WG(J)
(0343)100       CONTINUE
(0344)          SP=Q/3*(YG(1)+YG(K+1)+4*AS+2*BS)
(0345)          SH=Q/3*(WG(1)+WG(K+1)+4*APS+2*BPS)
(0346)          PM=NT/NO*100
(0347)          WRITE(6,177)TT,NO,NT,NTB,SP,SH,PM
(0348)          IF(NT.GE.NO)STOP
(0349)          IF(TT.LT.TT6)GOTO 50
(0350)          STOP
(0351)222       FORMAT(2E10.3)
(0352)333       FORMAT(3E10.3)
(0353)444       FORMAT(4E10.3)
(0354)964       FORMAT(1X,3E10.3)
(0355)974       FORMAT(1X,4E10.3)
(0356)975       FORMAT(1X,I3,4E10.3)
(0357)133       FORMAT(3X,3E10.3)
(0358)155       FORMAT(1X,5(X,G10.4))
(0359)177       FORMAT(1X,7E10.3)
(0360)          END
(0361)**END**
```

List of Symbols used in the Programs

A(J)	Richtmyer coefficient for phosphate
AA	$\theta f \Delta t/\Delta x^2$ (planar), $D_{LP}\theta f \Delta t/2\Delta r^2$ (granular)
ACT(J)	.524[I/(1+I)-.3I]
ACTS	ACT at s
AP	Richtmyer coefficient for base
AP(J)	Richtmyer coefficient for base
ASC	Simpson coefficient for calcium
ASH	Simpson coefficient for base
ASP	Simpson coefficent for phosphate
AZ(J)	ℓ for iteration
B(J)	Richtmyer coefficient for phosphate
BHS	b_{HS} (soil volume basis)
BHSI	b_{HS} (soil weight basis)
BP(J)	Richtmyer coefficient for base
BSC	Simpson coefficient for calcium
BSH	Simpson coefficient for base
BSP	Simpson coefficient for phosphate
BT(J)	-[HS]
C(J)	$[H_2PO_4^-]_L$
CA(J)	$[Ca^{2+}]_L$
CAB	$[Ca^{2+}]_L$ for iteration
CAI	$[Ca^{2+}]_L$ in native soil
CAS	$[Ca^{2+}]_L$ at s
CAT(J)	$[Ca^{2+}]_L^{t+1}$
CI	$[H_2PO_4^-]_L$ in native soil
CL	$[Cl^-]_L$
CP(J)	$[CaH_2PO_4^+]_L$

CPS	$[CaH_2PO_4^+]_L$ at s
CS	$[H_2PO_4^-]_L$ at s
CX	$[H_2PO_4^-]_L$ at 0
D(J)	Richtmyer coefficient for phosphate
DC	D_{LP}/D_{LH}
DE(J)	$\alpha°$
DEP	$\beta°$
DH	D_{LC}/D_{LH}
DP(J)	Rictmyer coefficient for base
D1	D_{LP}
D2	D_{LH}
D3	D_{LC}
E(J)	Richtmyer coefficient for phosphate
EP(J)	Richtmyer coefficient for base
F(J)	Richtmyer coefficient for phosphate
FA	Freundlich a parameter (soil volume basis)
FAI	Freundlich a parameter (soil weight basis)
FB	Freundlich b parameter (soil volume basis)
FP(J)	Richtmyer coefficient for base
F1	f
G, GG	fractional difference between iterated values
G(J)	Rictmyer coefficient for phosphate
GP(J)	Rictmyer coefficient for base
H(J)	$[H^+]_L$
HB	$b_{HS}/(2.303[H^+]_L)$
HC(J)	$[HCO_3^-]_L$
HCS	$[HCO_3^-]_L$ at s
HF	flux of base
HS	$[H^+]_L$ at s

HT(J)	$[H^+]_L^{t+1}$
HX	$[H^+]_L$ at 0
I	counter for time steps
II, III	counters for iterations
IN	counter for iterations
IS	I
J	counter for distance steps
K	total number of distance steps
KH	K^*
KSP	K_{SP}
K2	K_2
K3	K_3
L	θ
LPI	lime potential of native soil
NO	initial amount of DCPD in one granule
NT	total amount of phosphate dissolved (from flux across soil/mineral boundary)
NTB	total amount of base dissolved (from flux across soil/mineral boundary)
P	Δt
PB	abC_L^{b-1}
PD	ρ
PF	flux of phosphate
PH(J)	pH
PHI	pH of native soil
PHS	pH at s
PHX	pH at 0
PM	percentage of added DCPD dissolved
PO	total P concentration in native soil

PP	maximum value of P
PT(J)	total P concentration
P2(J)	$[HPO_4^{2-}]_L$
P2S	$[HPO_4^{2-}]_L$ at s
Q	Δx (planar), Δr (granular)
Q1	Δx in equation (2.54)
R	a_i
RL	R
R1	R_1
S	Δa
SC	total amount of calcium dissolved (from Simpson's rule)
SH	total amount of base dissolved (from Simpson's rule)
SP	total amount of phosphate dissolved (from Simpson's rule)
TC(J)	$[H_2PO_4^-]_L^{t-1}$
TCA(J)	$[Ca^{2+}]_L^{t-1}$
TCS	$[H_2PO_4^-]_L^{t-1}$ at s
TCX	$[H_2PO_4^-]_L^{t-1}$ at 0
TH(J)	$[H^+]_L^{t-1}$
THC(J)	$[HCO_3^-]_L^{t-1}$
THCS	$[HCO_3^-]_L^{t-1}$ at s
THS	$[H^+]_L^{t-1}$ at s
TNT	NT^{t-1}
TNTB	NTB^{t-1}
TPH(J)	pH^{t-1}
TPHS	pH^{t-1} at s
TP2(J)	$[HPO_4^{2-}]_L^{t-1}$

TP2S	$[HPO_4^{2-}]_L^{t-1}$ at s
TT	total time elapsed
TTn	total time elapsed
TZ(J)	ℓ^{t-1}
TZX	ℓ^{t-1} at -1
U(J)	$\Delta r/[2(\partial\bar{\ell}/\partial r+D_{LP}K_2/H\partial C/\partial r+2\bar{\ell}/r)]$
VC	average value of $[H_2PO_4^-]_L$ over Δt
VCA(J)	average value of $[Ca^{2+}]_L$ over Δt
VH(J)	average value of $[H^+]_L$ over Δt
WG(J)	$4\pi r^2$[base]
X(J)	x (planar), r (granular)
YG(J)	$4\pi r^2$[phosphate]
Z(J)	ℓ

Appendix C

Derivation of equation (4.61) for a particle dissolving in an infinite volume of soil (by P.H. Nye).

From Crank (1975) equation (6.60)

$$\frac{C_{Lr}-C_L'}{C_{Ls}-C_L'} = \frac{a_s}{r}\ \text{erfc}\ \frac{r-a_s}{2(D_{eff}t)^{1/2}} \qquad (a)$$

where $D_{eff}=D_{LP}\theta f/b_p$.

$$M_t = \int_{a_s}^{\infty} b_p(C_{Lr}-C_L')4\pi r^2\, dr \qquad (b)$$

Substituting from (a)

$$M_t = \int_{a_s}^{\infty} b_p(C_{Ls}-C_L')4\pi r_s\, \text{erfc}\ \frac{r-a_s}{2(D_{eff}t)^{1/2}}\, dr \qquad (c)$$

which may be written

$$M_t = b_p(C_{Ls}-C_L')4\pi a_s^3 \int_1^{\infty} \frac{r}{a_s}\, \text{erfc}\left(\frac{r}{a_s}-1\right)\left(\frac{a_s^2}{4D_{eff}t}\right)^{1/2} d\frac{r}{a_s} \qquad (d)$$

Using the result, obtained by integration by parts, that

$$\int_1^{\infty} R\ \text{erfc}\ A(R-1)\ dR = \frac{1}{A\pi^{1/2}} + \frac{1}{4A^2}$$

where A is a constant

$$M_t = b_p(C_{Ls}-C_L')4\pi a_s^3\left[\left(\frac{4D_{eff}t}{\pi a_s^2}\right)^{1/2} + \frac{D_{eff}t}{a_s^2}\right] \qquad (e)$$

REFERENCES

ABDOU, F.M. & LARSEN, S. 1964 A radioactive tracer method for measuring the stability of sparingly soluble phosphates in soil. Soil Science 98, 94-99.

AMELOKO, A.Y. 1983 "The Propagation of pH Changes in Soils, and the Effect of Liming." D.Phil. Thesis, University of Oxford.

ARNOLD, P.W. 1950 The nature of precipitated calcium phosphates. Transactions of the Faraday Society 46, 1061-1072.

BARROW, N.J. 1978 The description of phosphate adsorption curves. Journal of Soil Science 29, 447-462.

BARROW, N.J. 1984 Modelling the effects of pH on phosphate sorption by soils. Journal of Soil Science 35, 283-297.

BARROW, N.J. & SHAW, T.C. 1975 The slow reaction between soil and anions: 2. Effect of time and temperature on the decrease in phosphate concentration in the soil solution. Soil Science 119, 167-177.

BARROW, N.J. & SHAW, T.C. 1979 Effects of solution:soil ratio and vigour of shaking on the rate of phosphate adsorption by soil. Journal of Soil Science 30, 67-76.

BATES, R.G. & ACREE, S.F. 1943 pH values of certain phosphate chloride mixtures, and the second dissociation constant of phosphoric acid from 0 to 60°C. Journal of Research of National Bureau of Standards 30, 129-155.

BOULDIN, D.R. & SAMPLE, E.C. 1959 Calcium phosphate fertilizers. III. The effect of surface area on the availability coefficients of dicalcium phosphates. Soil Science Society of America Proceedings 23, 276-281.

BREEUWSMA, A. & LYKLEMA, J. 1973 Physical and chemical adsorption of ions in the electrical double layer of haematite (α-Fe_2O_3). Journal of Colloid and Interface Science 43, 437-438.

BREWSTER, J.L., BHAT, K.K.S. & NYE, P.H. 1976 The possibility of predicting solute uptake and plant growth response from independently

measured soil and plant characteristics. V. The growth and phosphorus uptake of rape in soil at a range of phosphorus concentrations and a comparison of the results with the predictions of a simulation model. Plant and Soil 44, 295-328.

BREWSTER, J.L., GANCHEVA, A.N. & NYE, P.H. 1975 The determination of desorption isotherms for soil phosphate using low volumes of solution and an anion exchange resin. Journal of Soil Science 26, 364-377.

BROWN, W.E. & LEHR, J.R. 1959 Application of the phase rule to the chemical behaviour of monocalcium phosphate monohydrate in soils. Soil Science Society of America Proceedings 23, 7-12.

CHIEN, S.H. & BLACK, C.A. 1976 Free energy of formation of carbonate apatites in some phosphate rocks. Soil Science Society of America Journal 40, 234-239.

CHIEN, S.H., CLAYTON, W.R. & McCLELLAN, G.H. 1980 Kinetics of dissolution of phosphate rocks in soils. Soil Science Society of America Journal 44, 260-264.

CHRISTOFFERSEN, J. 1980 Kinetics of dissolution of calcium hydroxyapatite. III. Nucleation-controlled dissolution of a polydisperse sample of crystals. Journal of Crystal Growth 49, 29-44.

CRANK, J. 1975 "The Mathematics of Diffusion." 2nd edn. Oxford University Press.

DAVIES, C.W. 1962 "Ion Association." Butterworths, London.

FOX, R.L. and KANG, B.T. 1976 Influence of phosphorus fertilizer placement and fertilization rate on maize nutrition. Soil Science 125, 34-40.

GLASSTONE, S., LAIDLER, K.J. & EYRING, H. 1941 "The Theory of Rate Processes." McGraw-Hill, New York.

GREGORY, T.M., MORENO, E.C. & BROWN, W.E. 1970 Solubilty of $CaHPO_4.2H_2O$ in the system $Ca(OH)_2$-H_3PO_4-H_2O at 5, 15, 25 and 37.5°C. Journal of Research of National Bureau of Standards 74A, 461-475.

HAYNES, R.J. 1982 Effects of liming on phosphate availability in acid soils. Plant and Soil 68, 289-308.

HELFFERICH, F. 1962 "Ion Exchange." McGraw-Hill, New York.

HOPE, G.D. α SYERS, J.K. 1976 Effects of solution:soil ratio on phosphate sorption by soils. Journal of Soil Science 27, 301-306.

HUFFMAN, E.O., CATE, W.E., DENNING, M.E. α ELMORE, K.L. 1957 Rates of solution of calcium phosphates in phosphoric acid solutions. Journal of Agricultural and Food Chemistry 5, 266-275.

JOHN, M.K. 1970 Colorimetric determination of phosphorus in soil and plant materials with ascorbic acid. Soil Science 109, 214-220.

KEAY, J.B., BIDDISCOMBE, E.F. α OZANNE, P.G. 1970 The comparative rates of phosphate absorption by eight annual pasture species. Australian Journal of Agricultural Research 21, 33-44.

KHASAWNEH, E.H. α DOLL, E.C. 1978 The use of phosphate rocks for direct application to soils. Advances in Agronomy 30, 159-206.

KINNIBURGH, D.G., SYERS, J.K. α JACKSON, M.L. 1975 Specific adsorption of trace amounts of calcium and strontium by hydrous oxides of iron and aluminium. Soil Science Society of America Proceedings 30, 464-470.

LEHR, J.R. 1980 Phosphate raw materials and fertilizers: Part 1 - A look ahead. In "The Role of Phosphorus in Agriculture" (eds. F.E. Khasawneh, E.C. Sample α E.J. Kamprath). American Society of Agronomy, Madison, Wisconsin.

LINDSAY, W.L. α STEPHENSON, H.F. 1959 Nature of the reactions of monocalcium phosphate monohydrate in soils. 1. The solution that reacts with the soil. Soil Science Society of America Proceedings 23, 12-17.

LONERAGAN, J.F. α ASHER, C.J. 1967 Response of plants to phosphate concentrations in solution culture. II. Rate of phosphate absorption and its relation to growth. Soil Science 103, 311-318.

LOPEZ-HERNANDEZ, I.D. α BURNHAM, C.D. 1974 The effect of pH on phosphate adsorption in soils. Journal of Soil Science 25, 207-216.

McCLELLAN, G.H. α LEHR, J.R. 1969 Crystal chemical investigation of natural apatites. American Mineralogist 54, 1374-1391.

MATTINGLY, G.E.G. 1963 Agricultural value of some water and citrate soluble fertilisers; an account of recent work at Rothamsted and elsewhere. Proceeedings of Fertiliser Society No. 75, 57-97.

MEKARU, T. α UEHARA, G. 1972 Anion adsorption in ferruginous tropical soils. Soil Science Society of America Proceedings 36, 296-300.

MORENO, E.C., BROWN, W.E. α OSBORN, G. 1960a Stability of dicalcium phosphate dihydrate in aqueous systems. Soil Science Society of America Proceedings 24, 94-98.

MORENO, E.C., GREGORY, T.M. α BROWN, W.E. 1968 Preparation and solubility of hydroxyapatite. Journal of Research of National Bureau of Standards 72A, 773-782.

MORENO, E.C., LINDSAY, W.L. α OSBORN, G. 1960b Reactions of dicalcium phosphate dihydrate in soils. Soil Science 90, 56-68.

MULLER, L.D. 1977 Laboratory methods of mineral separation. In "Physical Methods in Determinative Mineralogy" (ed. J. Zussman) 2nd edn. Academic Press, London.

MURMANN, R.P. α PEECH, M. 1969 Effect of pH on labile and soluble phosphate in soils. Soil Science Society of America Proceedings 33, 205-210.

NANCOLLAS, G.H. α MARSHALL, R.W. 1970 Kinetics of dissolution of dicalcium phosphate dihydrate crystals. Journal of Dental Research 50, 1268-1272.

NELSON, D.W. α SOMMERS, L.E. 1982 Total Carbon, Organic Carbon, and Organic Matter. In "Methods of Soil Analysis" (eds. A.L. Page, R.H. Miller α D.R. Keeney). Agronomy No. 9. Part 2. 2nd edn. American Society of Agronomy, Madison, Wisconsin.

NYE, P.H. 1966 The measurement and mechanism of ion diffusion in soils. I. The relation between self-diffusion and bulk-diffusion. Journal of

Soil Science 17, 16-32.

NYE, P.H. 1972 The measurement and mechanism of ion diffusion in soils. VIII. A theory for the propagation of changes of pH in soils. Journal of Soil Science 23, 82-94.

NYE, P.H. 1979 Diffusion of ions and uncharged solutes in soils and soil clays. Advances in Agronomy 31, 225-272.

NYE, P.H. 1983 The diffusion of two interacting solutes in soils. Journal of Soil Science 34, 671-691.

NYE, P.H. α TINKER, P.B. 1977 "Solute Movement in the Soil-Root System." Blackwell, Oxford.

OLSEN, R.A. 1975 Rate of dissolution of phosphate from minerals and soils. Soil Science Society of America Proceedings 39, 634-639.

PINNER, A. α NYE, P.H. 1982 A pulse method for studying effects of dead-end pores, slow equilibration and soil structure on diffusion of solutes in soils. Journal of Soil Science 33, 25-35.

PROBERT, M.E. α LARSEN, S. 1970 The stability of dicalcium phosphate dihydrate in soils. I. Laboratory studies. Journal of Soil Science 21, 353-358.

RAMZAN, M. α NYE, P.H. 1978 The measurement and mechanism of ion diffusion in soils. IX. Changes in soil acidity near a source of bicarbonate ions. Journal of Soil Science 29, 184-194.

RHOADES, J.D. 1982 Cation Exchange Capacity. In "Methods of Soil Analysis" (eds. A.L. Page, R.H. Miller α D.R. Keeney). Agronomy No. 9. Part 2. 2nd edn. American Society of Agronomy, Madison, Wisconsin.

RICHTMYER, R.D. 1957 "Difference Methods for Initial Value Problems." Inter-Science, New York.

ROBINSON, R.A. α STOKES, R.H. 1959 "Electrolyte Solutions." 2nd edn. Butterworths, London.

ROWELL, D.L., MARTIN, M.W. α NYE, P.H. 1967 The measurement and mechanism of ion diffusion in soils. III. The effect of moisture content on the self

diffusion of ions in soils. Journal of Soil Science 18, 204-221.

SANCHEZ, P.A. α SALINAS, J.G. 1981 Low input technology for managing oxisols and ultisols in tropical America. Advances in Agronomy 34, 280-398.

SANCHEZ, P.A. α UEHARA, G. 1980 Management considerations for acid soils with high phosphorus fixation capacity. In "The Role of Phosphorus in Agriculture" (eds. F.E. Khasawneh, E.C. Sample α E.J. Kamprath). American Society of Agronomy, Madison, Wisconsin.

SAWHNEY, B.L. 1974 Charge characteristics of soils as affected by phosphate sorption. Soil Science Society of America Proceedings 38, 159-160.

SMITH, G.D. 1965 "Numerical Solutions of Partial Differential Equations." Oxford University Press.

STUMM, W. α MORGAN, J.J. 1981 "Aquatic Chemistry." 2nd edn. Wiley-Interscience, New York.

THOMAS, G.W. 1982 Exchangeable Cations. In "Methods of Soil Analysis" (eds. A.L. Page, R.H. Miller α D.R. Keeney). Agronomy No. 9. Part 2. 2nd edn. American Society of Agronomy, Madison, Wisconsin.

WHITE, R.E. α TAYLOR, A.W. 1977 Effect of pH on phosphate adsorption and isotopic exchange in acid soils at high and low additions of soluble phosphate. Journal of Soil Science 28, 48-61.